UKI
AND _OGY
19 DECEMBER 1979 NO. 9, SEPTEMBER 1979

JPRS L/8823

19 December 1979

USSR Report

METEOROLOGY AND HYDROLOGY

No. 9, September 1979

FBIS FOREIGN BROADCAST INFORMATION SERVICE

NOTE

JPRS publications contain information primarily from foreign newspapers, periodicals and books, but also from news agency transmissions and broadcasts. Materials from foreign-language sources are translated; those from English-language sources are transcribed or reprinted, with the original phrasing and other characteristics retained.

Headlines, editorial reports, and material enclosed in brackets [] are supplied by JPRS. Processing indicators such as [Text] or [Excerpt] in the first line of each item, or following the last line of a brief, indicate how the original information was processed. Where no processing indicator is given, the information was summarized or extracted.

Unfamiliar names rendered phonetically or transliterated are enclosed in parentheses. Words or names preceded by a question mark and enclosed in parentheses were not clear in the original but have been supplied as appropriate in context. Other unattributed parenthetical notes within the body of an item originate with the source. Times within items are as given by source.

The contents of this publication in no way represent the policies, views or attitudes of the U.S. Government.

For further information on report content call (703) 351-2938 (economic); 3468 (political, sociological, military); 2726 (life sciences); 2725 (physical sciences).

APPROVED FOR RELEASE: 2007/02/08: CIA-RDP82-00850R000200030039-4

JPRS L/8823

19 December 1979

USSR REPORT

METEOROLOGY AND HYDROLOGY

No. 9, September 1979

Selected articles from the Russian-language journal METEOROLOGIYA I GIDROLOGIYA, Moscow.

CONTENTS PAGE

CONTENTS (Continued) Page

PUBLICATION DATA

English title	:	METEOROLOGY AND HYDROLOGY
Russian title	:	METEOROLOGIYA I GIDROLOGIYA
Author (s)	:	
Editor (s)	:	E. I. Tolstikov
Publishing House	:	Gidrometeoizdat
Place of Publication	:	Moscow
Date of Publication	:	September 1979
Signed to press	:	21 Aug 79
Copies	:	3870
COPYRIGHT	:	"Meteorologiya i gidrologiya", 1979

UDC 551.509.(322+323+324.2)

SHORT-RANGE FORECASTING OF AIR TEMPERATURE, CONTINUOUS PRECIPITATION AND WIND ON THE BASIS OF PROGNOSTIC PRESSURE CHARTS

Moscow METEOROLOGIYA I GIDROLOGIYA in Russian No 9, Sep 79 pp 5-15

[Article by Candidate of Geographical Sciences A. I. Snitkovskiy, USSR Hydrometeorological Scientific Research Center, submitted for publication 3 April 1979]

Abstract: The author investigates the possibilities of short-range forecasting of temperature, continuous precipitation and wind using regression analysis in accordance with the PP and MOS concepts. It is shown that for predicting weather phenomena and elements for 24 and 36 hours in advance it is preferable to write prognostic dependences on the basis of the MOS concept than on the basis of the PP concept, which at the present time is being used in operational synoptic practice.

[Text] As is well known, in the operational practice of short-range forecasting of weather phenomena and elements extensive use is made of the prognostic pressure and geopotential, on the basis of which advective temperature values, humidity and wind are determined at the initial points on the trajectories. On the basis of these data and observations at the forecasting point there is computation of virtually all weather phenomena and elements included in the text of the forecast.

Due to the absence of sufficiently reliable hydrodynamic models of weather forecasts of phenomena and elements, in operational weather forecasting use is made of different empirical dependences between the predicted phenomenon and the state of the atmosphere. In the USSR these dependences have long been based on factual (diagnostic) observational data, proceeding on the basis of existing physical concepts concerning the development of weather phenomena. In the case of a real forecast for 24 and 36 hours these relationships use prognostic parameters found from future charts, whereas in the case of a forecast for the current day, morning observational data are extrapolated for 12-18 hours in advance. Such an approach in the foreign

literature [10] has been given the name "perfect prognosis" (PP). Recently in the United States, Great Britain and a number of other countries, in addition to the PP concept, in the prediction of weather phenomena and elements extensive use has been made of the MOS concept (model output statistics) [10, 12]. The MOS concept makes use of the relationships found only in prognostic data [12-16]. The quality of forecasts of weather phenomena and elements on the basis of the MOS system is the greater the higher the quality of the prognostic models and the greater is the completeness and diversity of the meteorological elements obtained from models of meteorological elements and the greater is the archives of prognostic hydrodynamic fields, which makes it possible to write dependences for different forecasting points and different seasons of the year. In accordance with [10], the quality of the temperature and precipitation forecasts under the MOS system in the United States, beginning with an advance period of 24 hours or more, is higher than for the forecasts prepared by weathermen. As a rule, for writing the relationships for the MOS system the approach of multiple linear regression is employed.

In this paper we will examine the possibilities of short-range forecasting of minimum and maximum temperatures, continuous precipitation and wind for 24 and 36 hours for Moscow and Moskovskaya Oblast, making use of two approaches to forecasting -- PP and MOS.

At the present time it is difficult to create an MOS system superior in its indices to that created in the United States. There are many reasons for this and the most important of them are: a lower quality of the prognostic hydrodynamic schemes for predicting pressure and geopotential, whose relative error for 24 and 36 hours is 0.67-0.88 [11]; absence of numerical schemes for the prediction of temperature and humidity in the troposphere and schemes for predicting meteorological elements in the boundary layer; absence of archives of prognostic fields on machine carriers.

Accordingly, in the paper an attempt has been made to test the possibilities of short-range prediction of weather phenomena and elements on the basis of the MOS system by those means which were at our disposal. These are the archives of prognostic pressure fields at the earth's surface prepared manually by weathermen, the archives of prognostic maps of geopotential and vertical air movements in the troposphere based on the S. L. Belousov hydrodynamic scheme currently used in operational work and also a number of algorithms for the statistical processing of data.

Statistical Processing of Data

The statistical processing of data included the writing of multiple regression equations, paired correlation matrices and screening of predictors for inclusion in the prognostic scheme and evaluation of the regression equations using the absolute (δ) and relative (ε) errors, the correlation coefficient (r), the N. A. Bagrov reliability test (H) and the A. M. Obukhov accuracy test [6].

The multiple regression equations were written using the algorithm described in [4, 5], having definite differences from the standard programs for writing linear multiple regression equations employed in the mathematical support for the electronic computer. The regression employed in this study is not dependent on the function of distribution of variables and on the length of the sample. The basis for the idea was minimization of the mean minimum risk of the regression equation. The regression coefficients are computed for variables first transformed by means of othogonalization using the adopted base method [7, 8]. This makes it possible to reduce the dimensionality of initial criterial space. In order to evaluate the regression equation "from below" use is made of empirical risk (σ_{er}) -- the mean square error of the "teaching" equation. In this case there is a comparison of the predictant sigma (σ_y) in the teaching sample with the empirical risk. The greater the ratio σ_y/σ_{er}, the better is the "climatic forecast" for the particular regression sample. The evaluation "from above" is the mean minimum risk (σ_{mmr}) -- the theoretical mean square regression error for the general set. The greater the σ_y/σ_{mmr} ratio, the better is the "climatic" forecast made using the general set regression. As a rule, in well-selected equations there is satisfaction of the expression

$$\sigma_{er} < \sigma_{ex} < \sigma_{mmr} < \sigma_y. \tag{1}$$

where σ_{ex} is the mean square error of the equation for the "examination" sample.

The screening of predictors for inclusion in the prognostic equation was carried out in two ways. First, by means of comparison of the σ_{mmr} values for different groups of predictors. The lesser the σ_{mmr} value, the better do the predictors selected in the equation describe the considered weather phenomenon. Second, having paired correlation coefficients, standard deviations and the non-normalized regression coefficients, in accordance with [1] it was possible to find the contribution of the predictors to the dispersion of the predictant and the contribution of each predictor to the predictant.

Assume that r_{0l} are the paired correlation coefficients between the predictant and the predictors, σ_0 is the standard deviation of the predictant, σ_l is the standard deviation of the predictors, a_{0l} are the non-normalized regression coefficients. Then the contribution of an individual predictor will be

$$\Delta x_l = r_{0_l} \alpha_{0\,l}, \tag{2}$$

where $\alpha_{0l} = a_{0l}\sigma_l/\sigma_0$ are the coefficients of a normalized regression, and the fraction of each predictor in the determination of the predictant is

$$\delta x_l = \frac{|\Delta x_l|}{R^2}. \tag{3}$$

Here R is the multiple regression coefficient and R^2 is that contribution to the dispersion of the predictant which is given by the predictors.

In this case

$$R^2 = \sum_{l=1}^{L} |\Delta x_l|, \tag{4}$$

and

$$\sum_{l=1}^{L} \delta x_l = 1. \tag{5}$$

On the basis of the expression from [1]

$$\delta x_l > 2\frac{\sigma R}{R}, \tag{6}$$

where $\sigma R = 1 - R^2/\sqrt{n-2}$ (here n is the length of the sample) we can assert that if for a particular predictor the inequality (6) is satisfied, the use of this predictor in the multiple regression equation is feasible.

Initial Data

At our disposal we had prognostic pressure, geopotential and vertical air movements charts for 1976-1978 and also the advective temperature and humidity values at the earth and at the standard isobaric surfaces obtained using these charts. Accordingly, the selection of actual data on temperature, the quantity of continuous precipitation and wind was made for the three mentioned years. The dates of the investigated cases were selected from a table of random numbers.

Temperature. As the initial data on the minimum and maximum temperatures we used their values averaged for 7 stations in Moscow and 20 stations in the Moscow area. For predicting the minimum and maximum temperatures we used the MOS concept, since it is clear from physical considerations and in accordance with [2, 9] that the PP concept could not be applied to the forecasting of temperature. The prognostic predictors were selected for 24 and 36 hours in advance respectively.

The prognostic (at the initial points of the trajectories) predictors used in predicting minimum temperature were: T_3 -- temperature at 0300 hours, in °C; T_{850} -- temperature at the 850-mb level; T_{min} -- minimum temperature; T_{max} -- maximum temperature (on the day before); $(T - T_d)_{850}$ -- dew-point spread at the 850-mb level; $(T - T_d)^{fp}_{850}$ -- dew-point spread at the 850-mb level at the final point on the trajectory; u and v -- prognostic components of wind velocity at the earth, in m/sec; u_{850} and v_{850} -- prognostic components of wind velocity at the 850-mb level, in m/sec; λ is longitude of the day, in minutes.

The prognostic (at the initial points of the trajectories) predictors for predicting maximum temperature were: T^{pr}_{min} -- prognostic minimum temperature, obtained using the regression equation; T_{max}; T_{min}; T_{850}; $(T - T_d)^{fp}_{850}$; T^{fp}_{min}; u and v; u_{850} and v_{850}; λ.

Table 1 gives evaluations of that group of predictors which in the examination sample gave better evaluations of the regression equation.

Table 1

Evaluation of the Predictors Used for Predicting Spring Temperature in Moscow and Moskovskaya Oblast

Прогноз 1	Территория 2	Предикторы 3	R^2	Вклад предикторов в R^2, % 4	5 $\sigma_{эр}$	6 $\sigma_{экз}$	7 $\sigma_{смр}$	8 σ_y
9 $T^{пр}_{min}$	Москва 11	$T_з$, T_{850}, T_{min}, T_{max}, v, λ	75	25, 29, 23, 20, 1,2	2,24	2,21	2,61	6,1
	Московская область 12	то же 13	73	26, 28, 24, 19, 1,2	2,16	2,44	2,77	6,08
10 $T^{пр}_{max}$	Москва 11	$T^{пр}_{min}$, $T_{зк}$, T_{min}, T_{max}, v, λ	82	27, 20, 23, 21, 8,1	4,48	3,50	5,23	8,03
	Московская область 12	то же 13	77	28, 22, 24, 22, 2,2	4,27	3,42	4,98	8,0

KEY:

1. Prediction
2. Territory
3. Predictors
4. Contribution of predictors to R^2, %
5. er
6. ex
7. mmr
8. y
9. T^{pr}_{min}
10. T^{pr}_{max}
11. Moscow
12. Moskovskaya Oblast
13. Same

An analysis of the matrices of paired correlation between the minimum and maximum temperatures and the predictors indicates a high correlation between the predictants and predictors reflecting the temperature peculiarities of the boundary layer and also the longitude of the day (r = 0.60-0.85). At the same time there is a weak relationship between temperature and the dew point spread at the 850-mb level at the initial and final points of the trajectories, which, as is well known, characterizes the influence of cloud cover on air temperature at the earth, which proved to be erroneous at first glance. However, with a further examination of this fact it was found that since for prediction of T^{pr}_{min} and T^{pr}_{max}, among other predictors, use is made of the advective values of the minimum and maximum temperatures at the initial points of the trajectories, in whose values the influence of cloud cover was also reflected, therefore the dew-point spread at the 850-mb level in itself exerts no appreciable influence on the prognostic values of minimum and maximum temperatures.

It is known from synoptic experience how important it is, in predicting temperature, to estimate from what direction of the horizon the transfer of air masses will occur. It was found that the meridional components of the wind, especially at the earth's surface, correlate better with the predicted minimum and maximum temperatures than the zonal wind components.

The data on the explicable fraction of dispersion of minimum temperature (R^2) for Moscow is somewhat greater than for Moskovskaya Oblast, which is indicated by the known fact that there is a greater scatter of minimum temperature in the oblast than in the city.

The values of the different mean square errors (Table 1) for the most part conform to expression (1), which indicates the legitimacy of using the selected predictors in the regression equation.

For the purpose of taking into account the climatic and circulation peculiarities of the regression equation, for predicting the minimum and maximum temperatures in Moscow and Moskovskaya Oblast for 24 and 36 hours in advance we made separate determinations for each season of the year. The archives of initial data for each of the seasons consisted of 138 cases.

Continuous precipitation. The prediction of continuous precipitation for 24 hours in advance was examined. The initial data were taken for the cold season of the year from October through March. The predictant was the quantity of precipitation averaged for 7 stations in Moscow and 20 stations in Moskovskaya Oblast for the times of day from 2100 to 0900 hours.

A study was made of a total of 456 cases: 330 with precipitation and 126 without precipitation. The distribution of precipitation by gradations was as follows:

Gradations, mm	Without precipitation	0.0-0.3	0.4-3.0	3.1-10.0	$\geqslant$10.1
Number of cases (in parentheses, %)	126(27.6)	183(40.1)	113(24.8)	30(6.6)	4(0.9)

Information on precipitation of different gradations, as shown above, indicates the difficulty of prediction of both considerable continuous precipitation and the absence of precipitation. These same complexities arose in predicting the quantity of continuous precipitation in the United States [12].

The mentioned distribution of precipitation by gradations naturally found its reflection in the content of synoptic forecasts of precipitation. For example, the number of forecasts with precipitation (in the overwhelming majority small) was 25-30% greater than was observed, whereas the number of predictions without precipitation was 25-30% fewer than the actual number of cases of absence of precipitation.

As is well known, statistical methods for predicting weather phenomena and elements give better results when from the complex of different synoptic situations the predominanting situations are selected, for each of which a decisive statistical rule is formulated. If the predominating situation falls in a wide range of values, then, taking into account the possible errors in prognostic fields, the forecaster can determine this situation with a high degree of reliability.

An analysis of the selected cases indicated that of the 330 cases with precipitation, in 256 cases the precipitation was observed when the wind direction at the 500-mb surface was from 180 to 360°. For this reason for the investigation we selected a situation when the wind direction at the 500-mb level was from the western side of the horizon. As an absence of precipitation we used a case when the quantity of precipitation was 0.0 mm and when it was not observed.

The prediction of continuous precipitation by statistical methods is extremely difficult and therefore about 30 predictors were subjected to screening. It was found that the values of surface pressure, geopotential at the levels 850, 700 and 500 mb, temperature and dew point at the earth and at the 850-mb level and a number of other predictors have a weak correlation with precipitation. As a result of many numerical experiments we selected 10 predictors whose correlation with precipitation was satisfactory and good. These were: c_{500} -- wind velocity at the 500-mb level, m/sec; w_{700} -- ordered vertical air movements at the 700-mb level, mb/12 hours; k is a coefficient equal to $(H_{1000}+H_{500})-2H_{850}$; $\sum (T - T_d)$ is the total dew point deficit at the levels 800 and 750 mb; q_{pw} is the quantity of precipitable water in mm; Φ_{in} is the fact of initial precipitation at the point (or in the region) of the forecast in binary form (coding: $\Phi_{in} = 3$, when precipitation $\geqslant 0.1$ mm; $\Phi_{in} = 1$ in the remaining cases); q is the quantity of advective precipitation (the initial points of the trajectories are determined from the wind at the 700-mb level) in mm; Φ is the fact of advective precipitation in binary form (the coding is the same as for Φ_{in}).

It should be noted that a single-step prediction of the fact and quantity of continuous precipitation using the regression equations did not give satisfactory results. For this reason a number of predictors from among the selected predictors were represented in a binary form, which gave considerably better results in the prediction of the fact of precipitation. If the predicted value of the predictant exceeds a definite threshold (in our case -- two), then another equation is used in predicting the quantity of precipitation.

Table 2 gives estimates of the best predictors selected in the prognostic scheme. It can be seen that the explicable dispersion of the fact of continuous precipitation for Moskovskaya Oblast is greater than for Moscow, which is attributable to territorial averaging. It should be mentioned that allowance for w_{700} in the regression equation for Moskovskaya Oblast leads to nonsatisfaction of expression (1), $\sigma_{mmr} < \sigma_{ex}$. Therefore, in the regression equation only the fact of advective precipitation remains as a prognostic predictor.

Table 2

Explicable Dispersion (R^2) of Fact of Precipitation and Contribution of its Predictors

1 Концепция	2 Предикторы	R^2 %	Доля (в %) каждого предиктора в R^2 3	$\sigma_{эр}$ 4	$\sigma_{экз}$ 5	$\sigma_{смр}$ 6	σ_y 7
	12	8 Москва					
PP	w_{700}, $\Phi_{исх}$, Φ	28	60, 15, 25	0,85	0,95	0,98	1,00
	w_{700}, $\Phi_{исх}$, Φ, $\Phi_{син}$ 13	34	47, 12, 20, 21	0,83	0,91	0,95	1,00
MOS	w_{700}, $\Phi_{исх}$, Φ	17	40, 35, 25	0,93	0,93	1,06	1,00
	w_{700}, $\Phi_{исх}$, Φ, $\Phi_{син}$	23	30, 19, 19, 32	0,93	0,93	1,07	1,00
10 Синоптический прогноз		29		0,89	0,84	1,02	1,00
	12	9 Московская область					
PP	$\Phi_{исх}$, Φ	26	60, 40	0,80	1,00	1,02	1,00
	$\Phi_{исх}$, Φ, $\Phi_{син}$ 13	43	28, 12 60	0,80	1,00	1,02	1,00
MOS	$\Phi_{исх}$, Φ	28	58, 42	0,89	1,00	1,08	1,00
	$\Phi_{исх}$, Φ, $\Phi_{син}$	43	28, 12 60	0,89	1,00	1,02	1,00
11 Синоптический прогноз		33		0,85	1,03	0,98	1,00

KEY:

1. Concept
2. Predictors
3. Fraction (in %) of each predictor to R^2
4. er
5. ex
6. mmr
7. y
8. Moscow
9. Moskovskaya Oblast
10. Synoptic forecast
11. Synoptic forecast
12. in
13. syn

The regression equations, in which only a synoptic forecast of precipitation enters as a predictor, show that for Moscow $\sigma_{mmr} > \sigma_{ex}$, whereas for Moskovskaya Oblast $\sigma_{mmr} < \sigma_{ex}$, that is, the synoptic forecast of continuous precipitation for Moskovskaya Oblast must not be adequately successful, as is also indicated by the estimates of the probability of precipitation given in Table 4.

Table 3

Mean Probable Success of Forecasts of Minimum and Maximum Temperatures for Moscow and Moskovskaya Oblast in January, February and March 1979

Прогнозы 1	Месяц 2	3 Абсолютная ошибка, *град.*			
		4 $T^{пр}_{min}$		5 $T^{пр}_{max}$	
		Москва 6	Московская область 7	Москва 6	Московская область 7
8 Синоптиков	январь 10	1,6	1,8	2,1	2,2
9 По регрессии		2,0	2,3	1,9	1,8
Синоптиков	февраль 11	2,5	2,4	1,4	1,8
По регрессии		2,5	2,8	2,4	2,3
Синоптиков	март 12	1,8	1,4	3,0	2,6
По регрессии		0,9	1,2	2,8	2,6
Синоптиков	Средняя 13	2,0	1,9	2,2	2,2
По регрессии		1,8	2,1	2,4	2,2

KEY:

1. Forecasts
2. Month
3. Absolute error, degrees
4. T^{pr}_{min}
5. T^{pr}_{max}
6. Moscow
7. Moskovskaya Oblast
8. Weathermen
9. Using regression equations
10. January
11. February
12. March
13. Average

Wind. A study was made of a wind forecast for 24 and 36 hours in advance on the basis of the PP and MOS approaches. The period of time from September through May was investigated. Initially the number of predictors was about 20; then, taking into account the peculiarities of the correlation matrices, their number was reduced to 7. In the prognostic equations we left those predictors information concerning which could be read from the prognostic pressure and geopotential charts. The predictors included: c_g and d_g -- the velocity and direction of the geostrophic wind at the earth's surface in m/sec and degrees; C_{700} and d_{700} -- wind velocity and direction at the 700-mb level in m/sec and degrees; u_{850} and v_{850} -- wind velocity components at the 850-mb level in m/sec. In the regression equations for predicting wind velocity the predictant was the wind velocity itself, averaged for a two-minute interval, whereas for predicting wind direction -- the wind velocity components. Such an approach to the forecasting of wind velocity and direction is the most feasible [10].

Table 4

Evaluation of Regression Equations and Forecasts of Weathermen of Fact of Precipitation

1 Концепция	2 Предикторы	3 Оценка уравнений регрессии: r	H	Q	4 общая оправдываемость, %	5 оправдываемость осадков, %	6 оправдываемость отсутствия осадков, %
	8 Москва						
PP	w_{700}, $\Phi_{исх}$, Φ	0,29	0,40	0,40	70,2	64,5	76,0
	w_{700}, $\Phi_{исх}$, Φ, $\Phi_{син}$ 11	0,35	0,36	0,37	68,4	64,5	72,4
MOS	w_{700}, $\Phi_{исх}$, Φ 10	0,31	0,40	0,40	70,2	64,5	76,0
	w_{700}, $\Phi_{исх}$, Φ, $\Phi_{син}$	0,47	0,54	0,54	76,7	74,1	79,3
7 Синоптический прогноз	11	0,44	0,48	0,52	74,7	83,6	65,8
	9 Московская область						
PP	$\Phi_{исх}$, Φ	0,30	0,42	0,42	70,9	71,4	70,3
	$\Phi_{исх}$, Φ, $\Phi_{син}$	0,32	0,30	0,30	65,3	71,4	59,2
MOS	$\Phi_{исх}$, Φ	0,34	0,38	0,38	69,1	64,2	74,0
	$\Phi_{исх}$, Φ, $\Phi_{син}$	0,34	0,30	0,30	65,4	64,2	66,6
7 Синоптический прогноз		0,21	0,24	0,24	61,6	71,4	51,8

KEY:

1. Concept
2. Predictors
3. Evaluation of regression equations
4. Total probability of success, %
5. Probability of precipitation, %
6. Probability of absence of precipitation, %
7. Synoptic forecast
8. Moscow
9. Moskovskaya Oblast
10. in
11. syn

The initial sample of winds in a forecast for 24 hours was 134 cases, and in a forecast for 36 hours -- 164 cases. The overwhelming number of winds was with a velocity less than 10 m/sec. However, since the main purpose of the investigation was a clarification of the possibilities of predicting the wind in accordance with the MOS concept, such a formulation of the problem is entirely legitimate.

Table 5

Evaluation of Regression Equations for Wind Forecast

Заблаговременность, ч 1	Концепция 2	Оценки скорости ветра 3			Абсолютная ошибка направления ветра, град 4
		δ	ε	r	
24	PP	2,0	0,36	0,40	56,7
	MOS	1,9	0,34	0,54	57,7
36	PP	6,1	0,13	0,13	54,6
	MOS	1,9	0,32	0,40	56,6

KEY:

1. Advance period, hours
2. Concept
3. Estimates of wind velocity
4. Absolute error in wind direction, degrees

Results

The checking of the derived multiple regression equations for the prediction of temperature, continuous precipitation and wind was carried out on the basis of an independent examination sample, constituting approximately one third of the corresponding archives of initial data. This same third of the cases was used in evaluating the forecasts of weathermen, since at the present time the quality of the synoptic forecasts of the weather phenomena and elements for 24 and 36 hours is higher than for different computational and other forecasting methods.

Unfortunately, we were unable to make an evaluation of a synoptic forecast of the wind. It was also impossible to determine the correlation between the quantity of continuous precipitation in the forecast made by weathermen and the quantity of precipitation actually falling due to the fact that in the synoptic forecasts the quantity of anticipated precipitation has a qualitative formulation.

Temperature. The mean absolute error in predicting minimum temperature for 24 hours in advance for winter was for Moscow 1.8°C, for Moskovskaya Oblast -- 2.0°C; the maximum temperature for 36 hours was 1.9 and 1.8°C respectively. The forecasts of weathermen for this same sample for minimum temperature were 1.9 and 2.1°C respectively, and for maximum temperature -- 2.1 and 2.2°C. The correlation coefficients between the minimum and maximum temperatures predicted using the regression equations and the actual temperatures were 0.94 and 0.84.

Such a relationship of the evaluations of synoptic temperature forecasts and forecasts based on regression equations enabled us to carry out testing of the forecasts of minimum and maximum temperatures for Moscow and Moskovskaya

Oblast in January, February and March 1979. The results of these evaluations are given in Table 3. These results indicate entirely comparable evaluations of temperature forecasts with respect to regression equations and forecasts of weathermen. As a comparison we note that in the United States [14], using the MOS system, the mean absolute error in predicting minimum temperature for 24 hours in advance is 2.3°C; the maximum temperature for 36 hours -- 2.4°C. Accordingly, the evaluations cited in Table 3 for the temperature forecasts of weathermen and forecasts based on regression equations for Moscow are better than the corresponding evaluations of temperature forecasts in the United States. This indicates that despite the higher quality of the prognostic charts in the United States, the synoptic experience and choice of the corresponding predictors on the whole give better results in the prognostic equations. It must be remembered that the change in the mean absolute error by 0.2-0.3°C is approximately 10% of the success of the forecast.

Continuous precipitation. The checking of regression equations for predicting the fact of precipitation was carried out for the PP and MOS concepts. The results of this checking are given in Table 4. We should note one peculiarity in the analysis of these evaluations. In the forecast of the fact of precipitation for Moscow any of the combinations of predictors which we selected in the regression equations gives results which are worse than the forecasts of weathermen. Bearing in mind that in the preparation of operational forecasts weathermen daily use several prognostic schemes of forecasts of the quantity of precipitation, we decided to introduce a synoptic forecast of precipitation (precipitation or absence of precipitation (Φ_{syn}) as an additional predictor in binary form. The results of evaluations of these regression equations are given in the denominator of the corresponding rows in Table 4. It can be seen that the evaluations of the regression equations were now better and exceeded the evaluations of the forecasts of weathermen. The pattern of evaluations of the regression equations for forecasting the fact of precipitation in Moskovskaya Oblast (Table 4) is different. Here the evaluations of the regression equations with the predictors which we initially selected were better than the synoptic forecasts. The addition of a synoptic forecast of precipitation as a predictor in the regression equation worsened the results.

It is important to note that precipitation forecasts, in accordance with the MOS concept for Moscow and Moskovskaya Oblasts, were better than when using the PP concept.

The regression equations for predicting the quantity of continuous precipitation, in accordance with the MOS concept, were written in such a way that they included predictors having only the quantitative values of different atmospheric characteristics. We note that on the basis of the regression equations the quantity of precipitation is not predicted adequately satisfactorily. The correlation coefficient between the quantity of predicted precipitation and the actual quantity was not more than 0.41; the mean absolute error was 2.1. These evaluations are low but the available information [3] on the correlation coefficients between the quantity

of precipitation determined using different schemes and that actually observed do not exceed 0.38, and the mean absolute error in the gradation 0.0-4.00 mm is 0.7, and in the gradation 4-20 mm is 4.0-4.7. As a comparison we note that in the best diagnostic regression equation the correlation coefficient between the computed quantity of precipitation and the actual quantity is 0.65, and the absolute error is 1.8.

Wind. A comparison of evaluations of the regression equations written in accordance with the PP and MOS concepts (Table 5) shows that all evaluations made using the MOS system are higher than the evaluations made using the PP system. There is a tendency to a worsening of the results with an increase in the advance time of the forecast, which is directly governed by the quality of the prognostic charts.

Bearing in mind that the evaluations made relate to wind archives consisting for the most part of data on winds with a velocity less than 10 m/sec, we decided to check the conclusions drawn above using archives in which there are a sufficient number of cases of a wind with a force greater than 15 m/sec. For this purpose for a forecast for 24 hours, for Liyepaya station we prepared an archives of 134 cases, of which 43 were for a case of a wind greater than 15 m/sec. The results obtained using these data confirmed the conclusions drawn. It was found that evaluations for the MOS approach were better that the corresponding evaluations made by the PP approach. Thus, For example, for the absolute error this difference was 0.25, for the relative error -- 0.14, for the correlation coefficient -- 0.04.

Summary

The results for short-range (for 24 and 36 hours) forecasting of temperature, continuous precipitation and wind using the multiple regression equations indicate that at the present time for the writing of statistical dependences for the prediction of weather phenomena and elements it is better to use the MOS concept rather than the PP concept.

Despite the relatively high relative errors in the prognostic fields of pressure and geopotential of existing operational schemes, the use of these charts for the writing of prognostic dependences in accordance with the MOS concept for the short-range prediction of weather phenomena and elements is entirely possible.

The quality of predictions of weather phenomena and elements is dependent not only on how correctly the predictors in the prognostic equations were selected, but also on the correctness of choice of the initial data, which is exclusively associated with the accuracy of the prognostic fields of meteorological elements. Therefore, together with attempts to formalize the short-range forecasting of weather elements it is impossible to ignore the experience of the weatherman, who like no one else can best evaluate the nature of development of the synoptic situation and select the initial data.

BIBLIOGRAPHY

1. Alekseyev, G. A., OB"YEKTIVNYYE METODY VYRAVNIVANIYA I NORMALIZATSII KORRELYATSIONNYKH SVYAZEY (Objective Methods for the Smoothing and Normalization of Correlations), Leningrad, Gidrometeoizdat, 1971.

2. Bachurina, A. A., "Forecasting of Air Temperature and Dew Point in the Surface Layer of the Troposphere," PROGNOZ PRIZEMNOY TEMPERATURY, VLAZHNOSTI VOZDUKHA I DRUGIKH METEOROLOGICHESKIKH ELEMENTOV (Prediction of Surface Temperature, Air Humidity and Other Meteorological Elements), Leningrad, Gidrometeoizdat, 1970.

3. Bukreyeva, L. A., Veselova, G. K., "Results of Testing of Operational Numerical Scheme for the Synoptic-Hydrodynamic Forecasting of the Quantity of Precipitation," INF. SB. No 8, REZUL'TATY ISPYTANIYA RAZLICHNYKH SPOSOBOV I SKHEM KRATKOSROCHNOGO PROGNOSA POGODY (Results of Testing of Different Methods and Schemes for Short-Range Weather Forecasting), Moscow, Gidrometeoizdat, 1979.

4. Vapnik, V. N., Chervonenkis, A. Ya., "Uniform Convergence of the Frequencies of Occurrence of Events to Their Probabilities and the Problem of Seeking an Optimum Solution Using Empirical Data," AVTOMATIKA I TELEMEKHANIKA (Automation and Telemechanics), No 2, 1971.

5. Vapnik, V. N., VOSSTANOVLENIYE ZAVISIMOSTEY PO EMPIRICHESKIM DANNYM (Restoration of Dependences Using Empirical Data), Moscow, Nauka, 1979.

6. METODICHESKIYE UKAZANIYA PO PROVEDENIYU OPERATIVNYKH ISPYTANIY NOVYKH METODOV GIDROMETEOROLOGICHESKIKH PROGNOZOV (Systematic Instructions on Carrying Out Operational Tests of New Methods for Hydrometeorological Forecasts), Leningrad, Gidrometeoizdat, 1977.

7. Neymark, Yu. I., Vatalova, Z. S., Vasin, Yu. G., "Image Recognition and Medical Diagnosis," TRUDY MEZHDUNARODNOGO SIMPOZIUMA PO TEKHNICHESKIM I BIOLOGICHESKIM PROBLEMAM UPRAVLENIYA (Transactions of the International Symposium on Technical and Biological Problems in Control), Moscow, Nauka, 1971.

8. Romanov, L. N., Vinogradova, G. M., "Orthogonal Expansions of Synoptic Situations Using the Coordinates of an Adapted Base," TRUDY ZSRNIGMI (Transactions of the West Siberian Regional Scientific Research Hydrometeorological Institute), No 11, 1974.

9. Snitkovskiy, A. I., Ustinova, G. P., "Prediction of Minimum Air Temperature in Moscow With Use of Future Pressure Fields," TRUDY GIDROMETTSENTRA SSSR (Transactions of the USSR Hydrometeorological Center), No 225, 1979.

10. Snitkovskiy, A. I., Sonechkin, D. M., Fuks-Rabinovich, M. S., Shapovalova, N. S., OBZOR. SISTEMA OB"YEKTIVNOGO KRATKOSROCHNOGO PROGNOZA YAVLENIY I ELEMENTOV POGODY V SShA (Review. System of Objective Short-Range Forecasting of Weather Phenomena and Elements in the United States), Obninsk, Informatsionnyy Tsentr, 1978.

11. Ugryumov, A. I., Veselova, G. K., Chernova, V. F., Ageyeva, A. K., Bukreyeva, L. A., "Comparative Evaluation of Regional Schemes for the Numerical Forecasting of the Pressure Field for 24 and 36 Hours in Advance," INF. SB. No 6, "REZUL'TATY ISPYTANIYA RAZLICHNYKH SPOSOBOV I SKHEM KRATKOSROCHNOGO PROGNOZA POGODY"), Moscow, Gidrometeoizdat, 1978.

12. Bermowitz, R. Y., "An Application of Model Output Statistics to Forecasting Quantitative Precipitation," MON. WEATHER REV., Vol 103, No 2, 1975.

13. Hammons, G., Dallvalle, J., "MOS Maximum/Minimum Temperature Forecast Equations Based on Three-Month Seasons," TECHN. PROCEDURE BULL., No 155, 1976.

14. Hammon, G., Dallavalle, J., Klein, W. H., "Automated Temperature Guidance Based on Three-Month Seasons," MON. WEATHER REV., Vol 104, No 12, 1976.

15. Klein, W. H., Lewis, F., "Computer Forecast of Maximum and Minimum Temperature," J. APPL. METEOROL., Vol 9, 1970.

16. Klein, W. H., "On the Accuracy of Automatic Max/Min Temperature Forecast," J. APPL. METEOROL., Vol 11, No 8, 1972.

UDC 551.(509.313:558.21)

ALLOWANCE FOR OROGRAPHY IN NUMERICAL WEATHER FORECASTING MODELS

Moscow METEOROLOGIYA I GIDROLOGIYA in Russian No 9, Sep 79 pp 16-24

[Article by Doctor of Physical and Mathematical Sciences A. I. Romov, Ukrainian Scientific Research Hydrometeorological Institute, submitted for publication 8 January 1979]

Abstract: The author proposes a model for numerical weather forecasting using full equations in a σ-coordinate system with improved allowance for orography. Transformation of the equations of motion was carried out. This makes it possible to eliminate the errors caused by computation of small differences in the large values characteristic of the mentioned coordinate system in situations over mountain slopes. As a result, there is an increase in the accuracy of the computations of the pressure gradients, which here attains the usual accuracy level for an isobaric coordinate system. In the process of difference solution of the problem the need disappears for scaling geopotential to nonstandard isobaric surfaces. Thus, a solution is found for the known problem of allowance for orography in numerical weather forecasting problems.

[Text] In dynamic meteorology different coordinate systems are used, depending on the nature of the studied processes and the conditions under which they transpire. One of the principal, most commonly used systems at the present time is a p-system. The system of equations usually used in numerical weather forecasting schemes, without friction taken into account, in an x, y, p coordinate system has the following form [1]:

$$\frac{\partial u}{\partial t}+u\frac{\partial u}{\partial x}+v\frac{\partial u}{\partial y}+\omega\frac{\partial u}{\partial \zeta}=-g\frac{\partial H}{\partial x}+lv, \tag{1}$$

$$\frac{\partial v}{\partial t} + u\frac{\partial v}{\partial x} + v\frac{\partial v}{\partial y} + \omega\frac{\partial v}{\partial \zeta} = -g\frac{\partial H}{\partial y} - lu, \tag{2}$$

$$\frac{\partial T}{\partial t} + u\frac{\partial T}{\partial x} + v\frac{\partial T}{\partial y} + \omega\frac{\partial T}{\partial \zeta} = \frac{R\gamma_a T}{g\zeta}\omega, \tag{3}$$

$$\frac{\partial u}{\partial x} + \frac{\partial v}{\partial y} + \frac{\partial \omega}{\partial \zeta} = 0, \tag{4}$$

$$T = -\frac{g\zeta}{R}\frac{\partial H}{\partial \zeta}. \tag{5}$$

Here u and v are the wind velocity components along the x and y axes; H is the height of the isobaric surface; ζ is the ratio of pressure p to the standard value P = 1000 mb, playing the role of a vertical coordinate; ω is the full time derivative (time = t) of the ζ coordinate, representing the velocity of displacement of air particles relative to the isobaric surfaces; T is temperature; g is the acceleration of free falling; l is the Coriolis parameter; R is the gas constant; γ_a is the adiabatic temperature gradient.

The sought-for functions are u, v, H, T, ω. The forecasting equations in the form (1)-(5) are characterized by relative simplicity and convenience for a lowland territory. However, it is known that in a p-system it is difficult to describe the conditions at the lower boundary of the atmosphere, which is particularly important in prognostic problems for taking into account the influence of orography on weather.

In 1957 N. Phillips [8] introduced the vertical coordinate σ, equal to the ratio of pressure at a particular point to pressure at the earth's surface under this point, and proposed a rectifying σ-coordinate system whose advantages consist in convenience in stipulating the boundary conditions at the earth and solution of weather forecasting problems using a full system. This system, the same as the generalized Shuman and Hovermale variant [9], due to the mentioned advantages is intended for taking into account the influence of orography.

However, we note that up to this time virtually no one has succeeded in making full use of these important advantages. The fact is that in a σ-system, as is well known [1, 2, 6, 10], computations are made of the pressure gradients which figure in the equations of motion, with appearance of additional effects of "small differences of large values" of a higher order of magnitude than in the ordinary coordinate systems x, y, z and x, y, p. This is accompanied by great errors in the difference approximation in solving the equations of motion and instability of the computations [6, 10].

For a more detailed examination we will write equations (1)-(5) in one of the modifications of the σ-system examined in [3, 4]:

$$\frac{\partial u}{\partial t} + u\frac{\partial u}{\partial x} + v\frac{\partial u}{\partial y} + \frac{1}{\zeta^* - \zeta_{op}}(\omega - \sigma\omega^*)\frac{\partial u}{\partial \sigma} = \tag{6}$$

$$= lv - g\frac{\partial H}{\partial x} - \frac{\sigma RT}{\sigma\zeta^* + (1-\sigma)\zeta_{op}}\frac{\partial \zeta^*}{\partial x},$$

$$\frac{\partial v}{\partial t} + u\frac{\partial v}{\partial x} + v\frac{\partial v}{\partial y} + \frac{1}{\zeta^* - \zeta_{op}}(\omega - \sigma\omega^*)\frac{\partial v}{\partial \sigma} =$$

$$= -lu - g\frac{\partial H}{\partial y} - \frac{\sigma RT}{\sigma\zeta^* + (1-\sigma)\zeta_{op}}\frac{\partial \zeta^*}{\partial y^*}, \tag{7}$$

$$\frac{\partial T}{\partial t} + u\frac{\partial T}{\partial x} + v\frac{\partial T}{\partial y} + \frac{1}{\zeta^* - \zeta_{op}}(\omega - \sigma\omega^*)\frac{\partial T}{\partial \sigma} =$$

$$= \frac{RT\gamma_a \omega}{g[\sigma\zeta^* + (1-\sigma)\zeta_{op}]}, \tag{8}$$

$$\omega = \omega_{op} + \sigma\left(u\frac{\partial \zeta^*}{\partial x} + v\frac{\partial \zeta^*}{\partial v}\right) -$$

$$-\int_0^\sigma \left(\frac{\partial u(\zeta^* - \zeta_{op})}{\partial x} + \frac{\partial v(\zeta^* - \zeta_{op})}{\partial y}\right) d\sigma, \tag{9}$$

$$\omega^* = \omega + (1-\sigma)\left(u\frac{\partial \zeta^*}{\partial x} + v\frac{\partial \zeta^*}{\partial y}\right) -$$

$$-\int_\sigma^1 \left(\frac{\partial u(\zeta^* - \zeta_{op})}{\partial x} + \frac{\partial v(\zeta^* - \zeta_{op})}{\partial y}\right) d\sigma. \tag{10}$$

$$T = -\frac{g}{\kappa}\left(\sigma + \frac{\zeta_{op}}{\zeta^* - \zeta_{op}}\right)\frac{\partial H}{\partial \sigma}, \tag{11}$$

$$\frac{\partial \zeta^*}{\partial t} = \omega\ (x, y, 1, t) - \left(u_h\frac{\partial \zeta^*}{\partial x} + v_h\frac{\partial \zeta^*}{\partial y}\right), \tag{12}$$

$$\sigma = \frac{\zeta - \zeta_{op}}{\zeta^* - \zeta_{op}}; \tag{13}$$

$\zeta^* = \zeta^*(x, y, t)$ is the ζ value at the earth's surface (mountains); ω^* is the individual change in the ζ^* value; ζ_{oro} is dimensionless pressure at the isobaric surface ζ_{oro} = const, being the upper boundary of the "orographic" air layer in which the mountains are completely submerged and within the limits of which a σ-coordinate system is used.

ω_{oro} is the vertical velocity at the surface ζ_{oro} = const; H is the height of the surface σ = const above sea level; h is the height of the relief of the earth's surface; the h indices denote the values on this surface.

The same as in [3, 4], here we will propose that within the framework of one scheme use will be made of a combination of both coordinate systems: in the upper layer (above the surface ζ_{oro} = const) use is made of equations in the form (1)-(5), and in the lower layer -- in the form (6)-(12). We note that in the latter system, in place of the former five, we have seven equations, since here, besides the functions u, v, T, H and ω, we have additionally introduced and investigated the functions ω^* and ζ^*. The initial fields u, v, T, ζ^* must be stipulated. The region of solution of the problem is limited from above by the isobaric surface ζ_0 = const (0.1 or 0.2). The boundary conditions are:

$$\omega=0 \quad \text{when} \quad \zeta=\zeta_0,$$
$$H=h(x, y), \quad \text{when} \quad \sigma=1.$$

We note that the horizontal derivatives of one and the same function in both systems, speaking generally, differ greatly in their values. This is attributable to the fact that the isobaric surfaces always remain almost horizontal, whereas the surfaces σ = const can have different slopes in dependence on the nature of the relief and the thickness of the layer of submergence of the mountains (ζ_{oro} values).

These differences are particularly significant for the derivatives of geopotential (heights H). In each of the equations (6) and (7) the force of the pressure gradient is not represented by one term, as in (1) and (2), but by the last two terms on the right-hand sides, by the sum of these terms. Over the mountain slopes, in the lower air layers, these terms are opposite in sign and each of them can attain values two orders of magnitude greater than the resultant force of the pressure gradient. For example, with a mountain slope 10^{-2} the order of magnitude of each of the two mentioned terms on the earth is 10^{-1}, at the same time that their sum is 10^{-3}. (Here and in the text which follows the estimates are given in the MTS system of units).

Under such conditions computations of the pressure gradient in the final differences becomes impossible. This circumstance already over the course of a number of years serves as an obstacle for the effective use of a σ-coordinate system in the practice of numerical weather forecasts using full equations and in modeling of general circulation of the atmosphere.

In some studies, in order to eliminate the mentioned inconvenience, use is made of a method in which at each nodal point there is introduction of an auxiliary isobaric surface, its heights are interpolated by means of scaling from the surface σ = const and thus the horizontal pressure gradients are found [7, 10]. Such a method is rather unwieldy, inadequately economical, and the error associated with the scaling of geopotential can be comparable with the value of the pressure gradient itself.

In a study by S. O. Krichak [2] the influence of the mentioned shortcoming is softened by a corresponding choice of pressure at the upper boundary of the considered layer of the atmosphere at which a small horizontal variability of layer thickness is attained. In our case, with combined coordinates, the possibilities of such a choice are limited.

In this article we propose a method which makes possible a complete elimination of the additional effects of small differences of large values characteristic of a σ-coordinate system in situations over mountain slopes without having recourse to the introduction of auxiliary isobaric surfaces and scaling of heights. This is attained by a corresponding transformation of the equations themselves within the framework of a σ-coordinate system. In the layer of submergence of mountains we examine the dimensionless pressure function ζ, which is represented in the form of the sum of the main ζ value and the small deviation ζ_1:

$$\zeta=\bar{\zeta}+\zeta_1. \tag{14}$$

Now we will turn to the last term on the right-hand side of equation (6). Using an expression following from (13),

$$\zeta=\sigma\zeta^*+(1-\sigma)\,\zeta_{op}, \tag{15}$$

this term can be written as follows:

$$\frac{\sigma RT}{\sigma\zeta^*+(1-\sigma)\,\zeta_{op}}\frac{\partial\zeta^*}{\partial x}=\frac{RT}{\zeta}\frac{\partial\zeta}{\partial x}.$$

Then the sum of both terms in (6) representing the force of the pressure gradient, after the substitution (14), neglecting the squares of small values, can be represented in the form

$$-g\frac{\partial H}{\partial x}-\frac{RT}{\zeta}\frac{\partial\zeta}{\partial x}=-g\frac{\partial H}{\partial x}-\frac{RT}{\bar{\zeta}}\frac{\partial\bar{\zeta}}{\partial x}-\frac{RT}{\bar{\zeta}+\zeta_1}\frac{\partial\zeta_1}{\partial x}+ \tag{16}$$

$$+RT\frac{\zeta_1}{\bar{\zeta}^2}\frac{\partial\bar{\zeta}}{\partial x}.$$

We note that the first term on the left-hand side of (16) has the form of the pressure gradient force in a p-coordinate system and the second term -- in a z-system.

On the right-hand side of (16) the first two terms in the mountains have the order of magnitude 10^{-1}, the next two terms -- 10^{-3}. It is natural to attempt to avoid the first two terms, equating their sum to zero and determining from this equation the expression for $\bar{\zeta}$. For this it would be necessary to integrate it for x, which cannot be done with accuracy without knowing how temperature changes at the surfaces σ = const. In this case allowance for this change is significant, it cannot be neglected, and therefore first on the right-hand side of (16) it is necessary to carry out the following substitution:

$$RT\frac{\partial \ln\overline{\zeta}}{\partial x}=R\frac{\partial}{\partial x}(T\ln\overline{\zeta})-R\ln\overline{\zeta}\frac{\partial T}{\partial x}, \tag{17}$$

after which we obtain:

$$-g\frac{\partial H}{\partial x}-\frac{RT}{\zeta}\frac{\partial \zeta}{\partial x}=-g\frac{\partial H}{\partial x}-R\frac{\partial}{\partial x}(T\ln\overline{\zeta})-\frac{RT}{\overline{\zeta}+\zeta_1}\frac{\partial \zeta_1}{\partial x}+ \tag{18}$$

$$+RT\frac{\zeta_1}{\overline{\zeta}^2}\frac{\partial\overline{\zeta}}{\partial x}+R\ln\overline{\zeta}\frac{\partial T}{\partial x}.$$

Here on the right-hand side has appeared a term (dependent on $\partial T/\partial x$) with a value about 10^{-3}, but the $\overline{\zeta}$ function now is determined with accuracy from the condition of a full mutual compensation of the first two terms on the right-hand side of (18), having an identical and the highest order of magnitude (10^{-1}) among the other terms. We will assume

$$-g\frac{\partial H}{\partial x}-R\frac{\partial}{\partial x}(T\ln\overline{\zeta})=0. \tag{19}$$

Integrating (19) for x and assuming the condition $\overline{\zeta}$ = 1 with H = 0, we obtain the following expression for $\overline{\zeta}$, precisely satisfying equality (19):

$$\overline{\zeta}=e^{-\frac{gH}{RT}}. \tag{20}$$

Thus, if $\overline{\zeta}$ is computed using formula (20), we obtain the following expressions for the components of the pressure gradient force relative to the x and y coordinates respectively:

$$-g\frac{\partial H}{\partial x}-\frac{\sigma RT}{\sigma\zeta^*+(1-\sigma)\zeta_{op}}\frac{\partial\zeta^*}{\partial x}=-\frac{RT}{\overline{\zeta}+\zeta_1}\frac{\partial\zeta_1}{\partial x}+ \tag{21}$$

$$+RT\frac{\zeta_1}{\overline{\zeta}^2}\frac{\partial\overline{\zeta}}{\partial x}+R\ln\overline{\zeta}\frac{\partial T}{\partial x},$$

$$-g\frac{\partial H}{\partial y}-\frac{\sigma RT}{\sigma\zeta^*+(1-\sigma)\zeta_{op}}\frac{\partial\zeta^*}{\partial y}=-\frac{RT}{\overline{\zeta}+\zeta_1}\frac{\partial\zeta_1}{\partial y}+$$

$$+\frac{RT\zeta_1}{\overline{\zeta}^2}\frac{\partial\overline{\zeta}}{\partial y}+R\ln\overline{\zeta}\frac{\partial T}{\partial y}.$$

[op = oro]

Here the order of magnitudes of all the terms on the right-hand sides both over the plains and in the mountains no longer exceeds 10^{-3}.

It would be convenient to compute the $\overline{\zeta}$ fields using initial data and consider them to be approximately constant with time during the course of the entire period of the forecast. However, in a number of cases, due to the dependence on temperature, they can change significantly. The $\overline{\zeta}$ function does not satisfy

the "standardness" condition and therefore it is desirable that it be computed in each time interval in such a way that there be accurate satisfaction of expression (19). The latter is equivalent to the substitution of expressions following from (20) into equations (22) and (23),

$$\ln\bar{\zeta} = -\frac{gH}{RT},$$

$$\frac{1}{\bar{\zeta}}\frac{\partial\bar{\zeta}}{\partial s} = -\frac{g}{RT}\frac{\partial H}{\partial s} + \frac{gH}{RT^2}\frac{\partial T}{\partial s} \quad (s = x,\ y),$$

and the use of these equations in the following form:

$$\frac{\partial u}{\partial t} + u\frac{\partial u}{\partial x} + v\frac{\partial u}{\partial y} + \frac{1}{\zeta^* - \zeta_{op}}(\omega - \sigma\omega^*)\frac{\partial u}{\partial \sigma} = lv -$$

$$-\frac{RT}{\exp\left\{-\frac{gH}{RT}\right\} + \zeta_1}\frac{\partial \zeta_1}{\partial x} - g\zeta_1 \exp\left\{\frac{gH}{RT}\right\}\frac{\partial H}{\partial x} - \frac{gH}{T}\frac{\partial T}{\partial x} + \tag{24}$$

$$+\underline{\frac{gH}{T}\zeta_1 \exp\left\{\frac{gH}{RT}\right\}\frac{\partial T}{\partial x}},$$

$$\frac{\partial v}{\partial t} + u\frac{\partial v}{\partial x} + v\frac{\partial v}{\partial y} + \frac{1}{\zeta^* - \zeta_{op}}(\omega - \sigma\omega^*)\frac{\partial v}{\partial \sigma} = -lu -$$

$$-\frac{RT}{\exp\left\{-\frac{gH}{RT}\right\} + \zeta_1}\frac{\partial \zeta_1}{\partial y} - g\zeta_1 \exp\left\{\frac{gH}{RT}\right\}\frac{\partial H}{\partial y} - \frac{gH}{T}\frac{\partial T}{\partial y} + \tag{25}$$

$$+\underline{\frac{gH}{T}\zeta_1 \exp\left\{\frac{gH}{RT}\right\}\frac{\partial T}{\partial y}}.$$

[op = oro]

On the right-hand sides of equations (24) and (25), as before in (6) and (7), there are terms with $\partial H/\partial x$ and $\partial H/\partial y$, which after transformation became approximately two orders of magnitude smaller, since they were multiplied by $\bar{\zeta_1}/\zeta$. In place of the former terms with $\partial\zeta^*/\partial x$ and $\partial\zeta^*/\partial y$, after transformation their analogues, terms with $\partial\zeta_1/\partial x$ and $\partial\zeta_1/\partial y$, appeared; their values were also reduced by two orders of magnitude. In both equations two other terms appeared, these being dependent on the horizontal temperature gradients; the last (underlined) terms, which contain the factors ζ_1/ζ have the order of magnitude 10^{-5} and they can be neglected.

Thus, here the equations of motion were transformed to a form convenient for taking into account orography in numerical weather forecasts. For this purpose it is necessary that equations (6), (7) be replaced by equations (24), (25).

With respect to the derivatives of x and y in the advective terms for u, v, T in equations (6)-(10), they also experience certain changes in the σ-system. A compensation of the corresponding changes in the advection of meteorological functions enters into the terms taking into account vertical transfer, and although these values are not so significant as in a case with a pressure gradient, they can attain 100% of all the advection and they cannot be neglected. (The computation of advective terms is also somewhat complicated.) One important practical conclusion follows from what has been said: in a σ-coordinate system over mountainous regions in the equations of motion it is impossible to neglect the terms representing the vertical transfer of wind velocity.

The exclusion of derivatives of total pressure ζ^* and transformation to the deviations ζ_1^* together with (6) and (7) is also possible in the other equations. For example, equation (12) can be transformed and used in the following form:

$$\frac{\partial \zeta_1^*}{\partial t} = \left(1 - \frac{\gamma_a h \overline{\zeta^*}}{\overline{\zeta^* T_h}}\right) w_h - \left(u_h \frac{\partial \zeta_1^*}{\partial x} + v_h \frac{\partial \zeta_1^*}{\partial y}\right) + \\ + \frac{g \overline{\zeta^*}}{R \overline{T_h}} \left(u_h \frac{\partial h}{\partial x} + v_h \frac{\partial h}{\partial y}\right); \tag{12_1}$$

and accordingly in each time interval the ζ_1^* field is computed.

Now we will discuss the method for computing the initial values of the meteorological elements required in forecasting with use of the transformed equations. The surface $\zeta_{oro} = 0.7$ can be selected for taking into account orography over Europe. In our σ-coordinate system this corresponds to the equation $\sigma = 0$. The following surfaces are introduced: a) $\sigma = 1$, coinciding with the lower boundary of the atmosphere and b) $\sigma = 0.5$, lying in the interval between the earth and the 700-mb isobaric surface.

After objective analysis, which is usually carried out in an isobaric coordinate system, it is necessary to compute the initial grid fields (values at the grid points of intersection) of temperature T and pressure ζ on the two mentioned surfaces and H on the surface $\sigma = 0.5$.

First we will discuss computations of initial data at the earth's surface. If H_k and H_{k+1} are the heights of two adjacent working isobaric surfaces at a particular "node vertical" and at the same time h falls in the range

$$H_{k+1} \leqslant h \leqslant H_k, \tag{26}$$

then we have

$$\dot{T}_h = T_k + \gamma_k (H_k - h), \quad \gamma_k = \frac{T_{k+1} - T_k}{H_k - H_{k+1}}. \tag{27}$$

Formula (27) is used when $H_k = H_{700}$, $H_{k+1} = H_{850}$ and also when $H_k = H_{850}$, $H_{k+1} = H_{1000}$. If $h < H_{1000}$, then the T_k value is computed by means of extrapolation from the surface $\zeta = 1$ using a formula similar to (27) with the

mean value γ in the layer situated between the surfaces $\zeta = 1$ and $\zeta = 0.85$.

Surface pressure at the points of grid intersection under condition (26) is computed using the formula

$$\zeta^* = \zeta_k e^{\frac{g(H_k - h)}{RT_{cp}}}, \tag{28}$$

[cp = mean] where T_{mean} is the mean temperature in the air layer lying between the earth and the k-th working surface. This same formula is used if $H_k = H_{1000} > h$; here h can be both positive and negative.

Proceeding to the initial data on the surface $\sigma = 0.5$, we first compute the $\zeta_{\sigma = 0.5}$ values using a formula following from (15):

$$\zeta_{\sigma = 0,5} = 0,5\,(\zeta^* + \zeta_{op}). \tag{29}$$

[op = oro]

Then, using the integrated equation of statics (5) and interpolation of temperature, taking into account the mean vertical gradients in individual layers, with $\zeta_{k+1} \geqslant \zeta_{\sigma = 0.5} \geqslant \zeta_k$ we obtain

$$H_{\sigma = 0,5} = H_k - \frac{\bar{R}T_k}{\alpha g} \ln \frac{\zeta_{\sigma = 0.5}}{\zeta_k}, \tag{30}$$

$$T_{\sigma = 0,5} = T_k + \gamma_k (H_k - H_{\sigma = 0,5}),$$

where

$$\alpha = 1 - \frac{R\gamma_k}{2g} \ln \frac{\zeta_{\sigma = 0,5}}{\zeta_k},$$

ζ_k can be equal to 0.85 or 0.7 and ζ_{k+1} to 1.0 or 0.85 respectively.

Then, using formula (19), we compute the main pressure values at the surfaces $\sigma = 1$ and $\sigma = 0.5$:

$$\bar{\zeta} = \exp\left\{-\frac{gh}{RT_h}\right\}, \tag{31}$$

$$\bar{\zeta}_{\sigma = 0,5} = \exp\left\{-\frac{gH_{\sigma = 0,5}}{RT_{\sigma = 0,5}}\right\},$$

and their small deviations $\zeta_1^* = \zeta^* - \bar{\zeta}^*$,

$$\zeta_{1,\,\sigma = 0,5} = \zeta_{\sigma = 0,5} - \bar{\zeta}_{\sigma = 0,5}. \tag{32}$$

Now we have everything necessary for generalization of the quasi-implicit forecasting scheme presented in [4, 5] for the case of allowance for orography.

In the variant of the scheme with allowance for orography at the end of each time interval simple preparations are made for calculations in the next interval: the $\zeta_{\sigma=0.5}$ fields are computed using formula (29), $\bar{\zeta}^*$ and $\zeta_{\sigma=0.5}$ are computed using formula (31), $\zeta_{1,\sigma=0.5}$ using formula (32).

Otherwise the computations are carried out using the former scheme [3-5]. The only significant complication of the computations is with use of the second (fine) grid with "telescoping" over mountainous regions. Here it is also necessary to have a high-speed electronic computer.

The author expresses appreciation to L. S. Gandin for discussion of the problem, stimulating the carrying out of this study.

BIBLIOGRAPHY

1. Gandin, L. S., Dubov, A. S., CHISLENNYYE METODY KRATKOSROCHNOGO PROGNOZA POGODY (Numerical Methods for Short-Range Weather Forecasting), Leningrad, Gidrometeoizdat, 1968.

2. Krichak, S. O., "Allowance for Orography in a Baroclinic Prognostic Model Using the Full Equations of Hydrodynamics in a σ-Coordinate System," TRUDY GIDROMETTSENTRA SSSR (Transactions of the USSR Hydrometeorological Center), No 196, 1978.

3. Romov, A. I., "Numerical Modeling of Dynamics of Atmospheric Fronts," IZVESTIYA AN SSSR, FIZIKA ATMOSFERY I OKEANA (News of the USSR Academy of Sciences, Physics of the Atmosphere and Ocean), Vol 13, No 6, 1977.

4. Romov, A. I., "Scheme for Regional Numerical Weather Forecasting in a Combined Coordinate System With Telescopic Allowance for Interaction of Processes of Different Scales," TRUDY UkrNIGMI (Transactions of the Ukrainian Scientific Research Hydrometeorological Institute), No 154, 1977.

5. Romov, A. I., Lev, T. D., Kapitonova, V. A., "Quasi-implicit Scheme for Numerical Forecasting of Averaged Meteorological Elements," TRUDY UkrNIGMI, No 167, 1979.

6. Kasahara, A., "Various Vertical Coordinate Systems Used for Numerical Weather Prediction," MON. WEATHER REV., Vol 102, No 7, 1974.

7. Kurihara, Y., "Note on Finite Difference Expressions for the Hydrostatic Relation and Pressure Gradient Force," MON. WEATHER REV., Vol 96, No 9, 1968.

8. Phillips, N., "A Coordinate System Having Some Special Advantage for Numerical Forecasting," J. METEOROL., Vol 14, No 2, 1957.

9. Shuman, F. G., Hovermale, I. B., "An Operational Six-Layer Primitive Equation Model," J. APPL. METEOROL., Vol 7, No 4, 1968.

10. Smagorinsky, J., Strickler, R. F., Sangster, W. E., Manabe, S., Holloway, J. L., Hembree, G. D., "Prediction Experiment With a General Circulation Model," TRUDY MEZHDUNARODNOGO SIMPOZIUMA PO DINAMIKE KRUPNOMASSHTABNYKH ATMOSFERNYKH PROTSESSOV (Transactions of the International Symposium on Dynamics of Macroscale Atmospheric Processes), Moscow, 23-30 June 1965, Moscow, Nauka, 1967.

UDC 551.509.313

THE UPPER BOUNDARY CONDITION IN THE PROBLEM OF NUMERICAL FORECASTING OF METEOROLOGICAL ELEMENTS

Moscow METEOROLOGIYA I GIDROLOGIYA in Russian No 9, Sep 79 pp 25-33

[Article by V. A. Gordin and B. K. Dolmatov, USSR Hydrometeorological Scientific Research Center, submitted for publication 12 January 1979]

Abstract: For two variants of the linearized system of full equations in atmospheric dynamics in a p-coordinate system the authors have derived the boundary conditions for full absorption of waves passing through the upper boundary from the prognostic region. A similar boundary condition was derived for the difference analogue -- a variant of the operational prognostic model developed at the USSR Hydrometeorological Center. Numerical experiments demonstrated an improvement in the quality of the forecast when using this condition instead of the traditional condition.

[Text] Introduction. As is well known, baroclinic prognostic models of the atmosphere require the formulation of a correct boundary condition at the upper boundary of the prognostic region [9, 10, 14]. The best source of information for formulating such a boundary condition could be "splicing" with processing transpiring at altitudes considerably exceeding the prognostic (15-20 km) altitudes. Unfortunately, models of these processes have not been developed adequately and in the very near future one should not count on this source of information.

At the present time the condition most used for numerical models in a p-coordinate system (and also a number of others) when $p = p_{up}$ is the corollaries from the condition $\tau = 0$ when $p = 0$, where $\tau = dp/dt$, p_{up} is the upper computation level, whose correctness for the differential problem is validated using the conservation laws [9]. The correctness of such conditions for difference schemes is checked empirically [3]. However, these

corollaries are not entirely validated physically; in addition, they lead to the reflection of waves from the upper computation level [17].

In this study we propose use of the upper boundary condition of the type of total absorption of waves emerging from the prognostic region. This boundary condition is formulated for a specific linearized system of equations, differential or difference. Such a boundary condition is natural, taking into account that the points belonging to the upper computation level in no way differ from all the others and therefore there is no additional physically sound condition and no reflection of waves should occur at this level.

In order to clarify the physical sense of the total absorption condition we will examine the one-dimensional wave equation $u_{tt} = u_{xx}$.

The behavior of solution of this equation in the segment [0,1] is shown schematically in Fig. 1. As a comparison we have also given solutions with the same initial data, but with the Dirichlet and Neumann boundary conditions. The figure shows that with the Dirichlet and Neumann conditions there is reflection from the boundaries of the segment, which with solution of more complex equations can occur simultaneously with an intensification of fictitious waves. With respect to the total absorption conditions, in this case with $t \geqslant 1$, $x \in [0, 1]$ the solution $u(t, x) = 0$, that is, the same as if there was solution of the Cauchy problem with initial data continued indefinitely. In other words, there are no reflections at the points $x = 0; 1$.

We note that A. Sommerfeld was evidently the first to investigate the radiation condition at infinity for the multidimensional wave equation; this condition is close in its physical sense to the total absorption condition.

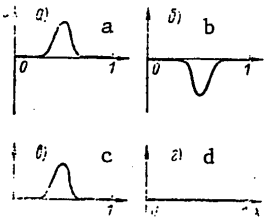

Fig. 1. Behavior of solution of wave equation $u_{tt} = u_{xx}$ in segment [0, 1] with different boundary conditions. a) $u(0, x)(u_t(0, x) = 0)$, b) $u(1, x)$ with Dirichlet conditions, c) $u(1, x)$ under Neumann conditions, d) $u(1, x)$ with total absorption conditions $u_x(t, 0) = u_t(t, 0)$, $u_x(t, 1) = -u_t(t, 1)$.

The total absorption conditions (under different names) were obtained independently in the studies of A. F. Bennet [14], M. Beland and T. Warn [13], and in the most general case, by one of the authors [4, 6]. Conditions of such a type have attracted the attention of both meteorologists [5, 7, 15, 18] and specialists in other fields (see bibliography to [15]).

In this paper we have derived the total absorption condition for a linearized baroclinic model of the atmosphere (#1) and for its difference analogue -- a six-level hemispherical prognostic model [3] used in an operational regime at the USSR Hydrometeorological Center (#2).

Similar considerations are also possible for other prognostic models.

In #3 we give the results of numerical experiments in which the total absorption condition is compared with the traditional condition.

#1. Total Absorption Condition for Differential Problem

As a prognostic model we will examine the following system of equations in a p-coordinate system [3] (the notations are those usually employed):

$$u_t + uu_x + vu_y + \tau u_p = lv - \Phi_x; \tag{1}$$

$$v_t + uv_x + vv_y + \tau v_p = -lu - \Phi_y; \tag{2}$$

$$u_x + v_y + \tau_p = 0; \tag{3}$$

$$T = -pR^{-1}\Phi_p; \tag{4}$$

$$T_t + uT_x + vT_y = RT(\gamma_a - \gamma)\, p^{-1} g^{-1} \tau. \tag{5}$$

In order to obtain the total absorption condition we will examine the following linearized system:

$$u_t = lv - \Phi_x; \tag{1'}$$

$$v_t = -lu - \Phi_y; \tag{2'}$$

$$\Phi_{pt} = -\varkappa\tau, \tag{6}$$

where $\varkappa = R^2T(\gamma_a - \gamma)p^{-2}g^{-1} > 0$.

These equations, together with (3), form a closed system of linear differential equations which we will henceforth denote by (D).

In order to investigate the correctness of the boundary conditions with $p = p_{up} > 0$ and in order to derive the boundary conditions for total absorption for the system (D), adhering to [6, 11], using the integral Fourier transforms $F_{\substack{x\to\xi\\ y\to\eta}}$ and Laplace transform $L_{t\to q}$, we transform the system (D) to an ordinary differential equation.

With zero initial data from (1') and (2') it follows that

$$u = -i(\xi q + l\eta)(q^2 + l^2)^{-1}\Phi, \qquad v = -i(\eta q - l\xi)(q^2 + l^2)^{-1}\Phi.$$

Substituting these expressions into equations (3) and (6) and excluding the function, we obtain

$$\frac{d^2\tau}{dp^2} = \varkappa \frac{\xi^2+\eta^2}{q^2+l^2}\tau. \tag{7}$$

In order to obtain the total absorption conditions for the system (D) it is necessary, in accordance with [6], to find a fundamental system of solutions for (7). In this case $\varkappa = \varkappa(p)$ and is dependent on the stratification assumed in the model. The simplest, evidently, is the case

a) $\varkappa = \text{const}$.

A more complex case, but on the other hand, more corresponding to reality, is

b) $\varkappa = c^2 p^{-2}$, $c = \text{const}$.

Such a stratification was assumed, in particular, in [3].

In both cases the fundamental system of solutions is easily found, and adhering to [6], the total absorption condition for (7) can be obtained in the form

$$\frac{d\tau}{dp}(p_в) = \alpha(q, \xi, \eta_l)\,\tau(p_в), \tag{8}$$

where $\alpha(q, \xi, \eta)$ is a function called the symbol of the boundary operator [1],

$$\alpha(q, \xi, \eta) = \begin{cases} \varkappa^{1/2}(\xi^2+\eta_l^2)^{1/2}(q^2+l^2)^{-1/2} & \text{in case a)} \\ p_в^{-1}\left[\frac{1}{2} + \sqrt{\frac{1}{4} + c^2\frac{\xi^2+\eta^2}{q^2+l^2}}\right] & \text{in case b).} \end{cases}$$

Using the inverse integral transforms [2, 6, 11], in final form we obtain the total absorption conditions

$$a)\ \frac{\partial\tau}{\partial p}(t, x, y, p_в) = 4\pi \int_0^t \int_{R^2} [(x-X)^2+(y-Y)^2]^{-1/2} J_0[l(t-T)] \times$$

$$\times \left(\frac{\partial^2}{\partial X^2} + \frac{\partial^2}{\partial Y^2}\right)\tau(T, X, Y, p_в)\,dX\,dY\,dT.$$

$$б)\ \frac{\partial\tau}{\partial p}(t, x, y, p_в) = 16\pi c^2 \int_{K_{x,y,t}} L(x-X, y-Y, t-T) \times$$

$$\times \tau(T, X, Y, p_в)\,dT\,dX\,dY,$$

where

$$K_{x,y,t} = \{(X, Y, T) \mid (x-X)^2+(y-Y)^2 < 4c^2(t-T)^2\},$$

$$L = f(x, y, t) - l\int_0^{\sqrt{t^2-(2c)^2(x^2+y^2)}} f(x, y, \sqrt{t^2-u^2})\,J_1(lu)\,du,$$

$$f = \left[(2c)^{-2}\frac{\partial^2}{\partial t^2} - \frac{\partial^2}{\partial x^2} - \frac{\partial^2}{\partial y^2}\right]^2 \chi\,(4c^2t^2 - x^2 - y^2)[t - (x^2+y^2)^{1/2}\,(2c)^{-1}],$$

J_0, J_1 are Bessel functions.

The total absorption boundary condition, thus, is not local; integral operators enter into it. Integration occurs over an infinite region. With increasing distance from the point x, y, t the kernels of the integral operators decrease -- the distant points enter into the boundary condition with a small weight.

The total absorption condition for a more realistic case (b) is also more physically sound -- integration does not occur over the entire half-space, but only along the "inverse light cone"; K is a situation characteristic for hyperbolic problems [5, 7]. This is attributable to the fact that in such problems perturbations are propagated with a finite velocity.

It follows from the evaluations for the Bessel functions that there is a power-law decrease of the kernels in the convolutions. A close result is also obtained in a difference case (with replacement of the integrals in the convolutions by infinite sums). In order to decrease the number of terms, and accordingly, in order to decrease the volume of the required memory and to accelerate computations we used the special procedures described below.

#2. Total Absorption Condition for Difference Problem

A description of an operational hemispherical model is given in [3] and we will employ the notations given there. As in #1, carrying out linearization in the difference system, we obtain

$$\overline{u}_t - l\overline{v}^t = -\overline{\Phi}^y_x;$$

$$v_t + l\overline{u}^t = -\overline{\Phi}^x_y; \qquad (P)$$

$$\frac{\tau(p+\Delta p)-\tau(p)}{\Delta p} = -\frac{1}{2}\{|\overline{[u(p)+u(p+\Delta p)]}^y_x + \overline{[v(p)-v(p+\Delta p)]}^x_y|;$$

$$\left[\frac{\Phi(p+\Delta p)-\Phi(p)}{\Delta p}\right]_t = -\frac{\varkappa}{2}[\tau(p)+\tau(p+\Delta p)].$$

Here, as in the model [3], it is assumed that the parameter of increase in a stereographic projection m = 1, and in contrast to the model, for simplification of the computations the time filter parameter $\nu = 0$. Applying the $Z_{t\to z}$ transform [8] and the Fourier transform to the system (P), making computations similar to those in #1, we obtain the system

$$\Phi(p+\Delta p)+\Phi(p)+b\tau(p+\Delta p)-b\tau(p)=0;$$

$$\Phi(p+\Delta p)-\Phi(p)+a\tau(p+\Delta p)+a\tau(p)=0,$$

where $a=\varkappa\Delta p\,\Delta t(z-z^{-1})^{-1}$; $b=h^2[(z-z^{-1})^2+\Delta t^2 l^2(z+z^{-1})^2]\times$

$\times[(z-z^{-1})\Delta p\,\Delta t S]^{-1}$, $S=2^{-1}(1-\cos 2\xi h\cos 2\eta h)$,

which can be rewritten in matrix form

$$\begin{pmatrix}\Phi(p+\Delta p)\\ \tau(p+\Delta p)\end{pmatrix}=B\begin{pmatrix}\Phi(p)\\ \tau(p)\end{pmatrix},\quad B=\begin{Vmatrix}\frac{a+b}{b-a}; & \frac{-2ab}{b-a}\\ \frac{-2}{b-a}; & \frac{a+b}{b-a}\end{Vmatrix}.$$

Assuming $\varkappa$ = const, we find the eigenvalues of the B matrix:

$$\lambda_{1,2}=(a+b\pm 2\sqrt{ab})(b-a)^{-1}\quad\text{and when}\quad |z|\gg 1\ |\lambda_1|>1>|\lambda_2|$$

The upper boundary condition, in a general case, is written in the form

$$(A_1,\ A_2)\begin{pmatrix}\Phi(p_n)\\ \tau(p_n)\end{pmatrix}=g(t,\ x,\ y), \tag{9}$$

[B = up(per)]

where g is some function, $A_{1,2}$ are difference operators, which like the operator (8) of the differential problem are not mandatorily local. The condition on the Shapiro-Lopatinskiy boundary operators A_1, A_2 [1, 11, 16], guaranteeing the correctness of the mixed boundary problem (P)-(9) (this means that with any initial data and any function g a solution of the problem exists and is continuously dependent on the initial data), is a nonorthogonality of the row of symbols (α_1, α_2) to the eigenvector of the matrix B, corresponding to α_2. The total absorption condition [4-7] involves an orthogonality of the row (α_1, α_2) to the eigenvector of the B matrix corresponding to α_1 (the first condition obviously follows from the second). For example, the first row of the matrix $(B-\lambda_1 E)$ satisfies this second condition:

$$(\alpha_1,\ \alpha_2)=\left(\frac{-2\sqrt{ab}}{b-a};\ \frac{-2ab}{b-a}\right)$$

or, proceeding to the normalization $\alpha_2=-1$, $\alpha_1=-(ab)^{-1/2}$. As a result, the total absorption boundary condition has the form

[B = up(per)]

$$\tau(p_n)=A_1\Phi(p_n).$$

The A_1 operator is the difference operator for an infinite number of points; its symbol α_1 is the product of the function of z and the function of ξ and η. In order to realize the total absorption condition on an electronic computer it is necessary to approximate the α_1 operator by a difference operator with the least possible number of points.

For an economical inverse Z-transformation [8] of the cofactor in α_1, dependent on z, we will use the Pade approximation, which has recently found application in different fields of mathematics and applied problems [12]. In this case the approximated function is replaced by a rational function (in our case this point is $z^{-1} = 0$) having the same derivatives to the order of magnitude N_1 as the approximated function.

The cofactor in α_1, dependent on ξ and η, is approximated by a sum in the form

$$\sum_{k,l} s_{kl} \exp(i\xi kh_x + i\eta lh_y).$$

These approximations are described in greater detail in the Appendix. After these approximations the total absorption condition, in accordance with the convolution theorem, assumes the form

$$\tau(p_s) = [1 - Q(z^{-1})]\,\tau(p_s) + P(z^{-1}) \sum_{k,l} s_{kl} \exp(i\xi kh_x + i\eta lh_y)\,\Phi(p_s)$$

or

$$\tau(t, x, y, p_s) = -\sum_{n=1}^{N} q_n \tau(t - n\Delta t, x, y, p_s) + \tag{10}$$

$$+ \sum_{n=0}^{M} p_n \sum_{k,l} s_{k,l}\,\Phi(t - n\Delta t, x - kh_x, y - lh_y, p_s).$$

The total absorption condition was used specifically in such a form in the model.

Thus, the total absorption boundary condition determines the vertical velocity value τ at the point of the spatial-temporal grid lying at the upper computation level (t, x, y, p_{up}) through the τ values at the preceding moments in time $t - n\Delta t$ and the geopotential values at this and preceding moments in time at the closest points also lying at the upper computation level. The method for computing the corresponding weights q_n, p_n, s_{kl} is described in the Appendix.

#3. Results of Numerical Experiments and Conclusions

Tests of the described approach were carried out using a regional variant of the model [3]. As the initial data we used archival data for 0000 hours on 1-10 April 1977 for the territory including the North Atlantic, Europe, North Africa, Near East, Central Asia and Western Siberia.

The interval for the horizontal variables was 300 km, the time interval was 12 minutes.

With replacement of the traditional boundary condition at the upper boundary by the condition of total absorption of the emerging waves there were appreciable changes in the prognostic fields at all levels. In particular,

due to the absence of reflection from the upper boundary there was a decrease in the kinetic energy, there was in increase in divergence of the wind field, artificially understated by the traditional condition [3].

Table 1

1 Срок прогноза	2 Уровень, мб											
	1000	850	700	500	300	100	1000	850	700	500	300	100
	3 Коэффициент корреляции						4 Относительная ошибка					
5 3 сут	0,01	0,02	0,03	0,02	0,02	0,04	−0,03	−0,04	−0,05	−0,04	−0,03	+0,04
4 сут	0,00	0,01	0,02	0,02	0,02	0,04	−0,04	−0,05	−0,07	−0,07	−0,03	+0,05

KEY:

1. Time of forecast
2. Level, mb
3. Correlation coefficient
4. Relative error
5. days

Table 1 gives the improvements (the correlation coefficient increases, the relative error usually decreases) due to use of the total absorption condition at the upper boundary in place of the traditional condition in forecasting for three and four days in advance. All the evaluations, except for the relative error at 100 mb, are better in case of use of the total absorption condition, which evidently must be considered preferable.

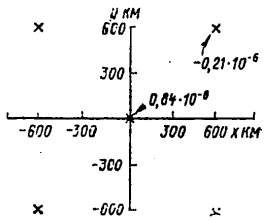

Fig. 2. Overlay and weights (mb·sec/m^2) of operator for horizontal variables approximating Π operator.

The possible ways to bring about further improvement in approximation of the total absorption condition (9) are: 1) careful selection of the optimum (for example, in the statistical sense [4, 5]) coefficients of the boundary operator s_{kl}; 2) allowance for smoothing ($\nu \neq 0$) in formulating the boundary condition (9); 3) shifting to variant (b) in the case of linearization of the model, that is, to that which is used in model [3]. For this it is necessary to find a fundamental system of solutions of a second-degree difference equation with variable coefficients, which is a complex problem.

A more detailed discussion of the mathematical and computational aspects will be given in a separate publication.

The authors express appreciation to M. S. Fuks-Rabinovich for constant attention to the study and useful consultations.

Appendix

Method for computing the coefficients in the total absorption boundary operator for emerging waves for difference baroclinic model

For the inverse Z- transformation of the symbol $(ab)^{-1/2}$ it is necessary, in accordance with [8], to carry out expansion into a Laurent series with $z = \infty$.

We have
$$(ab)^{-1/2} = \Pi (1 - z^{-2})(1 - 2\mu z^{-2} + z^{-4})^{-1/2} =$$
$$= \Pi \left\{ 1 + \sum_{k=1}^{\infty} z^{-2k} [P_k(\mu) - P_{k-1}(\mu)] \right\},$$

where
$$\Pi = S^{1/2} \varkappa^{-1/2} h^{-1} (1 + \Delta t^2 l^4)^{-1/2}, \quad \mu = (1 - \Delta t^2 l^2)(1 + \Delta t^2 l^2)$$

P_k is the k-th Legendre polynomial. The coefficients of the power series in even powers of z^{-1} with $\mu = 0.97$ decrease, but extremely slowly. The number of terms in the Laurent series to which we limit ourselves is equal to the number of time layers in the total absorption boundary condition and therefore, due to the limitations on the electronic computer memory resources and speed it cannot be too great. At the same time, limitation only to the one first term of the expansion was too approximate.

Accordingly, for approximation of the expression in braces we made use of the Pade approximation [12, 19]
$$\left\{ 1 + \sum_{k=1}^{\infty} z^{-2k} [P_k(\mu) - P_{k-1}(\mu)] \right\} \approx P^n(z^{-2}) / Q^m(z^{-2}),$$

where P^n, Q^m are polynomials of the powers n and m, $Q^m(0) = 1$, and the approximate equation, by definition of the Pade approximation, results in a coincidence of the Laurent expansions to the number $N_1 = n + m$ inclusive; in the case m = 0 this is simply a cutoff of an infinite series.

As a measure of the approximation error we used
$$\varepsilon = \sum_{N_1}^{N_2} a_k^2,$$

where a_k is the difference of the Laurent coefficients with the numbers k of the approximated function and its approximation. In the evaluations we assumed $N_2 = 30$. A good result was obtained with m = n = 2: $\varepsilon = 0.006$.

We note once again that n + 1 and m + 1 are the numbers of the time layers of the H and τ functions which enter into the boundary condition. If m = 0, that is, the Pade approximation is not used, then it is necessary that

$n \geqslant 5$, which would lead to insuperable difficulties in application.

In order to obtain the coefficients of the polynomials P^n and Q^m we used the program which we wrote and a more general program carried out using the description in [15] and

$$P^2 = 1{,}0000 - 1{,}9925\, z^{-2} + 0{,}9997\, z^{-4}, \quad Q^2 = 1{,}0000 - 1{,}9777\, z^{-2} + 0{,}9997\, z^{-4}.$$

The expansion of the $\Pi(\xi, \eta)$ function into a double Fourier series can be carried out, for example, numerically, using the so-called fast Fourier transform. Only the coefficients $s_{k\ell}$ with a sum of the indices a multiple of four are different from zero (this can also be demonstrated analytically). With a cutoff of the series, which is necessary due to restrictions on the electronic computer resources, the sum of the $s_{k\ell}$ coefficients, that is, the value of the cut-off series with $\xi = \eta = 0$, is different from zero, whereas $\Pi(0,0) = 0$. Thus, the approximation of the Π symbol in the zero harmonic is impaired. It is possible to approximate Π in a form optimum in the statistical sense with the limitation that the symbol of the approximating operator becomes equal to zero when $\xi = \eta = 0$ [4, 5].

In the cited experiments we limited ourselves to a very simple overlay of five points (see Fig. 2); the weights at the lateral points are -1/4 of the weight of the central point, which was selected empirically and in the final experiments was selected equal to $0.84 \cdot 10^{-6}$.

BIBLIOGRAPHY

1. Agranovich, M. S., "Boundary Problems for Systems of First-Degree Pseudo-differential First-Order Operators," USPEKHI MATEMATICHESKIKH NAUK (Advances in the Mathematical Sciences), No 1, p 24, 1969.

2. Beytmen, G., Erdeyn, A., TABLITSY INTEGRAL'NYKH PREOBRAZOVANIY (Tables of Integral Transforms), Vol I, Moscow, Nauka, 1969.

3. Belousov, S. L., et al., "Operational Model of Numerical Forecasting of Meteorological Elements for the Northern Hemisphere," TRUDY GIDROMETTSENTRA SSSR (Transactions of the USSR Hydrometeorological Center), No 212, 1978.

4. Gordin, V. A., "Some Mathematical Problems in Hydrodynamic Forecasting," Tezisy DOKLADOV NA II VSESOYUZNOY KONFERENTSII MOLODYKH SPETSIALISTOV GIDROMETSLUZHBY SSSR (Summaries of Reports at the Second All-Union Conference of Young Specialists of the USSR Hydrometeorological Service), Obninsk, 1976.

5. Gordin, V. A., "Some Mathematical Problems in Numerical Hydrodynamic Forecasting," DOKLADY NA II VSESOYUZNOY KONFERENTSII MOLODYKH SPETSIALISTOV GIDROMETSLUZHBY SSSR (Reports at the Second All-Union Conference of Young Specialists of the USSR Hydrometeorological Service), Obninsk, 1977.

6. Gordin, V. A., "Mixed Boundary Problem Simulating the Cauchy Problem," USPEKHI MATEMATICHESKIKH NAUK, Vol 33, No 5, 1978.

7. Gordin, V. A., "Mixed Boundary Problem for a Barotropic Atmospheric Model," TRUDY GIDROMETTSENTRA SSSR, No 196, 1978.

8. Dech, G., RUKOVODSTVO K PRAKTICHESKOMU PRIMENENIYU PREOBRAZOVANIYA LAPLASA I Z-PREOBRAZOVANIYA (Manual on the Practical Use of the Laplace Transform and the Z-Transform), Moscow, Nauka, 1972.

9. Dikiy, L. A., TEORIYA KOLEBANIY ZEMNOY ATMOSFERY (Theory of Oscillations of the Earth's Atmosphere), Leningrad, Gidrometeoizdat, 1969.

10. Kibel', I. A., VVEDENIYE V GIDRODINAMICHESKIYE METODY KRATKOSROCHNOGO PROGNOZA POGODY (Introduction to Hydrodynamic Methods for Short-Range Weather Forecasting), Moscow, Gostekhizdat, 1957.

11. Shilov, G. Ye., MATEMATICHESKIY ANALIZ. VTOROY SPETSKURS (Mathematical Analysis. Second Special Course), Moscow, Nauka, 1965.

12. Baker, G. A., Jr., ESSENTIALS OF PADE APPROXIMANTS, Acad. Press, New York, 1975.

13. Beland, M., Warn, T., "The Radiation for Transient Rossby Waves," J. ATMOS. SCI., Vol 32, No 10, 1975.

14. Bennet, A. F., "Open Boundary Conditions for Dispersive Waves," J. ATMOS. SCI., Vol 33, No 2, 1975.

15. Engquist, B., Majda, A., "Boundary Condition," MATH. COMPUT., Vol 31, 1977.

16. Gustafsson, B., Kreiss, H.-O., Sundstrom, A., "Stability Theory of Difference Approximations for Mixed Initial Boundary Value Problems, II," MATH. COMPUT., Vol 26, 1972.

17. Kirkwood, E., Derome, J., "Some Effects of the Upper Boundary Condition and Vertical Resolution on Modeling Forced Stationary Planetary Waves," MON. WEATHER REV., Vol 105, No 10, 1977.

18. Miyakoda, K., Rosati, A., "One-Way Nested Grid Models: the Interface Conditions and the Numerical Accuracy," MON. WEATHER REV., Vol 105, No 9, 1977.

19. Starkard, Y., "Subroutine for Calculation of Matrix Pade Approximants," COMPUT. PHYS. COMM., Vol 11, 1976.

UDC 551.558.2

VERTICAL CURRENTS IN THE TROPOSPHERE

Moscow METEOROLOGIYA I GIDROLOGIYA in Russian No 9, Sep 79 pp 34-43

[Article by Candidate of Physical and Mathematical Sciences V. A. Shnaydman, Odessa Hydrometeorological Institute, submitted for publication 12 December 1978]

Abstract: Vertical currents in the troposphere are determined by solution of a differential equation derived from the vorticity equation, heat influx equation, continuity equation and equation of statics, in which the following are taken into account: advection of absolute vorticity, heat advection and frictional currents at the upper boundary of the planetary boundary layer. The latter are found from solution of a closed system of equations, including the equations of motion and the equation for the balance of kinetic energy of turbulence and semiempirical closing hypotheses. Standard aerosynoptic data are used as the initial data. The results of computations for specific synoptic situations are given. It is shown that frictional vertical currents, computed using the proposed method, agree better with the precipitation field than the currents determined using the the Dyubyuk formula.

[Text] Prognostic schemes using the full equations of hydrothermodynamics have now come into broad use. It is known that the main difficulty in applying these schemes is the filtering of meteorologically insignificant noise, which to the greatest degree exerts an influence on the values of two-dimensional divergence, and accordingly, vertical currents. The employed filtering methods for small-scale disturbances make it possible to devise prognostic schemes which are stable in computational respects and to obtain a reliable description of the geopotential and wind fields. However, use of these fields for computing differential characteristics of the type of divergence is accompanied by considerable errors. Therefore, the idea of

computing vertical currents using the vorticity equation, heat influx equation, continuity equation and equation of statics from the following differential equation remains acceptable for practical purposes:

$$(l\zeta)^2 \frac{\partial^2 \omega}{\partial \zeta^2} + \Delta\left[(lm)^2 \omega\right] = -R\zeta\Delta A_T - l\zeta^2 \frac{\partial A_\Omega}{\partial \zeta}; \tag{1}$$

where $l = 14{,}58 \cdot 10^{-5} \sin\varphi$; $\zeta = \frac{p}{1000}$, $\omega = \frac{d\zeta}{dt}$,

$$m^2 = R^2 T(\gamma_a - \gamma)/gl^2, \quad \Omega_a = l + \Omega_z = l + \left(\frac{\partial v}{\partial x} - \frac{\partial u}{\partial y}\right);$$

$$A_T = -\left(u\frac{\partial T}{\partial x} + v\frac{\partial T}{\partial y}\right), \quad A_\Omega = -\left(u\frac{\partial \Omega_a}{\partial x} + v\frac{\partial \Omega_a}{\partial y}\right).$$

Here p is pressure; T is temperature; u, v are the horizontal components of the wind velocity vector in a standard coordinate system; γ_a, γ are the dry adiabatic and geometric vertical temperature gradients; φ is latitude; R is the gas constant; g is the acceleration of gravity; ζ is reduced pressure; ω is isobaric vertical velocity; Ω_a, Ω_z is the vertical component of absolute and relative vorticity; m is the stability parameter; l is the Coriolis parameter; A_Ω, A_T is the horizontal advection of absolute vorticity and temperature; ω is isobaric vertical velocity.

With use of the diagnostic equation (1) it is possible to take into account the principal physical factors determining the field of vertical currents. In particular, this includes the advection of absolute vorticity and thermal advection.

For convenience in writing the computation algorithm equation (1) was written in the form

$$b^2\zeta^2 \frac{\partial^2 \omega}{\partial \zeta^2} + M^2 \Delta^{(d)}(a\omega) = F(x, y, \zeta), \tag{2}$$

where $b = l / l_0$, $a = (\gamma_a - \gamma)/(\gamma_a - \gamma_0)$;

$$M^2 = R^2 T(\gamma_a - \gamma_0)/gl_0^2 d^2;$$

$$F = -R\zeta\Delta A_T \left| l_0^2 - b\frac{\partial A_\Omega}{\partial \zeta} \right| l_0;$$

$$l_0 = 2\omega \sin\varphi_0; \qquad \varphi_0 = 45°; \qquad \gamma_0 = 0{,}65 \cdot 10^{-2}\ °C/м;$$

$\Delta^{(d)}\omega$ is the Laplace finite-difference operator with the interval d.

An important factor in writing an algorithm for computing vertical currents in the atmosphere is allowance for the planetary boundary layer near the underlying surface. Such an allowance can be made approximately using the

lower boundary condition for equation (1). We will assume that the lower boundary of the region, where equation (1) is used, coincides with the upper boundary of the boundary layer; the latter is some isobaric surface ζ_H. We will assume that on this surface the vertical currents are known and equal to ω_H. The algorithm for their computation is formulated on the basis of solution of the problem of the planetary boundary layer. As the upper boundary of the considered computation region we will assume the level of the second extremum of the vertical currents, situated in the lower stratosphere, to be approximately $\zeta = \zeta_h \approx 0.25$. Then the boundary conditions along the vertical are written in the following way:

$$\begin{gathered} \zeta = \zeta_H; \quad \omega = \omega_H; \\ \zeta = \zeta_h; \quad \frac{\partial \omega}{\partial \zeta} = 0. \end{gathered} \tag{3}$$

In order to substitute the boundary conditions in the horizontal plane we will make the assumption that on the surfaces bounding the region of computation of vertical currents the following relationship is correct

$$\omega(\zeta) = \omega_H + \frac{1}{l}\left[A_{\Omega h}(\zeta - \zeta_H) - \int_{\zeta_H}^{\zeta} A_\Omega(\zeta')\, d\zeta'\right], \tag{4}$$

that is, on the boundary surface we take into account only the dynamic processes caused by the advection of absolute vorticity. We feel that although expression (3) is approximate, it is nevertheless better than the stipulation of zero vertical currents at the limiting surface, since on the average the contribution of the dynamic factor to the formation of the field of vertical currents is predominant.

Now we will discuss the method for computing vertical currents at the upper boundary of the planetary boundary layer (PBL) or frictional currents (ω_H).

If we write the equations of motion with allowance for the turbulent terms, from them we find an expression for divergence and integrate within the limits of the boundary layer; for vertical currents at the upper boundary of the boundary layer we obtain

$$\omega_H = -\frac{g}{lp_{00}}\,\mathrm{rot}\,\vec{\tau}_0 - \frac{1}{l}\,\mathrm{rot}\int_1^{\zeta_H}\frac{d\vec{v}}{dt}\,d\zeta, \tag{5}$$

where p_{00} = 1000 mb is standard pressure at the earth, $\vec{\tau}_0$ is the vector of surface frictional shearing stress.

An evaluation of the terms in expression (4), obtained taking into account the $\vec{\tau}_0$ values, computed using the drag laws [2, 3, 8], indicated that the second term in (4) is an order of magnitude less than the first and therefore it can be assumed approximately that

$$\omega_H \cong -\frac{g}{lp_{00}}\,\mathrm{rot}\,\vec{\tau}_0. \tag{6}$$

The frictional shearing stress is computed using the semi-empirical theory of a baroclinic boundary layer [5, 6]. The computation algorithm provides for computation of the geostrophic friction coefficient ($\chi = v_*/c_g$, where $v_* = \sqrt{|\tau_0|/\rho}$) and the angle of deviation of the actual wind from the geostrophic wind near the underlying surface (α) as functions of the following parameters:

-- Rossby numbers $Ro = c_g/\mathfrak{l} z_0$;

-- stratification parameters $\mu = \frac{\lambda Q_0/c_p \rho}{l v_*^2}$; $\nu = \frac{\varkappa^4 \left(\frac{\partial \theta}{\partial z}\right)_H}{l^2}$;

-- baroclinicity parameters $\lambda_x = \frac{\lambda}{l^2}\frac{\partial T}{\partial x}$; $\lambda_y = \frac{\lambda}{l^2}\frac{\partial T}{\partial y}$.

Here v_* is dynamic velocity; Q_0 is the turbulent heat flow near the underlying surface; $(\partial\theta/\partial z)_H$ is the vertical gradient of potential temperature near the upper boundary of the boundary layer; c_g is the velocity of the geostrophic wind at the earth; z_0 is the roughness parameter; c_p is the specific heat capacity at constant pressure; ρ is air density at the earth; $\lambda = g/T$ is the buoyancy parameter; $\chi = 0.38$ is the Karman constant.

The developed computation method for the χ and α parameters is based on information determined directly in the prognostic model. In order to find the determining dimensionless parameters it is necessary to have information on geopotential and temperature at the main computation levels. In the first approximation for "restoring" the temperature field it is possible to use the equation of statics. Then for computing vertical currents it is sufficient to have data on the geopotential field, which at the present time is precomputed with an acceptable degree of accuracy [1].

In order to determine the thermal stratification parameters we will use the averaged dependence, proposed in [4], for the vertical gradient of potential temperature $\partial\theta/\partial z$ on height

$$\frac{\partial \theta}{\partial z} = -\frac{Q_0/c_p \rho}{\varkappa v_* z} + \left(\frac{\partial \theta}{\partial z}\right)_H \frac{z}{z_N}, \qquad (7)$$

where z_N is the height of the upper computation level in the layer where the vertical temperature profile is approximated by the cited dependence.

If for determining the stratification parameters μ and ν use is made of the temperature difference in the layers between the computation levels z_1 and $z_2(T_1 - T_2)$, z_3 and z_N $(T3 - T_N)$, the lower layer is within the limits of the boundary layer and the upper layer is directly over the upper boundary of the planetary boundary layer, the dependences for finding μ and ν will have the form

$$\mu = [M_2 (z_2^2 - z_1^2)/z_N^2 - M_1 (z_N^2 - z_3^2)/z_N^2]/[[1 - (z_3/z_N)^2] \ln (z_2/z_1) - - [(z_2^2 - z_1^2)/z_N^2] \ln (z_N/z_3)] \chi;$$
$$\nu = R_1 [M_2 \ln (z_2/z_1) - M_1 \ln (z_N/z_3)]/[[1 - (z_3/z_N)^2 \ln (z_2/z_1) - - [(z_2^2 - z_1^2)/z_N^2] \ln (z_N/z_3)], \quad (8)$$

where

$$M_1 = \lambda \varkappa^2 [\gamma_a (z_2 - z_1) - (T_1 - T_2)]/lC_g;$$
$$M_2 = \lambda \varkappa^2 [\gamma_a (z_N - z_3) - (T_3 - T_N)]/lC_g;$$
$$R_1 = 2 \varkappa^2 C_g/lz_N.$$

The value of the geostrophic friction coefficient μ included in the expression for χ is found in the process of an iteration procedure used in solution of a closed system of equations for determining the characteristics of the boundary layer.

Thus, for computing the parameters of the baroclinic planetary layer in the considered method use is made of the following information:
1) surface pressure field, from which the components and modulus of velocity of the geostrophic wind are computed;
2) mean temperature in the boundary layer, from which the components and modulus of the horizontal temperature gradient are found;
3) temperature drops in the lower and upper parts of the boundary layer, from which the thermal stratification parameters are determined;
4) values of the roughness and Coriolis parameters.

It is easy to show that the above algorithm is suitable when there is information only on the basic isobaric surfaces, that is, when using only standard aerosynoptic information. Such information was used in computations in this study. As the initial data we took the values of surface pressure and temperature, geopotential and temperature at the isobaric surfaces AT_{850} and AT_{700}. Using these data at the points of intersection of a regular grid we computed the velocity vector of the geostrophic wind at the earth, the Rossby number, the stratification and baroclinicity parameters. From solution of the closed system of equations we found the geostrophic friction coefficient, the angle of deviation of the actual wind from the geostrophic wind and the components of the vector of frictional shearing stress

$$\tau_{0x} = \rho \varkappa^2 \chi^2 C_g (u_g \cos \alpha - v_g \sin \alpha);$$
$$\tau_{0y} = \rho \varkappa^2 \chi^2 C_g (u_g \sin \alpha + v_g \cos \alpha). \quad (9)$$

Replacing the differential operator rot $\vec{\tau}_0$ by the difference operator, we computed the velocities of the vertical currents at the upper boundary of the boundary layer, which were related to the 850-mb level, that is, ζ_H was assumed equal to 0.85. The profile of vertical currents in the free atmosphere was determined by the ω values at the levels 700, 500 and 300 mb. At these levels we computed the values of the advection of absolute vorticity and temperature in a geostrophic approximation. The $\partial A_\Omega / \partial \zeta$ value in

the noted AT_{300}-AT_{250} layer was assumed equal to the derivative in the layer AT_{500}-AT_{300} and from this condition we computed the $A_{\Omega h}$ value, which was used only for the boundary contour of the region. Thus, the ω values on the boundaries of the region (lower and lateral) and the values of the determining physical factors (A_{Ω} and A_T) within the region were computed and it is possible to proceed to a determination of ω within the region at the considered isobaric surfaces 700, 500 and 300 mb. In this study it was assumed that a = 1, b = 1, d = 300 km, then $M^2 = 7.065$.

A numerical solution of equations (2) was found in the following way. After replacement of the derivatives of the vertical and horizontal coordinates by final differences equation (2) was solved in explicit form relative to the vertical velocity value at a point of intersection in the regular grid ω_{ijk}:

$$\omega_{ijk} = \beta_k \omega_{ij\,H} - \sum_{s=1}^{3} \alpha_{sk} [F_{ijs} - M^2 (\omega_{i+1,\,js} + \omega_{i-1,\,js} + \omega_{ij+1,\,s} + \omega_{ij-1,\,s})]. \quad (10)$$

The coefficients α_{sk} and β_k are given in Table 1.

Table 1

Values of the Constants α_{sk} and β_k

k	α_{sk}			β_k
	$s=1$	$s=2$	$s=3$	
1	$1{,}70 \cdot 10^{-2}$	$5{,}94 \cdot 10^{-3}$	$1{,}18 \cdot 10^{-3}$	$31{,}8 \cdot 10^{-2}$
2	$2{,}63 \cdot 10^{-3}$	$2{,}58 \cdot 10^{-2}$	$5{,}12 \cdot 10^{-3}$	$49{,}2 \cdot 10^{-3}$
3	$2{,}52 \cdot 10^{-4}$	$2{,}48 \cdot 10^{-3}$	$3{,}24 \cdot 10^{-2}$	$47{,}1 \cdot 10^{-4}$

The finding of vertical velocities for the entire region of determination was accomplished using an iteration procedure. If the required accuracy was stipulated $10^{-2} |\omega_{ijk}|_{max}$, the number of iterations, as a rule, did not exceed 10.

We will illustrate the effectiveness of use of the proposed method for vertical currents, taking into account the boundary layer effects in two cases of a cyclonic pressure field with a clearly expressed system of atmospheric fronts over the European territory of the Soviet Union. First of all, we compared the fields of actual and computed surface winds; these were found to be sufficiently close. Figure 1 illustrates the mentioned fields and the synoptic situation for 26 December 1976.

The similarity of the fields of computed and actual velocities of the surface wind vector gives basis for hoping that the computed frictional currents will reproduce the real fields of vertical velocities at the upper boundary of the boundary layer.

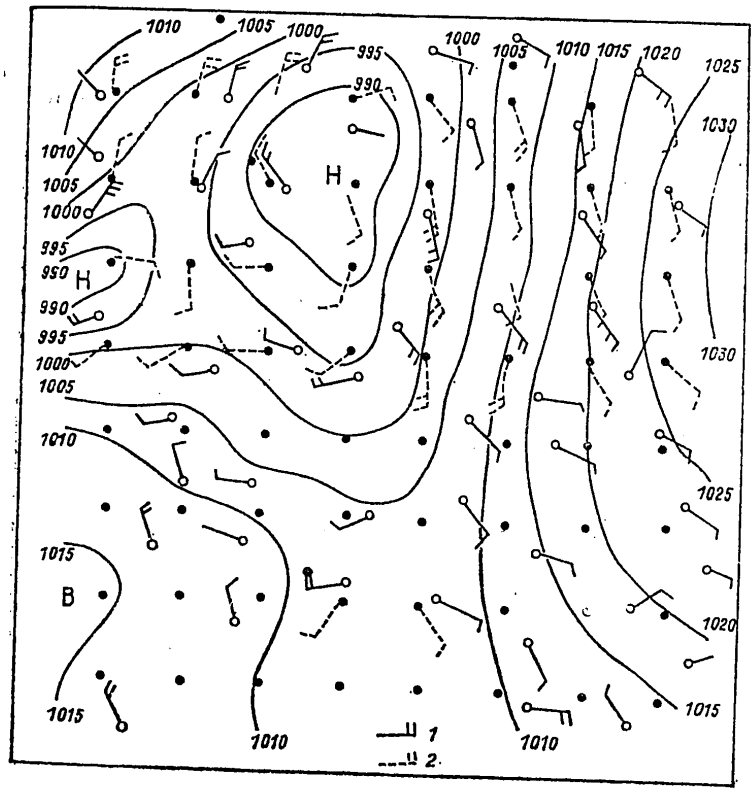

Fig. 1. Surface pressure field, actual (1) and computed (2) wind velocities at vane height on 26 December 1976. H = low

In order to compute the frictional vertical currents by solving a closed system of equations for the baroclinic boundary layer we found the components of the frictional shearing stress vector near the underlying surface for the points of intersection of a regular grid covering the European USSR with a 300-km interval. The frictional vertical currents were computed using expression (5) and the Dyubyuk formula with use of a constant turbulence coefficient equal to 10 m^2/sec. The roughness of the underlying surface at all points of intersection in a regular grid was stipulated as 10 cm.

We examined the sign of the frictional currents and the fact of falling or absence of precipitation. The results of the analysis are given in Table 2. The numerator indicates the percentage of recurrence of ascending and descending frictional currents in the presence and absence of precipitation, whereas the denominator gives the recurrence of cases of falling or absence of precipitation when there are ascending and descending frictional currents.

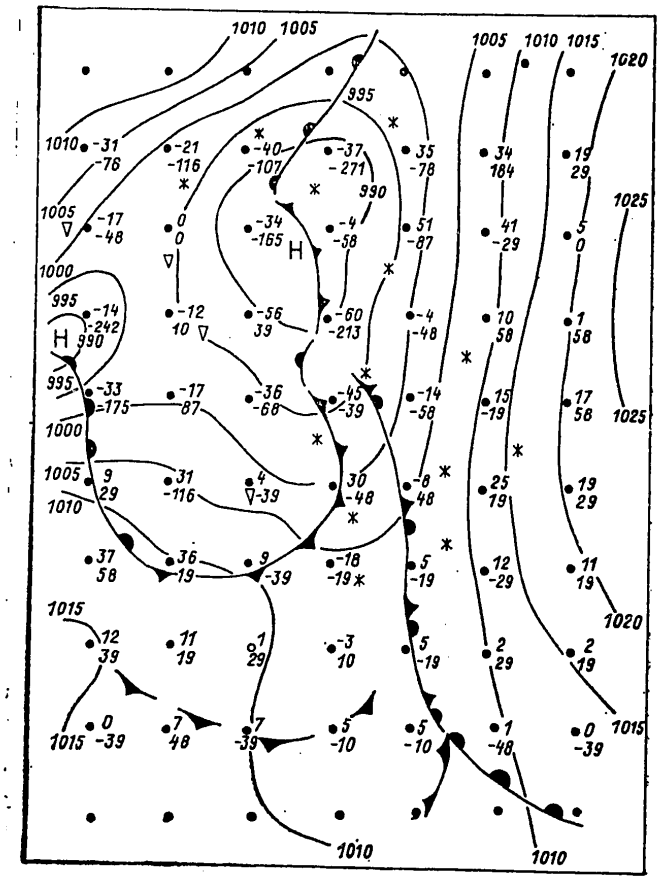

Fig. 2. Surface pressure field and frictional vertical currents on 26 December 1976. H = low

Table 2

Presence or Absence of Precipitation in Presence of Ascending and Descending Frictional Currents

Осадки 1	Восходящие 2		Нисходящие 3	
	ППС 4	Дюбюк 5	ППС 4	Дюбюк 5
6 Наличие	84/60	62/50	16/10	38/29
7 Отсутствие	25/40	43/50	75/90	57/71

KEY:

1. Precipitation
2. Ascending
3. Descending
4. Planetary boundary layer
5. Dyubyuk
6. Presence
7. Absence

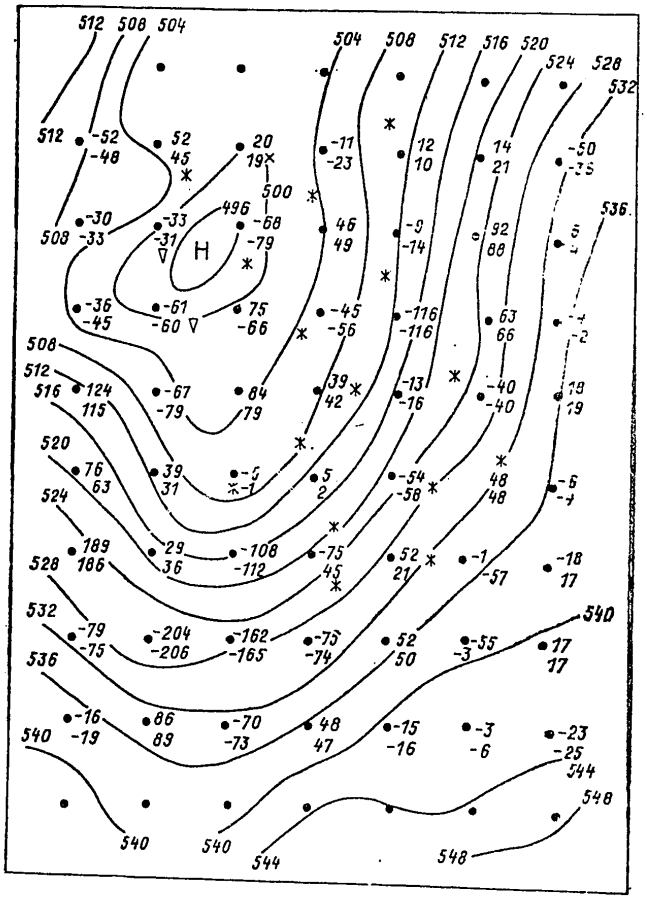

Fig. 3. Isolines of geopotential and vertical currents at AT_{500} on 26 December 1976. H = low

We should note the circumstance that the descending currents, computed using the planetary boundary layer program, are encountered during the falling of precipitation 2.5 times less frequently than those computed by the Dyubyuk method (38%). The fact of falling of precipitation when there are descending currents is noted in only 10% of the cases when using the planetary boundary layer method, whereas according to the Dyubyuk formula this value is three times greater (29%). All this makes it possible to conclude that computations of frictional vertical currents by the planetary boundary layer method is preferable. If it is taken into account at the same time that when using the planetary boundary layer method only 2, and when using the Dyubyuk formula, only 33 of the 112 values of the frictional vertical currents exceed 75 mb/12 hours in absolute value, it can be concluded that the planetary boundary layer method reproduces more realistically the fields of vertical currents characteristic for large-scale atmospheric processes.

As a rule, the sign of the frictional currents when using the planetary boundary layer method is opposite the sign of the Laplacian of surface pressure, but this is by no means always observed. In a number of cases sufficiently large positive values of the surface pressure Laplacian correspond to the descending frictional currents computed by the planetary boundary layer method and vice versa.

The patterns cited above are clearly traced in Fig. 2, which shows the synoptic situation, frictional vertical currents and precipitation on 26 December 1976. The two rows of vertical current values correspond to: upper -- computed by the planetary boundary layer method, lower -- computed using the Dyubyuk formula.

For the mentioned synoptic situations we computed the vertical currents at the isobaric surfaces 700, 500 and 300 mb, taking into account the frictional currents determined by the planetary boundary layer method (ω_1) and using the Dyubyuk formula (ω_2). Figure 3, which gives the ω values at AT_{500} for 26 December 1976, gives ω_1 in the numerator and ω_2 in the denominator, near each point of intersection in a regular grid. Here also the isolines of geopotential AT_{500} are shown. The values of the vertical currents in the free atmosphere for the considered synoptic situations vary in a rather wide range: descending movements in the region of a well-expressed trough and a high cyclone can (in absolute value) exceed 100 mb/12 hours. The characteristic value falls in the range 50-80 mb/12 hours. The descending currents in the region of the anticyclonic field as a rule are less; their maximum values do not exceed 100 mb/12 hours and the characteristic values fall in the range 30-50 mb/12 hours. A distinguishing feature of the field of vertical currents is their great spatial variability: in the region of a trough the maximum differences in the values of the vertical currents at two adjacent points of intersection in a regular grid often exceed 50 mb/12 hours; frequently at adjacent points of intersection in a regular grid there are vertical currents of opposite signs. All this, unquestionably, leads to spottiness in the distribution of precipitation, which was observed in the considered cases.

This analysis of vertical movements in the troposphere makes it possible to conclude that the developed method for taking into account the effects of the planetary boundary layer and the principal physical factors in computing the values of vertical velocities can be used in numerical forecasting of the cloud cover and precipitation fields.

BIBLIOGRAPHY

1. Belousov, S. L., "Operational Numerical Short-Range Forecasts of Meteorological Elements," METEOROLOGIYA I GIDROLOGIYA (Meteorology and Hydrology), No 6, 1978.

2. Zilitinkevich, S. S., DINAMIKA POGRANICHNOGO SLOYA ATMOSFERY (Dynamics of the Atmospheric Boundary Layer), Leningrad, Gidrometeoizdat, 1970.

3. Yordanov, D. L., Penenko, V. V., Aloyan, A. Ye., "Parameterization of a Stratified Baroclinic Boundary Layer for Numerical Modeling of Atmospheric Processes," IZVESTIYA AN SSSR, FIZIKA ATMOSFERY I OKEANA (News of the USSR Academy of Sciences, Physics of the Atmosphere and Ocean), Vol 14, No 8, 1978.

4. Laykhtman, D. L., FIZIKA POGRANICHNOGO SLOYA ATMOSFERY (Physics of the Atmospheric Boundary Layer), Leningrad, Gidrometeoizdat, 1970.

5. Tarnopol'skiy, A. G., Shnaydman, V. A., "Parameterization of the Planetary Boundary Layer in Prognostic Models," TRUDY GIDROMETTSENTRA SSSR (Transactions of the USSR Hydrometeorological Center), No 145, 1974.

6. Tarnopol'skiy, A. G., Shnaydman, V. A., "Parameterization of the Baroclinic Planetary Boundary Layer of the Atmosphere," TRUDY GIDROMETTSENTRA SSSR, No 180, 1976.

7. Shklyarevich, O. B., "Profile of Strong Winds," TRUDY GGO (Transactions of the Main Geophysical Observatory), No 362, 1976.

8. Arya, S. P., "Suggested Revisions to Certain Boundary Layer Parameterization Schemes Used in Atmospheric Circulation Models," MON. WEATHER REV., Vol 105, No 2, 1977.

UDC 551.509.616:621.375.826

INFLUENCE OF SMALL-SCALE TURBULENCE ON CLEARING OF AN AQUEOUS AEROSOL

Moscow METEOROLOGIYA I GIDROLOGIYA in Russian No 9, Sep 79 pp 44-48

[Article by S. D. Pinchuk, Institute of Experimental Meteorology, submitted for publication 29 January 1979]

Abstract: This paper presents the results of an experimental investigation of the influence of small-scale turbulence on clearing of an aqueous aerosol by a beam from a continuous CO_2 laser in a stationary operating regime. The measurements were made in a model medium with an artificially created mechanical turbulence. In the case of an intensity distribution uniform in the beam section, the experimental data are approximated by computed curves obtained using formulas for uniform movement with introduction into the thermal effect function of a term which characterizes the transport of aerosol as a result of turbulent diffusion. Taking into account the results of the experiment and information on the value of the coefficient of turbulent diffusion in the surface layer of the atmosphere, a hypothesis is advanced relative to the influence of small-scale turbulence on clearing of the cloud medium.

[Text] The recently published results of investigations of evaporation of a water droplet and clearing of an aerosol by the radiation of a CO_2 laser [2, 5, 7, 9, 10, 13] have indicated the fundamental possibility of a ray effect on clouds and fogs for the purpose of creating zones of increased transparency. One of the factors determining the clearing by a beam of a continuous CO_2 laser is movement of the medium -- existing (wind) and induced (free convection). Cases when the existing movement is uniform (that is, constant in time and in space) and convection arises in an initially motionless medium were studied in [13, 5]. Since in the atmosphere the movement has a turbulent nature, it is of interest to investigate clearings in the presence of turbulence, in particular, that which is

small-scale in comparison with beam diameter. Within the framework of the model in which the efflect of fluctuations of the velocity of movement of the medium is characterized by the coefficient of turbulent diffusion, a theoretical study was made of individual problems: dynamics of formation of the cleared zone [11], its "blurring" after the laser is deactivated [6]. In this communication we give the results of an experimental investigation of the influence of small-scale turbulence on clearing of an aqueous aerosol in a stationary laser-effect regime.

The experimental apparatus is illustrated schematically in Fig. 1.

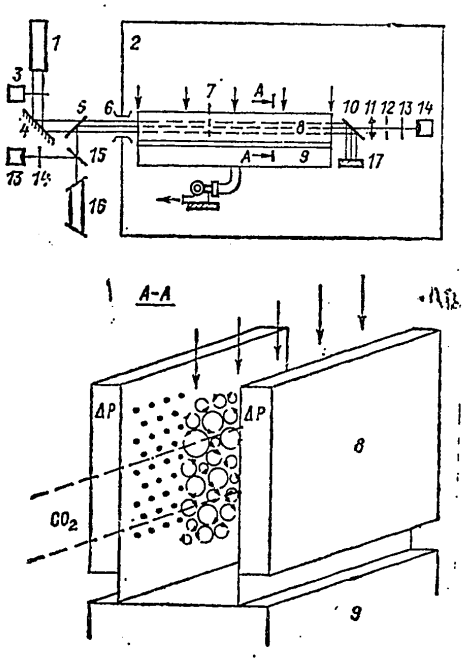

Fig. 1. General diagram of experimental apparatus. 1) CO_2 laser (λ = 10.6 μm), 2) aerosol chamber, 3) electromechanical shutter, 4) rotating mirror, 5) mixing plate of NaCl, 6) entrance window, 7) sensor of instrument for measuring velocity, 8) turbulent cell, 9) wind apparatus, 10) quartz plate, 11) lens, 12) diaphragm, 13) light filter, 14) photodiode, 15) light-dividing plate, 16) He-Ne laser (λ = 0.63μm), 17) absorber

The measurements were made in a model cloud medium created in the aerosol chamber [4] by means of adiabatic expansion of moist air. The microstructure of the aqueous aerosol forming in the chamber is close in its characteristics to the droplet spectrum of natural clouds and fogs. The temperature

of the medium is 18-21°C. The effect was attained using the beam of a continuous CO_2 laser; the intensity of the radiation is about 800 W; the beam, with a diameter $2a \approx 45$ mm, contains several transverse modes (by a careful adjustment of the mirrors it was possible to achieve an intensity distribution approximately uniform in the beam section). The clearing effect, as which we selected the change in the optical thickness of the medium as a result of the exposure $\Delta\tau_\lambda$, was registered using the narrow sounding ray of a He-Ne laser propagating along the axis of the produced beam.

The principle of creating artificial mechanical turbulence is similar to that described in [12]. A turbulent cell consists of two identical rectangular boxes, with a length of 2 m, situated opposite one another. In the box wall there are apertures through which the compressed air fed inside emerges (the diameter of the apertures is 1.5 mm, the distance between them is 10 mm). With collision of the oppositely directed jets and their mixing in the central region of the cell a quite uniform and isotropic random velocity field with eddies measuring $l \lesssim 2a$ is formed. The cell was matched with the wind apparatus [1], which ensured a directed movement of the medium with the velocity $\bar{v}$. The characteristics of the velocity field $v = \bar{v} + v'$ were checked using a "Disa" thermoanemometer. The degree of turbulence of the flow was varied by the air pressure in the boxes (ΔP), determining the dispersion of velocity fluctuations σ_v, or by means of a change in $\bar{v}$.

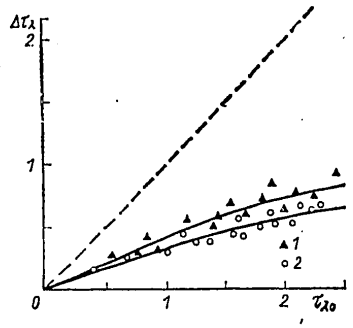

Fig. 2. Dependence of degree of clearing under conditions of forced convection on initial optical thickness of medium in presence (2) and absence (1) of fluctuating velocity component.

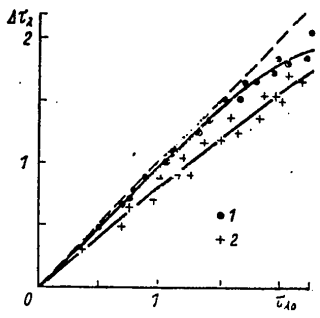

Fig. 3. Dependence of degree of clearing under conditions of free convection on initial optical thickness of medium in presence (2) and in absence (1) of fluctuating velocity component.

An analysis of the results of the model experiment made it possible to ascertain some peculiarities of the clearing of aerosol in the case of turbulent movement in comparison with that when the fluctuating velocity component is absent.

With exposure under conditions of forced convection the degree of clearing of the turbulent medium is less than for uniform movement with a velocity equal to the mean velocity of the turbulent flow. The difference increases with an increase in the degree of turbulence. Figure 2 shows the dependence of $\Delta\tau_\lambda$ on the initial optical thickness of the medium $\tau_{\lambda 0}$ for homogeneous movement with v = 25 cm/sec (1) and with a degree of flow turbulence $\sigma_v/v \approx 50\%$ (2). The figure shows that the relative contribution of turbulence to blurring of the cleared zone is approximately identical in the investigated measurement interval $\tau_{\lambda 0}$.

If the exposure occurs under free convection conditions, the clearing is dependent on whether there is random movement in the medium and on what the σ_v value is. A purely convective mechanism of blurring of the cleared zone occurs when $\sigma_v = 0$. The initial transparency "burst" characteristic for this mechanism directly after onset of the exposure and the $\Delta\tau_\lambda$ value in a stationary regime decrease with an increase in σ_v. The disappearance of the burst is evidence that the transfer of aerosol in the beam zone is caused predominantly by turbulent diffusion.

Figure 3 shows the dependence of $\Delta\tau_\lambda$ on $\tau_{\lambda 0}$ for σ = 12 cm/sec (2) and when σ_v is close to zero (1). As can be seen from the figure, in contrast to clearing during forced convection, under free convection conditions the relative contribution of turbulence to blurring of the cleared zone decreases with an increase in $\tau_{\lambda 0}$, which is associated with an increase in the velocity of induced movement.

Thus, the noted peculiarities in clearing of an aqueous aerosol in the presence of a fluctuating velocity component can be qualitatively attributed to the presence of an additional (diffusion) mechanism of blurring of the cleared zone in the medium. Experimental data on the change of optical thickness of the medium on the beam axis are satisfactorily approximated by the computed curves constructed using the formulas for uniform movement [3] with introduction into the thermal effect function of a term responsible for the diffusion transport of aerosol:

$$\Theta_\tau = \frac{3}{4}\frac{\beta_T I_0 A_\pi}{L\rho}\left(\frac{a}{v + A\frac{4D_T}{a}}\right). \qquad (1)$$

Here β_T is the fraction of energy absorbed by a droplet which is expended on evaporation, I_0 is the intensity of radiation,

$$A_\pi = 10^3 см^{-1},$$

[π = abs] L, ρ is the heat of evaporation and water density respectively, v is the convection (forced or free) rate, D_T is the coefficient of turbulent diffusion.

Using the coefficient $A \leqslant 1$, reducing the effective rate of diffusion transport, an allowance is made for the circumstance that during turbulent movement partially evaporating droplets are introduced into the beam zone. The A value in a general case is dependent on I_0, σ_v and, in addition, on the

method for determining the turbulent diffusion coefficient, which is usually found from physical considerations on the basis of a classical determination ($D_T = 1/3\ u'\ l'$, where u', l' are the velocity and the mixing path respectively), and for the surface layer of the atmosphere either on the basis of empirical data [12] or using the Richardson-Obukhov formula [8]. In the computations it was assumed that $D_T = 1/3\ \sigma_v\ a$, and for the above-mentioned experimental conditions the A value is 0.5 and the term in θ_T responsible for the diffusion transport of aerosol is $2/3\ \sigma_v$. For estimating the relative contribution of turbulence to blurring of the cleared zone it is possible to use the parameter $\Gamma = 4\ D_T/av$, which represents the ratio of the conductive and convective terms in the equation for transforming the droplet spectrum in the beam. If $\Gamma > 1$, the prevailing blurring mechanism is diffusion; if $\Gamma < 1$ -- convection.

It should be emphasized that the function θ_T can be represented in the form (1) only in a case of an intensity distribution which is uniform in the section of the beam. It was discovered experimentally that the influence of small-scale turbulence on clearing is essentially dependent also on the structure of the transmitted beam, and in particular, on the relative positioning of the sounding ray and the region with a high intensity of radiation. The minimum value of the $\Delta\tau_\lambda$ ratio in the presence and in the absence of a fluctuating velocity component is realized when the ray is on the leeward side. With other positionings the mentioned ratio can be of the order of and greater than unity.

Taking into account the results of the model experiment, and also the information cited in the literature on turbulent diffusion in the atmospheric surface layer [8, 12], a hypothesis can be made concerning the influence of small-scale turbulence on the clearing of natural aerosol. This requires computation of the value of the Γ parameter. In computing D_T in the turbulence spectrum it is necessary to take into account only those inhomogeneities whose characteristic dimensions are less than and of the order of magnitude of beam diameter. Corresponding estimates show that for $2a \leqslant 10$ cm and $\bar{v} \geqslant 10^2$ cm/sec the influence of small-scale turbulence on the clearing of a natural aerosol will be negligible. However, it must be taken into account for broader beams and in so-called "stagnation" regions arising during scanning [12].

In conclusion the author expresses appreciation to L. G. Akul'shin for assistance in carrying out the measurements.

BIBLIOGRAPHY

1. Belyayev, V. P., Volkovitskiy, O. A., Nerushev, A. F., Nikolayev, V. P., Pinchuk, S. D., Skripkin, A. M., "Experimental Investigation of Clearing of a Fog by Laser Radiation With $\lambda = 10.6\ \mu m$," IZVESTIYA AN SSSR, FIZIKA ATMOSFERY I OKEANA (News of the USSR Academy of Sciences, Physics of the Atmosphere and Ocean), Vol 11, No 10, 1975.

2. Bisyarin, V. P., Kolosov, M. A., Pozhidayev, V. N., Sokolov, A. V., "Interaction Between Laser Radiation in the UV, Visible and IR Ranges and an Aqueous Aerosol," IZVESTIYA VUZOV SSSR, FIZIKA (News of Higher Schools of Education USSR, Physics), No 11, 1977.

3. Volkovitskiy, O. A., "Experimental Investigation of the Influence of Radiation of CO_2 Lasers on a Droplet Cloud Medium," METEOROLOGIYA I GIDROLOGIYA (Meteorology and Hydrology), No 9, 1977.

4. Volkovitskiy, O. A., "Complex of Experimental Apparatus for Geophysical Investigations," METEOROLOGIYA I GIDROLOGIYA, No 6, 1965.

5. Zuyev, V. Ye., Kuzikovskiy, A. V., "Thermal Clearing of Aqueous Aerosols by Laser Radiation," IZVESTIYA VUZOV SSSR, FIZIKA, No 11, 1977.

6. Kobzev, V. V., Petrov, G. D., "Decrease in Attenuation of Laser Radiation in a Fog," TRUDY MOSK. INST. RADIOTEKHNIKI, ELEKTRONIKI I AVTOMATIKI (Transactions of the Moscow Institute of Radio Engineering, Electronics and Automation), Vol 4, No 40, 1969.

7. Korotin, A. V., Svetogorov, D. Ye., Sedunov, Yu. S., Semenov, L. P., "Formation of Zones of Clearing in Clouds and Fogs," DOKLADY AN SSSR (Reports of the USSR Academy of Sciences), Vol 220, No 4, 1975.

8. Matveyev, L. T., OSNOVY OBSHCHEY METEOROLOGII. FIZIKA ATMOSFERY (Principles of General Meteorology. Atmospheric Physics), Leningrad, Gidrometeoizdat, 1965.

9. Romanov, G. S., Pustovalov, V. K., "Clearing of the Cloudy Atmosphere Containing Water Droplets by Intensive Monochromatic Radiation," ZHURNAL PRIKLADNOY SPEKTROSKOPII (Journal of Applied Spectroscopy), Vol XIX, No 2, 1973.

10. Sukhorukov, A. P., Shumilov, E. N., "Clearing of a Polydisperse Fog," ZHURNAL TEKHNICHESKOY FIZIKI (Journal of Technical Physics), Vol 43, No 5, 1973.

11. Sukhorukov, A. P., Khokhlov, R. V., Shumilov, E. N., "Dynamics of Clearing of Clouds by a Laser Beam," PIS'MA V ZHURNAL EKSPERIMENTAL'NOY I TEORETICHESKOY FIZIKE (Letters to the Journal of Experimental and Theoretical Physics), Vol 14, No 4, 1971.

12. Gebhardt, F. G., Smith, D. C., Buser, R. G., Rohde, R. S., "Turbulence Effects on Thermal Blooming," APPL. OPT., Vol 12, No 8, 1973.

13. Glickler, S. L., "Propagation of a 10.6 Laser Through a Cloud Including Droplet Vaporization," APPL. OPT., Vol 10, No 3, 1971.

UDC 551.510.42

COMPUTATION OF ATMOSPHERIC PROPAGATION OF EFFLUENT OF HIGH INDUSTRIAL SOURCES IN THE PRESENCE OF INVERSIONS ALOFT

Moscow METEOROLOGIYA I GIDROLOGIYA in Russian No 9, Sep 79 pp 49-55

[Article by Candidates of Physical and Mathematical Sciences F. A. Gisina and S. M. Ponomareva, Leningrad Hydrometeorological Institute, submitted for publication 25 May 1978]

Abstract: This article gives a brief review of statistical data on inversions aloft for different points and existing methods for determining the concentrations of impurities under such anomalous conditions. The authors propose a routine method for computing the propagation of impurities during inversions aloft, based on network aerological data. The influence of inversions of different intensity and thickness on contamination of the surface air layer by effluent of high point sources is considered.

[Text] It is known that in the case of formation of an inversion aloft there is a considerable increase in air contamination at the earth by effluent of high sources situated in the layer beneath the inversion. Since within the inversion turbulent exchange is considerably attenuated, this layer acts as a "lid," preventing the scattering of impurities; at the same time, in the layer beneath the inversion it is common to observe convective conditions favoring the transfer of impurities to the underlying surface. Many authors consider temperature inversions as one of the main components of the potential of air contamination [1-6]. At many places the frequency of recurrence of such unfavorable conditions is extremely high. For Moscow, according to the data in [8], the frequency of recurrence of inversions aloft in the lower 500-m layer during the year is 33-34% (for observation times 0400 and 1600 hours); in the cold half-year such inversions are observed still more frequently.

The relative increase in the degree of contamination in comparison with an inversion-free situation is dependent on the structure of the blocking layer -- its thickness, intensity, altitude of the lower boundary, and also

the relative positioning of the latter and the level at which the impurity escapes. A study of these parameters is especially important for major industrial centers where inversions are characterized by a great thickness and intensity. According to [11], for Leningrad the height of the lower boundary of inversions aloft falls in the interval 100-400 m in 84% of the cases at nighttime (observation time 0400 hours) and 74% during the daytime (1600 hours). Such conditions prevent the upward transfer of impurities even for high stacks.

Until now no adequately reliable methods have been developed for computing concentrations under the anomalous conditions of propagation of the inversion aloft type. Several studies are known which are devoted to a theoretical solution of the problem, usually employing numerical experiments. Within the framework of the so-called statistical approach the effect of inversions aloft is taken into account extremely schematically. Source [6] gives two formulas for computing volume concentration in the presence of an inversion aloft, but it is noted that the results obtained using these formulas differ substantially and it is impossible to make a choice between them without experimental checking. The indeterminancy increases since there are no recommendations on the choice of the dispersions σ_y, σ_z entering into these formulas in the case of formation of a blocking layer.

Within the framework of the diffusion approach the influence of inversions aloft was examined in studies [2, 6, 13]. Heines and Peters [13], for determining the concentration of impurities, used a three-dimensional turbulent diffusion equation in which the exchange coefficients in the vertical and transverse directions were considered constant with altitude but proportional to distance: $K_y = A_y x^q$, $K_z = A_z x^n$. The inversion layer was assumed to be impermeable for the impurity, that is, it was assumed that the flux $K_z \frac{\partial q}{\partial z}$ at the lower boundary of the inversion is equal to zero.

The computations were made for different source altitudes. The wind velocity was stipulated constant; the coefficient $A_y = A_z$ and $n = q$. It can be seen from the computed data that the influence of the inversion layer increases with increasing distance from the source and an increase in the ratio of stack height to the altitude of the lower boundary of the inversion H_u. With $h/H_u = 1$ the concentration in the presence of an inversion layer increases by a factor of three at the distance $x = 10$ km, or by more than an order of magnitude with $x \geqslant 100$ km in comparison with an inversion-free situation.

Monograph [2] gives some results of numerical experiments for investigating atmospheric contamination in the presence and absence of inversion layers aloft. For computing the concentration use was made of a three-dimensional turbulent diffusion equation in which wind velocity was considered variable with altitude in accordance with a logarithmic law, the horizontal diffusion coefficient was stipulated proportional to wind velocity $K_y = au$, and the profiles of the vertical diffusion coefficient were postulated taking into account the sharp attenuation of exchange in the inversion layer. A study was made of five characteristic K(z) profiles, for each of which

the ratio of the surface concentration was computed in the presence and absence of an inversion layer. Unfortunately, for the computed cases there is not always an indication of the parameters with which the numerical estimates of the effect of inversions (wind velocity, source height) were obtained. This makes difficult their use and interpretation. It is also not clear what vertical distribution of the turbulence coefficient corresponds to an inversion-free case. It follows from the data cited in [2] that in dependence on the considered profile the surface concentration in the presence of a layer with attenuated turbulence over the stack can increase at the distance 1 x 10 km by a factor of 1-1.9.

The objective of this study is a numerical investigation of propagation of an impurity from high sources in the presence of uplifted inversions, taking their actual structure into account. Computations of the contamination level in the surface layer corresponding to each type of inversions with operation of sources of different height were carried out in the following way. The wind velocity profiles and the turbulence coefficient, as well as the height of the mixing layer, determining the intensity of exchange, are found from solution of a closed system of equations for a stationary, horizontally homogeneous atmospheric boundary layer, formulated in [5]. The velocity of the geostrophic wind, roughness parameter and Coriolis force are considered known. In addition, on the basis of radiosonde data there is stipulation of the actual temperature distribution. By such a method, using a semi-empirical model, it is possible first to find the profiles of the principal turbulence characteristics in the boundary layer for different cases of temperature distribution with height, including for different types of uplifted inversions. In such a formulation the problem was for the first time solved by us in [3].

The distribution of concentrations of a weightless impurity arriving from a high source is then computed by numerical integration of the two-dimensional diffusion equation

$$u\frac{\partial S}{\partial x}=\frac{\partial}{\partial z}K_z\frac{\partial S}{\partial z} \tag{1}$$

and computations of the volume concentration q(x, y, z) — using the formula [11]

$$q(x, y, z)=S(x, z)\exp\left(-y^2/\sqrt{2\pi\sigma_y^2}\right)/\sqrt{2\pi\sigma_y^2}. \tag{2}$$

In the case of presence of a blocking layer over a source use is made of an ordinary boundary condition -- equality of the concentration of impurity to zero at the height of the mixing layer, determined in the course of the system of equations for the boundary layer as the level at which frictional stress is less than 10% of its surface value. Support for such a formulation of the boundary condition is given, for example, by the experiments of Olsson [15], indicating that the level of penetration of the impurities can substantially exceed the height of the lower boundary of the inversion.

Table 1

Ratios of Surface Concentrations in Presence and Absence of Inversion for Stacks With Height h = 50–200 m at Different Distances from Source

x км	1 Случаи A: ΔH=90÷300 м, ΔT=1,7° C, 2 Hп=426 м			B: ΔH=100÷450 м, ΔT=2,8° C, Hп=268 м				C: ΔH=220÷380 м, ΔT=2,2° C, 2 Hп=710 м		
	50	80	100	50	80	100	200	100	150	200
0,6	0,5	0,3	0,1	1,4	2,6	$6\cdot10^{-4}$		$6\cdot10^{-4}$	0,1	0,1
1	0,8	0,6	0,4	2,4	5,5	$2\cdot10^{-2}$	$<10^{-7}$	$2\cdot10^{-3}$	0,3	0,2
2	1,2	1,0	1,1	3,5	5,5	0,5		0,1	0,7	1,0
3	1,4	1,3	1,3	3,9	5,4	1,3	$3\cdot10^{-5}$	1,3	1,3	1,4
5	1,7	1,7	1,7	4,6	5,7	2,8	$2\cdot10^{-2}$	0,8	1,5	1,2
6	1,8	1,8	1,8	4,7	5,7	3,3	$4\cdot10^{-2}$	1,0	1,5	2,4
8	1,9	1,9	1,8	4,8	5,8	4,3	0,1	1,4	1,9	2,5
10	2,0	1,8	1,8	5,4	6,1	5,1	0,3	1,7	2,1	2,6

KEY:
1. Cases
2. H_{mix}

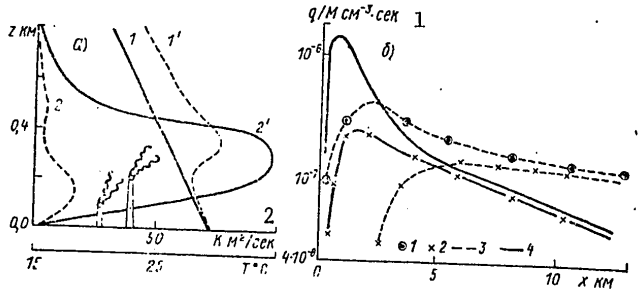

Fig. 1. Initial temperature profiles T(1, 1') and mixing coefficient K (2, 2') in atmospheric boundary layer in presence of inversion (1', 2) and after its destruction (1, 2') (case C from Table 1) (a), and also change in surface normalized axial concentration q/M in dependence on distance x for sources with a height 100 (1) and 200 (2) m in presence of inversion layer above them (3) and in inertialess case (4) (b).

KEY:
1. $cm^{-3}\cdot sec$
2. m^2/sec

The transverse dispersion σ_y^2, determining the volume concentration in accordance with (2), is computed using an interpolation formula satisfying the limiting expressions following from the Taylor formula

$$\sigma_y^2 = \bar{b}x^2/u^2(1+\bar{b}x/\alpha\,\bar{u}\bar{K}), \tag{3}$$

where $\alpha = 66$ is an empirical constant. This expression, proposed in [4], relates σ_y^2 to the energy values b and the turbulence coefficient K, and also wind velocity u, vertically averaged in the layer from z = 0 to z = h, where h is source height. Thus, the dispersion is dependent not only on the distance and the meteorological parameters, but also on height. However, in the computations for industrial sources, usually having stacks with a height of about 50-200 m, the dependence of dispersions on altitude is relatively weak.

Now we will examine the results of computations of concentrations by the method described above, carried out for different inversion situations. As an example, Table 1 gives the ratios of the surface concentrations at different distances x from sources of different height in the presence of inversion layers with the thickness ΔH and the intensity ΔT and after their destruction. The heights of the stacks were stipulated in such a way that the scatter of the impurity occurred either below or within the layer with attenuated exchange. The initial temperature profiles were selected from observations in summer in the steppe (O'Neil, August 1953 [14]). A study was made of cases with moderate wind velocities (dynamic velocity of about 0.3 m/sec). For each of the three cases Table 1 gives the computed values of the height of the mixing layer H_{mix}.

Table 2

Ratio of Surface Axial Concentrations q_B/q_A for Two Types of Uplifted Inversions

x км	h м		
	50	80	100
1	1,1	0,4	0,1
2	1,5	1,0	0,5
3	1,6	1,2	0,9
5	2,0	1,4	1,2
8	2,1	1,9	1,7
10	2,5	2,3	2,2

As an inertialess case a study was made of a situation characteristic for the midday hours in summer over the steppe (the temperature profile corresponded to 1200 hours on 22 August 1953 on the basis of data in [14]. The computed values of the K coefficient and the thickness of the mixing layer substantially increased (K_{max} = 102 m^2/sec, H_n = 990 m) in comparison with inversion situations (in the case C, for example, K_{max} = 17.2 m^2/sec, H_n = 710 m). The dynamic velocity was stipulated in both cases as a constant value and according to measurement data was equal to 0.3 m/sec. Figure 1a illustrates the transformation of the temperature profiles and the turbulence coefficient with a change in the temperature stratification for this numerical experiment. The distribution of the axial concentration, normalized for the scatter, for two heights of stacks in the presence of an inversion and after its destruction is given in Fig. 1b.

It follows from the computed data that in the case of an uplifted inversion there can be formation of rather complex K profiles. The concentrations near the earth increase in comparison with an inertialess situation, beginning at some distance. The position of the maximum is displaced into the direction of large x. Although the shape of the q(x, 0,0) curves does not change, the concentrations at all distances, the values and position of the maximum in the case of a fixed height of the discharge are essentially dependent on the structure of the "blocking" layer. A quantitative estimate of the inversion effect is given not only in Table 1, but also in Table 2, which gives the ratios of the surface concentrations for cases A and B, when the position of the lower boundary of the inversion layers differed insignificantly, but their extent and intensity were different.

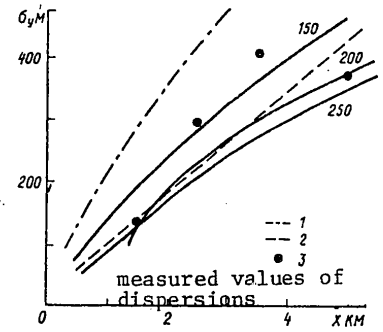

Fig. 2. Dependence of transverse dispersion σ_y, computed using formula (3), on distance x for different heights of stacks h = 150, 200, 250 m in presence of an inversion (experiment 1). 1) $\sigma_y(x)$ distribution for inertialess conditions, 2) computations using $\sigma_y = 0.2\ x^{0.9}$.

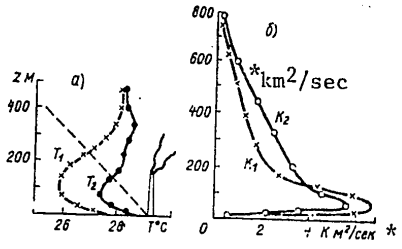

Fig. 3. Initial profiles of temperature T_1 (experiment 1, 1100-1130) and T_2 (experiment 2, 1300-1330) (dashed line -- dry adiabat) (a) and corresponding computed profiles of turbulence coefficient K_1 and K_2 in presence of uplifted inversion (b).

If we compare the surface concentrations from 50- and 100-m stacks for cases A and B, it can be seen that the ratios of the concentrations change in dependence on distance from 0.1 to 2.5. The increase in contaminations begins at lesser distances and is all the more conspicuous (with the same lower boundary of the inversion), the more intense it is. The greatest increase in the concentrations is by a factor of 5-6 in comparison with an inertialess situation and was obtained in the case B, when the inversion had a maximum thickness (from 100 to 400 m) and intensity ($\Delta T = 2.8°C$). Their differences are attributable to the fact that each type of inversion corresponds to the specific distribution K(z) -- the main argument of this problem.

In dependence on the relative position of the level of maximum exchange and the mouth of the stack, the influence of one and the same layer is different. The greatest increase in concentrations for case B corresponds to stacks with heights 50 and 80 m. The mouth of a 100-m stack is already situated in

the zone of decreased exchange and the ratios of the concentrations become less, especially near the stack and in the zone of the maximum. With h = 200 m, as a result of the blocking effect, far less impurity is transported toward the earth (see Table 1) than in the absence of an inversion when the mixing is developed very strongly.

As a result of the difference in approaches it is impossible to compare the results with those described above [2, 7, 13]; it can only be noted that the qualitative picture of the influence of uplifted inversions on contamination of the surface layer is identical for all models. The method described in [2] is characterized by an appreciably lesser increase in the concentrations in the layer beneath the inversion than for our model and that proposed in [13].

Unfortunately, there are no experimental data on the detailed picture of air contamination in the presence of uplifted inversions; there are only indications of a substantial increase in the concentrations under these conditions. In particular, it is noted in [7] that during experiments with smoke from a 355-m stack it was found that with a "smoking" type of jet the concentration on the average is an order of magnitude greater than the maximum concentration computed using the Sutton formula.

An attempt was made to use the results of the diffusion experiments made by Sato [16] for checking the model described above. Although source [16] described the results of only several half-hour experiments carried out under conditions of strong horizontal nonuniformity on the sea shore (which was not taken into account in the model), this source draws attention to the fact that it contains a relatively complete description of the initial meteorological data and the diffusion parameters. A study was made of two cases with the most clearly expressed uplifted inversion layers, for which the source gave both detailed temperature profiles and the corresponding measurement data for transverse dispersions and surface concentrations at different distances from a source with a height of 150 m. The impurity was ejected directly beneath the inversion layer (experiment 1, 27 July 1968, 1100-1130), or in its lower part (experiment 2, 27 July 1968, 1300-1330 hours).

Figure 2 gives the actual temperature profiles for these experiments and the distributions of the turbulence coefficient K(z) computed from them. The roughness parameter was selected equal to 0.3 m. The effective height of the source varied with distance from 150 to 300 m and was stipulated on the basis of measurement data. The heights of the mixing layer were obtained for these experiments; these were equal to 540 and 595 m respectively. The stratification parameter was $\mu_0 = -30$ and -28.

Figure 3 gives some idea concerning the transverse dispersion at different distances, computed from the profiles of the coefficient and turbulent energy and wind velocity using formula (3) and measured in the course of the experiments at several distances. The numerical experiments indicate that

the effect of inversions, taking into account the dependence of dispersions on the structure of the inversion layer, becomes still more conspicuous. For example, the surface concentration further increases in the zone of the maximum on the average by 30% (for comparison the computations were made using a simple power-law formula for the dispersion $\sigma_y = 0.2\ x^{0.9}$).

Table 3

Comparison of Computed Values of Surface Concentrations With Measured Values ((qu/M)·10^{-7})

x км	Опыт 1 1		Опыт 2 2	
	расч. 3	эксп. 4	расч. 3	эксп. 4
1,5	7,4	15	4	9
2,0	14	9	10	15
3,5	2,3	4	1,6	8
4,8	2,1	2,1	3,4	5
7,5	1,4	1,2	—	—

KEY:

1. Experiment 1
2. Experiment 2
3. Computed
4. Experimental

The computed and measured values of the axial concentration qu/M at different distances, normalized for scatter and wind velocity, are given in Table 3. It can be seen that they differ on the average by a factor of 1.5-2.

Finally, checking on the basis of materials from individual field experiments is clearly inadequate. Nevertheless, our comparison makes it possible to hope that it is possible to obtain a rather realistic picture of the distribution of concentrations under inversion conditions. An important positive peculiarity of the described method is the possibility of computing air contamination in the case of a complex distribution of temperature with height, when the theoretical models, based on an a prior stipulation of the temperature profiles, are inapplicable.

BIBLIOGRAPHY

1. Bezuglaya, E. Yu., "On Determination of the Potential for Air Contamination," TRUDY GGO (Transactions of the Main Geophysical Observatory), No 234, 1968.

2. Berlyand, M. Ye., SOVREMENNYYE PROBLEMY ATMOSFERNOY DIFFUZII I ZAGRYAZNENIYA ATMOSFERY (Modern Problems in Atmospheric Diffusion and Atmospheric Contamination), Leningrad, Gidrometeoizdat, 1975.

3. Gisina, F. A., Ponomareva, S. M., "Use of Characteristics of the Temperature Field for Determining Some Turbulence Parameters in the Atmospheric Boundary Layer," TRUDY IEM (Transactions of the Institute of Experimental Meteorology), No 27, 1972.

4. Gisina, F. A., Sal'man, O. Ye., "Evaluation of Transverse Dispersion of Particles Entering the Atmosphere from a Continuous High Point Source," FIZIKA I ISSLEDOVANIYE ATMOSFERY (Physics and Investigation of the Atmosphere), No 62, 1977.

5. Laykhtman, D. L., FIZIKA POGRANICHNOGO SLOYA ATMOSFERY (Physics of the Atmospheric Boundary Layer), Leningrad, Gidrometeoizdat, 1970.

6. METEOROLOGIYA I ATOMNAYA ENERGIYA (Meteorology and Atomic Energy), translated from English, Leningrad, Gidrometeoizdat, 1971.

7. METEOROLOGIYA I ATOMNAYA ENERGIYA (Meteorology and Atomic Energy), translated from English, IL, Moscow.

8. Petrenko, V. K., "Temperature Inversions as the Principal Component of the Potential of Air Contamination in Moscow," TRUDY TsVGMO (Transactions of the Central High-Elevation Hydrometeorological Observatory), No 4, 1975.

9. Ponomareva, S. M., Khandozhko, L. A., "Classification of the Vertical Temperature Gradient Using Synoptic Criteria and Evaluation of Dangerous Air Contaminations," TRUDY LGMI (Transactions of the Leningrad Hydrometeorological Institute), No 52, 1975.

10. Son'kin, G. R., Razbegayeva, Ye. A., Terekhova, K. M., "On the Problem of Meteorological Causality of Air Contamination Over a City," TRUDY GGO, No 185, 1966.

11. Son'kin, L. R., Matveyeva, T. M., "Some Peculiarities of Formation of Temperature Profiles in the Lower 500-m Layer Over the European USSR," TRUDY GGO, No 207, 1968.

12. Dickson, R., "Meteorological Factors Affecting Particulate Air Pollution of a City," BULL. AMER. METEOROL. SOC, Vol 42, No 8, 1964.

13. Heines, T. S., Peters, L. K., "The Effect of Horizontal Inversions Layer Caused by a Temperature Inversion Aloft on the Dispersion of Pollutants in the Atmosphere," ATMOS. ENVIRON., Vol 7, 1973.

14. Lettau, H. H., Davidson, B., "Exploring of the Atmosphere's First Mile," Vol 1-2, London-New York-Paris, Pergamon Press, 1957.

15. Olsson, L. E., et al., "An Observational Study of the Mixing Layer in Western Oregon," ATMOS. ENVIRON., Vol 8, 1974.

16. Sato, J., "The Vertical Spread of Concentration in a Stable Layer," PAPERS IN METEOROLOGY AND GEOPHYSICS, Vol 24, No 4, 1973.

UDC 551.50:629.13:003.1

ECONOMIC EFFECTIVENESS OF METEOROLOGICAL SUPPORT OF CIVIL AVIATION

Moscow METEOROLOGIYA I GIDROLOGIYA in Russian No 9, Sep 79 pp 56-60

[Article by Candidate of Technical Sciences E. I. Monokrovich, Kazakh Scientific Research Hydrometeorological Institute, submitted for publication 6 February 1979]

Abstract: The article describes a method for computing the economic effect from taking weather forecasts into account in the implementation of passenger flights. As an alternative variant, the author examines the execution of flights only when the actual weather is taken into account. The method was tested at the Kustanay and Ust'-Kamenogorsk AMSG (Air Weather Stations of the Civil Air Fleet). It was established that the gain from use of meteorological information is 2-3 times greater than the expenditures on the meteorological support of civil aviation.

[Text] Meteorological information is of great importance not only for ensuring flight safety, but also for increasing the economy of aviation work.

Among all the types of information used for the meteorological support of flights, the most important is weather forecasts for the landing point and information on weather conditions along the flight route. Among all the types of aviation work the most important, unquestionably, is the transport of passengers. Accordingly, it is desirable to examine the problem of the economic effectiveness of use of the mentioned types of meteorological information in carrying out passenger flights.

Either a zero or ideal hypothesis is used for ascertaining the effectiveness of forecasts. In the first case the results of use of operational forecasts are compared with the computed (conditional) results of orientation of the user on an inertial forecast, the norm for the meteorological element, etc. In the second case -- with the conditional results of use of ideal forecasts.

Whereas in order to determine the degree of perfection of the prognostic method an ideal forecast is more suitable, in order to ascertain the absolute effect of forecasts it is necessary to use a zero hypothesis. In this case an alternative evaluation of the synoptic forecast for the landing point can be made on the basis of the actual weather, firm adherence to the schedule, climatic forecast, etc. I believe that the most realistic approach is a comparison of the results of evaluation of synoptic forecasts with the computed results of flights against "the actual weather." Incidentally, during the first years of work of civil aviation, before creation of the network of AMSG stations (Air Weather Stations of the Civil Air Fleet), information on the actual weather at the landing point and in the neighborhood of emergency airports completely determined the takeoff decision.

Thus, in accordance with the adopted hypothesis a forecast for the landing point will be useful in two situations: a) when with the actual flight weather taken into account, a forecast is received that weather deterioration is expected in the next few hours; b) when actual nonflight weather is taken into account, weather improvement is predicted.

In the first case an economic gain is obtained because the return of an aircraft or its diversion to an emergency airport is prevented (assuming that a takeoff would occur, since the actual weather at the landing point at the time of takeoff was favorable). With the strategy of confidence in the forecast the takeoff of the aircraft in this case is delayed. The economic loss from delay in aircraft departure is several times less than from an interrupted flight. Here the importance of the forecast for ensuring flight safety is entirely obvious.

In the second situation the forecast makes possible timely initiation of preparation of the aircraft, crew and passengers for takeoff. This brings about a reduction in the idle time of the aircraft and the losses associated with this.

It is understandable that a forecast "with unfavorable phenomena" which proves to be incorrect results in an unjustifiable delay of the aircraft, whereas an unsuccessful forecast "without phenomena" results in diversion of the aircraft to an emergency airport or return to the takeoff point. Accordingly, the overall effect of prognostic servicing can be represented as the difference between the total gain from correct forecasts and the total loss from incorrect forecasts.

Thus, the possibility of computing the effectiveness of forecasts is becoming real if we know the specific losses from interrupted flights and delays of aircraft of different types. The determination of these losses is an extremely complex problem. There are no official instructions for their computation. This matter is also not examined in the literature on the economics of civil aviation. Sometimes workers in planning-economic agencies of aviation enterprises approximately compute the losses suffered by individual aviation detachments from disruption of flight regularity. But even so, no attempts are made to evaluate the losses in the social sphere, that is, the losses associated with loss of time by the passengers.

Therefore, the author had to develop a method for computing these losses independently. In order to estimate the specific losses of profit of aviation detachments from delays in takeoff and interrupted flights we employed report materials and standards of the Kazakh Civil Aviation Administration characterizing all the items of cost in operation of aircraft of different types, the amount of profit per one hour of flight, etc. In order to determine the social loss we used data from the Central Statistical Administration on the cost of the national product of the Kazakh SSR, the number of man-hours wasted during a year in the national economy of the republic and other data. It was calculated that on the average each man-hour yields a product of 3.8 rubles. Taking into account that not less than 50% of the Aeroflot passengers are workers and that the ratio of the mean annual amount of working time to the total duration of the year is 0.21, one lost passenger-hour on the average results in a social loss of 0.4 ruble. By knowing the number of passenger seats in aircraft of different types and the occupancy ratio, it is easy to calculate the loss inflicted on society when a takeoff is delayed one hour. The method and results of calculations of losses for all presently used types of aircraft are set forth in greater detail in [1].

The proposed method for evaluating the effectiveness of aviation forecasts is validated using the following reasonings. The effect of one forecast will be dependent on how many and what aircraft should, in accordance with the schedule, land at a particular point in the time interval for which the forecast is prepared. The usefulness of the forecasts issued by the AMSG for some calendar period (for example, a month) will also be dependent on the number of observed continuous periods of nonflight weather and on the quality of the forecasts issued during this time. The latter factor is quite fully characterized by three indices:
-- successful notification of dangerous phenomena -- φ ;
-- probable success of forecasting "with phenomena" -- η ;
-- probable success of forecasting "without phenomena" -- θ.

All three indices are in fractions of unity.

The number of periods of nonflight weather noted during a month will be denoted by l . In the computations it is necessary to take precisely this number and not the number of noted dangerous phenomena, since sometimes 2 or 3 dangerous phenomena are observed simultaneously. Moreover, the reckoning of dangerous phenomena is done differently at different AMSG.

In order to calculate the airport load factor we must know the number of serviced aircraft-takeoffs and also the structure of the serviced aircraft fleet by types of aircraft. It is most convenient to characterize the airport load by the number of serviced conditional aircraft takeoffs. As one "conditional aircraft-takeoff" we used the takeoff of one AN-24. Each type of aircraft was assigned a conversion factor representing the ratio of the cost of one hour of operation of an aircraft of a particular type to the

cost of operation of the AN-24. These factors, which we computed using civil aviation data, are given in Table 1.

Table 1

Type of aircraft, helicopter	Conversion factor
AN-24	1.00
IL-62	5.74
TU-154	4.84
TU-104	2.59
TU-124	2.30
IL-18	1.70
YaK-40	0.96
IL-14	0.72
AN-2	0.28
MI-8	1.27
MI-4	0.66
MI-2	0.48
MI-1	0.29

Then, multiplying the number of takeoffs of aircraft of each type, taken from the schedule or using data from the TsDA, by the corresponding conversion factors, we find the number of serviced conditional aircraft-takeoffs for a particular airport.

Detailed computations have shown that with an airport load characterized by the number of conditional aircraft-takeoffs serviced in the course of a month equal to 4,360, the mean effectiveness of one successful three-hour forecast "with phenomena" is 8,900 rubles. We took specifically three-hour time intervals rather than six-hour time intervals because according to the Instructions on Meteorological Support of Civil Aviation (NMO GA-73) forecasts for 6 and 9 hours are prepared each 3 hours and each 6-9-hour forecast is subdivided in the text into 2-3 three-hour forecasts; an evaluation of the probable success of forecasts is made for each three-hour period.

Taking into account the linear dependence of the forecasting effect on the number of serviced takeoffs, for any monthly value u it is possible to find the mean effect of one forecast "with phenomena":

$$E_0 = 8900/4360\ u = 2.04\ u \text{ rubles.}$$

As was already mentioned above, the effect of a successful forecast "with phenomena" is simultaneously a measure of the losses in the case of a forecast "without phenomena" which proved to be unjustified.

Similarly it was computed that the mean loss from one forecast "with phenomena" which proved to be unjustified (as a result of which the takeoff delays are unjustified) is

$$U_0 = 0.48u \text{ rubles.}$$

This same value is a measure of the gain from one successful forecast "without phenomena," issued during actual nonflight weather.

As a result, the expression for computing the monthly economic effect from forecasts for the landing point can be written in the following way:

$$E = ul\left[2{,}04\ \varphi + 0{,}48\ \theta - 0{,}48\ \varphi\left(\frac{1}{\eta} - 1\right) - 2{,}04\ (1 - \varphi)\right] \text{ rubles.}$$

In this formula the first two terms in the brackets express the gain from successful forecasts "with phenomena" and "without phenomena," and the third and fourth terms represent the losses from forecasts which have proven to be unjustified.

This method underwent practical testing at the Ust'-Kamenogorsk and Kustanay AMSG. The results of the computations, carried out by the personnel of these AMSG, are given in Table 2.

Table 2

Results of Practical Testing of Method for Computing the Economic Effect from Aviation Weather Forecasts at the Ust'-Kamenogorsk and Kustanay Aviation Meteorological Stations of the Civil Air Fleet

φ	θ	η	Σl	Σu	$\Sigma Э$ тыс. руб. 1
2 Усть-Каменогорск (февраль—май 1978 г.)					
0,93	0,98	0,79	50	5044	134,8
3 Кустанай (январь—май 1978 г.)					
0,94	0,96	0,88	102	6273	290,5

KEY:
1. Thousands of rubles
2. Ust'-Kamenogorsk (February-May 1978)
3. Kustanay (January-May 1978)

As we see, the results of the computations objectively reflect the nature of operation of the AMSGs during the time when the tests are made (airport load, nature of the weather, quality of the forecasts). The time required for the computations was 3-4 man-hours. The resulting economic effect exceeds by a factor of 2-3 the total expenditures on the operation of these AMSG.

Incidentally, the author's computations indicated that the potential effectiveness of the forecasts issued by the Alma-Ata Aerometeorological Center on the average exceeds by a factor of three the expenditures on its maintenance. Taking into account the proposals made in the course of testing of the method at the Kustanay and Ust'-Kamenogorsk AMSG, the Kazakh Scientific Research Hydrometeorological Institute issued the "Methodological Recommendations on Evaluation of the Economic Effectiveness of Aviation Weather Forecasts." These recommendations were approved by the Scientific and Technical

Council of the Administration of the Hydrometeorological Service Kazakh SSR for use at the Kazakhstan AMSG.

In addition to the forecasts for the landing point, a definite economic effect is given by information on weather conditions along the flight trajectory and in regions of emergency airports. For example, the wind direction and velocity along segments of the flight trajectory exert a direct influence on the flight duration, and accordingly, on the quantity of fuel expended. The greater the weight of the fuel taken, the greater is its expenditure; in addition, in individual cases an increase in the fuel supply leads to a decrease in the commercial load of the aircraft, and this means that there is an increase in transport cost.

When there is unstable weather in the neighborhood of a close emergency airport a fuel supply is taken for flight to the point of destination, for flight to a distant emergency airport and for 30 additional minutes of flight. Thus, the greatest fuel supply is taken on when there is unstable weather in the neighborhood of a near emergency airport and when there is a strong head wind along the flight trajectory. In each case the fuel supply must be calculated specifically for these most unfavorable conditions if the ship crews do not have appropriate meteorological information. In actual practice, however, they also receive information on the actual weather along the path of the impending flight and a weather forecast for the next few hours. For example, receiving information on an accompanying (tail) wind, the navigator, in accordance with the Instructions, takes a calm into account, which makes it possible to carry a lesser fuel supply than when there is a head wind.

We carried out an analysis of 150 aircraft logs with report data on flights by IL-62, TU-154 and IL-18 aircraft. As a result, it was established to what extent the actual navigational supply on each flight differed from the maximum (which it would be necessary to take in the absence of meteorological information). The quantity of saved fuel was determined using the formula

$$\Delta B = (B_m - B_{act})bT \text{ kg}.$$

Here B_m and B_{act} are the maximum and actual navigational supplies, in tons, respectively; b is the specific hourly fuel expenditure, kg/tons/hour; T is the flight time, hours.

By means of a comparison of the ΔB values with the actual fuel expenditures on a flight we determined its saving in percent. The results of the computations are given in Table 3.

The mean percentage of fuel economy for the considered flights is 3.3. In addition, in computing the fuel supply for the worst conditions, in a number of cases an aircraft with approach to the point of designation would have a weight exceeding the admissible landing weight. In these cases it is necessary either to dump the excess fuel in the air or fly extra over the landing point for some time in order to expend the excess fuel. We did not take such direct fuel losses into account. On some types of aircraft

the taking of the maximum fuel supply on board would lead in individual cases to a decrease in the commercial load, which would result in a corresponding decrease in the profit. We also did not take these cases into account. Thus, this value of the economic effect must be adopted as a minimum estimate.

Table 3

Route	Type of aircraft	Number of flights	Mean fuel savings
Alma-Ata - Domodedovo	IL-62	60	3.5
Domodedovo-Semipalatinsk	TU-154	28	2.5
Kustanay-Domodedovo	TU-154	28	3.1
Alma-Ata-Shevchenko	IL-18	34	3.8

We note in conclusion that the expenditures on meteorological support constitute, according to our computations, only 2% of the entire sum of expenditures on the operation of aircraft.

BIBLIOGRAPHY

1. Monokrovich, E. I., "Simplified Method for Evaluating the Economic Effectiveness of AMSG Activity," INFORMATSIONNOYE PIS'MO UGMS KazSSR (Information Letter No 3 Administration of the Hydrometeorological Service KazSSR), Alma-Ata, 1977.

UDC 551.464.3

SUBSURFACE SALINITY MAXIMUM IN THE ACTIVE LAYER OF THE OCEAN AND CONVECTIVE PENETRATIONS

Moscow METEOROLOGIYA I GIDROLOGIYA in Russian No 9, Sep 79 pp 61-65

[Article by Candidate of Physical and Mathematical Sciences A. A. Kutalo and Ye. B. Chernyavskiy, USSR Hydrometeorological Scientific Research Center, submitted for publication 2 August 1978]

Abstract: Evaporation at the ocean surface leads to the formation of a film of cold and saline water. It is postulated that this water, being detached from the surface and penetrating to the depth of hydrostatic equilibrium, forms or replenishes the subsurface salinity maximum. Data from a survey of the southwestern part of the Sargasso Sea are used in validating the hypothesis.

[Text] In oceanology it is usually assumed that the waters of the subsurface salinity maximum (SSM) acquire their properties by being in contact with the free surface of the ocean [4, 6]. Two factors are regarded as responsible for SSM waters losing contact with the free surface: due to horizontal advection of waters from the centers of formation and their sinking beneath the lighter surrounding waters [4, 6, 7] and as a result of the formation of a surface, lighter layer of freshened waters, caused by seasonal variability of hydrometeorological conditions at the ocean surface, in the very regions of formation of SSM waters [8].

In this paper we propose to substantiate still another mechanism for the formation of the subsurface salinity maximum. It is postulated that a source of SSM waters is a thin surface layer, colder and more saline than the underlying waters, created during evaporation from the ocean surface. The formation of the SSM occurs as a result of the detachment of volumes of water of increased density from the ocean surface, the so-called surface layer, and their convective sinking to the depths of hydrostatic equilibrium.

The depth of the SSM is usually about 100 m. Therefore, the postulated mechanism of SSM formation is possible only with an insignificant exchange of salts and heat of the sinking water volumes with the surrounding less

saline and warmer waters. Such convective sinking, without a change in salinity and temperature of water volumes of increased density in the surface layer to the depths of hydrostatic equilibrium will be called "convective penetrations of the intermediate water layer."

There are no data from direct instrumental investigations of such a process in the ocean. We will demonstrate the reality of its existence in the following way. We note that an important condition for the realization of convective penetrations is the presence of a thin surface layer of cooled, heavier water. The existence of such a layer has been noted in many studies [1, 5]. A temperature decrease in such a surface layer is possible due to heat losses by the ocean for three main reasons: as a result of evaporation, radiation and contact heat exchange with the atmosphere. The latter two factors cannot cause a change in the salt composition of the surface layer and independently, without evaporation, cannot cause the formation of a salinity maximum by means of convective penetrations.

We will assume that the parameters of the surface cooled layer, being the source of SSM waters, for the most part are determined by evaporation processes. We will call this layer the evaporation layer. We will examine the premises for such an assumption. Convective (contact) heat exchange, in the case of small temperature differences between the water and air, as is observed in regions where the SSM is observed, is insignificant. The effective radiation of the ocean is an integral effect of some surface layer. Taking into account that evaporation is a purely surface phenomenon, it can be hoped that the layers of cooling generated by the mentioned factors will have different vertical dimensions and to an adequate degree will be independent.

Assuming the existence of convective penetrations, we also will not take into account the exchange of salts and heat of the evaporation layer with the underlying waters. With the assumptions made we will examine the conditions for the salt and heat balances of some volume of waters in the evaporation layer during the lifetime of this volume between two successive convective penetrations. Assume that V_1, S_1, T_1 are such a volume, its salinity and the time of detachment from the surface and V_0, S_0, T_0 are its initial parameters, corresponding to the moment of formation of the evaporation layer. S_0 and T_0 can be identified with the generally accepted values of surface salinity and temperature, obtained when making measurements with standard hydrological instruments. The conditions for conservation of the quantity of salts in the discriminated volume and the heat balance have the form

$$S_0V_0=S_1V_1; \tag{1}$$

$$cT_0V_0=cT_1V_1+L(V_0-V_1), \tag{2}$$

where $V_0 - V_1$ is the volume of evaporating water, c is the specific heat capacity of water, L is the latent heat of vaporization.

Excluding V0 and V_1 from (1) and (2), we obtain the relationship between the salinity and temperature of the water volume in the evaporation layer at the initial moment and at the moment of its convective penetration:

$$\frac{S_1 - S_0}{S_0} = \frac{T_0 - T_1}{L/c - T_0}. \quad (3)$$

Thus, if the SSM waters are formed by the described convective penetrations mechanism, relationship (3) should be satisfied for them. S_1, T_1 are salinity and temperature measured by standard methods in the SSM layer and S_0, T_0 at the ocean surface. The discovery of regions in the ocean where relationship (3) is observed can be regarded as demonstration of the existence of the described mechanism of formation of the subsurface salinity maximum. For this purpose we carried out an analysis of data for 295 stations in a hydrological survey in the western part of the Sargasso Sea during the 23d voyage of the scientific research weather ship "Passat" (September-October 1977, see Figure 1). The dots denote the hydrological stations on the runs. In the western part of the region the dashed line outlines a rectangle of a mesosurvey consisting of 49 stations. The coefficient α, characterizing the degree of satisfaction of expression (3), was computed:

$$\alpha = \frac{S_1 - S_0}{S_0} - \frac{T_0 - T_1}{L/c - T_0}. \quad (4)$$

The inset in Fig. 1 shows histograms of the distribution of the parameters α, $\Delta S = S_1 - S_0$ and $\Delta T = T_0 - T_1$. We note a clearly expressed bimodality of these distributions. In the light of the above it can be interpreted in the following way. The ΔS and ΔT values, corresponding to the main peak on the histograms, have mean values 0.40°/oo and 5.52°C. In accordance with (4) this gives $\alpha = 3 \cdot 10^{-4}$, which is virtually equivalent to zero, since the terms in (4) have the order of magnitude $1 \cdot 10^{-2}$. The mean α value, corresponding to the main maximum on the histogram, computed using data for each station, has the value $\bar{\alpha} = 1.2 \cdot 10^{-3}$. This is about 10% of the value of the terms in (4). It can be asserted that for the main maximum stations with the histogram of the distribution of α, ΔS and ΔT the expression (3) is satisfied with adequate accuracy.

The second maximum on the histograms corresponds to large α and ΔS values and small ΔT values, that is, for stations of this maximum the expression (3) is not satisfied. It can be asserted that in the corresponding regions the considered convective penetrations mechanism plays no decisive role in formation of the SSM.

The α distribution over the area of the hydrological survey (Fig. 1) reveals a distinct regional localization of α values. In constructing the map use was made of three-point moving averaging of values along the hydrological runs. All the values corresponding to the main maximum on the histogram ($\alpha = 1.2 \cdot 10^{-3}$) were distributed in the northwestern region, whereas the second maximum ($\alpha = 4.8 \cdot 10^{-3}$) was in the southeastern region. Thus, in the survey area two regions are defined: in one of them there is satisfaction of expression (3), whereas in the other it is not satisfied. The boundary

between the regions can be regarded as the isoline $\alpha = 1 \cdot 10^{-3}$. The possibility of defining an extensive region in the ocean in which expression (3) is satisfied indicates the reality of existence of the considered mechanism of SSM formation through convective penetrations. It can be asserted that to the northwest of the isoline $\alpha = 1 \cdot 10^{-3}$ the subsurface salinity maximum has a local origin, but to the southeast is determined by the mechanisms in accordance with [4, 6, 7]. These conclusions are confirmed by the different nature of the vertical distributions of salinity and temperature, their different values in the SSM layer (Fig. 2).

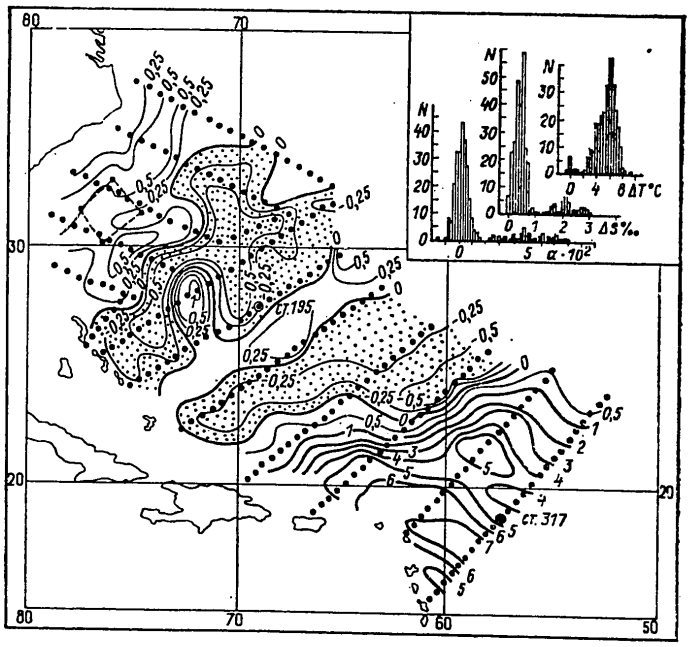

Fig. 1. Map of distribution of the α index. The inset shows histograms of the frequency of recurrence of the α, ΔT and ΔS values at survey stations.

We note that in each of the two defined regions there is a universal medium-scale intermittence of α values. It is manifested in the presence, on each of the hydrological runs, of extensive segments with a length of 200-500 km with low and high α values. The commensurability of such segments with the distances between runs makes the procedure of constructing a map of positioning of the first unambiguous. The map shown as Fig. 1 was constructed taking into account the correspondence between the defined medium-scale structures and the results of hydrodynamic modeling [2, 3]. According to these results, the horizontal circulation of the baroclinic layer in the

ocean has an intermittent cellular nature. In Fig. 1 the regions of negative α values are stippled. We note that the α distribution allows cellular interpretation. This fact can be regarded as a manifestation of the influence of the sign of vorticity of mesoscale circulation cells on the conditions of formation of the SSM. However, solution of this problem, like others relating to the adopted assumptions, is beyond the scope of this paper. We also note the problem of evaluation of the influence of temporal noncorrespondence between the measured salinity and temperature values in the SSM layer and at the surface. For satisfaction of expression (3) it is required that the S_1, T_1 values correspond to the water masses of the SSM layer forming from the surface waters at the times when the measurements are made.

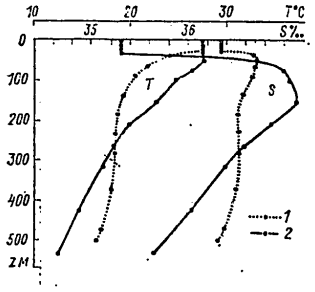

Fig. 2. Distribution of temperature and salinity with depth at two survey stations. 1) station 195 ($a = 1.3 \cdot 10^{-3}$); 2) station 317 ($\alpha = 4.3 \cdot 10^{-2}$). The location of the stations is shown in Fig. 1.

It is surprising that with all the adopted simplifications the resulting indirect criteria indicate the reality of the mechanism of SSM formation by the considered convective penetrations. Both macroscale and mesoscale ordering in the distribution of α over the area of the hydrological survey precludes randomness in obtaining such results.

The great importance of the corollaries associated with critical analysis of existing concepts concerning the mechanisms of energy exchange between the ocean and the atmosphere, following in the case of reality of the considered mechanism of SSM formation, requires a strictly unambiguous answer. However, in any case, whether such convective penetrations are confirmed or not, the observed phenomenon in the distribution of α requires further investigations.

BIBLIOGRAPHY

1. Bortkovskiy, R. S., Byutner, E. K., Malevskiy-Malevich, S. P., Preobrazhenskiy, L. Yu., PROTSESSY PERENOSA VBLIZI POVERKHNOSTI RAZDELA OKEAN-ATMOSFERA (Transfer Processes Near the Ocean-Atmosphere Discontinuity), Leningrad, Gidrometeoizdat, 1974.

2. Kutalo, A. A., "Horizontal Circulation of a Baroclinic Layer and Westerly Boundary Currents in the Ocean," OKEANOGRAFICHESKIYE ISSLEDOVANIYA (Oceanographic Investigations), No 25, Moscow, Sovetskoye Radio, 1976.

3. Kutalo, A. A., "Hydrodynamic Principles of Stability of Vertical Structures of Hydrological Fields in the Ocean," TRUDY GIDROMETTSENTRA SSSR (Transactions of the USSR Hydrometeorological Center), No 200, 1978.

4. Khanaychenko, N. K., SISTEMA EKVATORIAL'NYKH PROTIVOTECHENIY V OKEANE (System of Equatorial Countercurrents in the Ocean), Leningrad, Gidrometeoizdat, 1974.

5. Chernous'ko, Yu. L., Shumilov, A. V., "Evaporation and Microconvection in the Thin Surface Layer," OKEANOLOGIYA (Oceanology), Vol 11, No 6, 1971.

6. Defant, A., "The Atlantic Ocean Troposphere," WISS. ERGEBNISSE DTSCH. ATLANT. EXPEDITION AUF DEM "METEOR" 1925-1927, Bd. VI, T 1, Lief 3, 1936.

7. Montgomery, R. B., "Circulation in Upper Layers of Southern North Atlantic Deduced With Use of Isentropic Analysis," PAPERS IN PHYSICAL OCEANOGRAPHY AND METEOROLOGY, Vol VI, No 2, 1938.

8. Neumann, G., "Quantitative Relationships of Near-Surface Salinity Variations and Their Causes in an Area of the Western Tropical Atlantic," DEUTSCHE HYDROGRAPHISCHE ZEITSCHRIFT, Jg. 25, H 4, 1972.

UDC 551.464

VARIABILITY OF WATER SALINITY IN THE COASTAL ZONE OF THE SEA

Moscow METEOROLOGIYA I GIDROLOGIYA in Russian No 9, Sep 79 pp 66-70

[Article by Candidate of Technical Sciences G. S. Ivanov and Candidate of Geographical Sciences A. N. Ovsyannikov, State Oceanographic Institute, submitted for publication 20 November 1978]

Abstract: Observations of shore stations are used in determining the temporal and spatial variability of water salinity in the coastal zone of some Russian seas. The probability of different variability values is established and on this basis an optimum accuracy of ±0.1°/oo and a measurement method are recommended.

[Text] Water salinity in the oceans and open regions of seas is determined with an accuracy to ±0.02°/oo. The same high accuracy in determining water salinity has also been adopted in the network of sea shore stations in the coastal zone of Russian seas [2]. A relatively expensive and complex argentometric method is used for ensuring this accuracy at stations.

At the network of sea shore stations salinity samples are taken systematically, usually once a day. Along the coast the stations are separated from one another by a distance of tens and hundreds of kilometers. The question arises: is there justification for this accuracy in determining salinity at sea coastal stations under the conditions of the existing temporal and spatial discreteness?

For answering this question the authors examined the temporal (diurnal) and spatial (along the shoreline) variability of salinity in the surface layer of the coastal zone of Soviet seas. On the basis of the results it is possible to recommend the optimum accuracy in determining water salinity in the network of sea shore hydrometeorological stations.

Temporal Variability of Salinity

In order to ascertain the variability of water salinity with time we computed the differences in its values each 24 hours on the basis of data from shore stations (ΔS_{24}) and each 1 hour (within the 24-hour period) using data from roadstead stations (ΔS_1). Since at shore stations salinity is determined every day, a one-year series of observations is entirely adequate for our purposes. Data for 1964 were processed. At the considered roadstead stations (observations are not made more than 10 km from the shore) salinity is determined each hour in the course of 24 hours once a month. In order to have an adequate number of determinations, the processing included materials for several years (from 1961 through 1974). In each sea we selected stations situated in areas where there is a mixing of sea and fresh water and where it is virtually absent.

On the basis of the ΔS_{24} and ΔS_1 values for each station we calculated their probability. As an example, Fig. 1 shows the probability curve ΔS_{24} (n = 365) for the hydrometeorological station Klaypeda on the Baltic Sea. From similar probability curves for the considered 17 stations we read the values of the difference ΔS_{24} with 1, 5, 50, 68 and 95% probability. We computed the mean annual salinity values (S) and the ranges of its variability ($\Delta S_{24}max$). These values are given in Table 1.

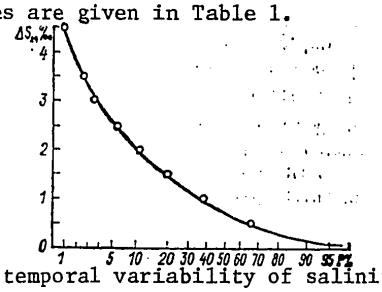

Fig. 1. Probability of temporal variability of salinity according to data from the Klaypeda hydrometeorological station.

It follows from this table that the variability of salinity is not dependent on its mean values but is dependent on the morphometric peculiarities of the place where the samples were taken and on the hydrometeorological processes characteristic for the particular sea area. The greatest variability of salinity is observed at stations situated near the mouths of rivers flowing into the sea. Such stations are Murmansk (mouths of the Kola and Tuloma Rivers), Okhotsk (Okhota River), Odessa (Dnestr River), Tyuleniy Island (Volga River) and others. The minimum salinity variability is observed at stations situated far from the influence of river runoff (Mysovoye, Moshchnyy, Ogurchinskiy Island). The fluctuations of temporal variability of salinity at the site where samples are taken are influenced by the wind direction and velocity, causing surges in the sea, tides and high waters in rivers.

At all the considered stations the variability of salinity at the σ level is considerably greater than 0.2°/oo. In sea areas subjected to the influence of river runoff, and they predominate in the coastal zone of the sea,

Table 1

Море 1	Станция 2	$\overline{S}$ ‰	ΔS_{24} max ‰	3 ΔS_{24} обеспеченностью, %				
				1	5	50	68	95
4 Азовское	13 Мысовое *	11,7	0,9	0,8	0,3	0,1	0,07	0,04
5 Аральское	14 Барса—Кельмес *	10,2	0,9	0,8	0,5	0,1	0,07	0,04
6 Балтийское	15 Клайпеда	5,4	4,5	4,3	2,6	0,7	0,4	0,1
	16 Мощный *	5,2	1,0	0,9	0,7	0,2	0,1	0,06
7 Баренцево	17 Мурманск	23,9	9,0	8,5	6,0	1,5	1,0	0,5
	18 Д. Зеленецкая	33,7	4,7	4,2	2,2	0,2	0,1	0,06
8 Белое	19 Кандалакша	13,0	7,5	7,2	4,6	1,3	0,9	0,4
9 Каспийское	20 о. Тюлений	4,8	4,0	3,5	2,3	0,6	0,5	0,3
	21 Астара	11,3	2,0	1,7	1,0	0,3	0,2	0,08
	22 о. Огурчинский *	13,6	1,0	0,8	0,4	0,1	0,07	0,04
10 Охотское	23 Охотск	31,2	4,5	4,0	2,0	0,5	0,4	0,3
11 Черное	24 Севастополь *	18,1	0,9	0,5	0,3	0,1	0,07	0,04
	25 Ялта	18,1	1,5	1,1	0,7	0,1	0,07	0,04
	26 Одесса	15,7	4,8	4,5	2,5	0,6	0,5	0,3
12 Японское	27 Владивосток	32,5	1,4	1,1	0,7	0,2	0,1	0,06
	28 Холмск	33,2	1,5	1,4	0,7	0,2	0,1	0,06
	29 Золотой *	33,0	1,0	0,8	0,6	0,2	0,1	0,04

30 * В районе станции нет стока пресных вод.

KEY:

1. Sea
2. Station
3. Probability
4. Sea of Azov
5. Aral Sea
6. Baltic Sea
7. Barents Sea
8. White Sea
9. Caspian Sea
10. Sea of Okhotsk
11. Black Sea
12. Sea of Japan
13. Mysovoye
14. Barsa-Kel'mes
15. Klaypeda
16. Moshchnyy
17. Murmansk
18. D. Zelenetskaya
19. Kandalaksha
20. Tyuleniy Island
21. Astara
22. Ogurchinskiy Island
23. Okhotsk
24. Sevastopol'
25. Yalta
26. Odessa
27. Vladivostok
28. Kholmsk
29. Zolotoy
30. * In the station region there is no runoff of fresh water

The accuracy of an individual salinity determination is ±0.1°/oo; with a discreteness of 24 hours this is ensured in 80-95% of the cases. Salinity variability values also remain considerable with a discreteness of its determinations to 1 hour. This is indicated by ΔS_1 values with probabilities 1, 5, 50, 68 and 95%, cited in Table 2.

This table shows that the salinity variability at the 68% probability level, even with a discreteness of determination of 1 hour, considerably exceeds 0.02°/oo and for the considered 6 points is 0.07-1.4°/oo. An increase in the variability values in hour time intervals in comparison with 24-hour intervals (Murmansk, Odessa) is attributable, on the one hand, to a change in the site of taking of samples, and on the other hand, the considerably greater and long-term series used in processing the roadstead stations. The change in the place of taking the samples also exerts an influence on mean salinity (Murmansk, Odessa). The ΔS_1 values show that with a considerable decrease in the discreteness in determining salinity to 1 hour an accuracy of ±0.02°/oo is excessive.

Table 2

Море 1	Рейдовая станция 2	$\overline{S}$ °/oo	ΔS_1 max °/oo	3 ΔS_1 обеспеченностью, % 1	5	50	68	95	Число наблюдений 4
5 Азовское	9 Темрюк	10,9	5,3	5,3	2,6	0,4	0,3	0,2	688
6 Баренцево	10 Мурманск	16,5	8,7	8,7	6,2	1,8	1,4	1,0	1430
7 Каспийское	11 Огурчинский	13,5	0,9	0,8	0,5	0,1	0,07	0,04	997
	12 Изберг	11,6	3,8	3,8	1,8	1,3	1,0	0,7	1308
8 Черное	13 Туапсе	17,5	1,1	1,0	0,6	0,1	0,07	0,05	1030
	14 Одесса	14,7	8,6	8,6	4,3	1,2	0,9	0,7	1099

KEY:

1. Sea
2. Roadstead station
3. Probability
4. Number of observations
5. Sea of Azov
6. Barents Sea
7. Caspian Sea
8. Black Sea
9. Temryuk
10. Murmansk
11. Ogurchinskiy
12. Izberg
13. Tuapse
14. Odessa

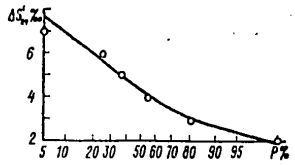

Fig. 2. Probability of values of spatial variability of salinity between hydrometeorological stations Neftechala and Svinoy Island.

Spatial Variability of Salinity

In order to determine the variability of salinity along the shoreline of the coastal zone of the sea we computed the differences ($\Delta S'_{24}$) of its synchronous determinations at adjacent stations for the 15th of each month during the

Table 3

1	Пары станций	$\Delta S'_{24}$ 5%	$\Delta S'_{24}$ 50%	$\Delta S'_{24}$ 95%	Расстояние L, км 2	$\frac{\Delta S'_{50}}{L}$
3	Азовское море					
6	Таганрог	0,4	5,0	2,8	115	0,04
7	Жданов	6,8	4,0	2,2	70	0,06
8	Бердянск	4,2	2,0	1,1	295	0,01
9	Мысовое	6,4	1,8	1,0	70	0,02
10	Опасное	9,4	4,7	2,6	60	0,08
11	Темрюк	9,2	4,7	2,6	110	0,04
12	П. Ахтарск	7,4	4,0	2,2	115	0,03
13	Ейск	10,4	7,3	4,0	80	0,09
4	Каспийское море (западное побережье)					
15	Астара	3,0	2,5	1,4	90	0,03
16	Нефтечала	7,7	4,3	2,4	70	0,06
17	о. Свиной	0,6	0,3	0,2	70	0,004
18	Баку	2,0	0,4	0,2	70	0,01
19	Жилой	4,0	1,8	1,0	145	0,01
20	Кызыл-Буруи	3,5	2,2	1,2	125	0,02
21	Дербент	3,0	1,8	1,0	65	0,03
22	Изберг	4,0	2,8	1,6	60	0,05
5	Черное море					
24	Приморское	5,1	2,8	1,4	130	0,02
25	Одесса	4,7	2,0	1,1	65	0,03
26	Тендра	5,3	3,0	1,8	125	0,02
27	Скадовск	1,4	0,4	0,2	30	0,01
28	Хорлы	2,5	1,3	0,7	115	0,01
29	Черноморское	1,2	0,3	0,2	95	0,003
30	Евпатория	0,8	0,3	0,2	65	0,005
31	Севастополь	0,7	0,3	0,2	10	0,03
32	Херсонес	0,6	0,2	0,1	75	0,003
33	Ялта	1,0	0,5	0,3	115	0,004
34	Феодосия	1,2	0,5	0,3	115	0,003
35	Анапа	1,3	0,6	0,3	45	0,01
36	Новороссийск	1,0	0,4	0,2	30	0,01
37	Геленджик	2,0	1,0	0,6	95	0,01
38	Туапсе	5,4	2,3	1,4	255	0,01
39	Очамчире	3,8	1,3	0,7	65	0,02
40	Поти	3,1	1,3	0,7	65	0,02
41	Батуми					

KEY TO TABLE 3

1. Pairs of stations
2. Distance L, km
3. Sea of Azov
4. Caspian Sea (western shore)
5. Black Sea
6. Taganrog
7. Zhdanov
8. Berdyansk
9. Mysovoye
10. Opasnoye
11. Temryuk
12. P. Akhtarsk
13. Yeysk
14. Taganrog
15. Astara
16. Neftechala
17. O. Svinoy
18. Baku
19. Zhiloy
20. Kyzyl-Burun
21. Derbent
22. Izberg
23. Makhachkala
24. Primorskoye
25. Odessa
26. Tendra
27. Skadovsk
28. Khorly
29. Chernomorskoye
30. Yevpatoriya
31. Sevastopol'
32. Khersones
33. Yalta
34. Feodosiya
35. Anapa
36. Novorossiysk
37. Gelendzhik
38. Tuapse
39. Ochamchire
40. Poti
41. Batumi

---

period from 1961 through 1970. The $\Delta S'_{24}$ probability values were computed. As an example, Fig. 2 shows the probability curve for $\Delta S'_{24}$ between Neftechala and O. Svinoy stations (Caspian Sea), situated at a distance of 70 km apart. A study of the curve shows that the difference in the salinity values between these stations at one and the same moments in time attains 7.7°/oo with a probability 5%; 4.3°/oo with a probability 50% and 2.3°/oo with a probability 95%, that is, on the average in this water body salinity varies by 0.06°/oo in a distance of 1 km. The $\Delta S'_{24}$ values with a probability 5, 50 and 95% for pairs of stations in the Sea of Azov, Black Sea and along the western shore of the Caspian Sea are given in Table 3, from which it follows that with the existing positioning of the sea stations along the shore in not one of the considered seas is spatial interpolation of salinity in the coastal zone of the sea ensured with an accuracy to 0.02°/oo. Even in order to compute the salinity field between the stations with an accuracy to 0.1°/oo the distances between the stations in the Sea of Azov must average 2 km, in the Caspian Sea -- 3 km, in the Black Sea -- 10 km.

This investigation makes it possible to draw the following conclusions:

1. The temporal variability of salinity in the coastal zone of the seas is considerable and even with determinations each 1 hour is considerably greater than 0.02°/oo. Therefore, with the discreteness of 24 hours adopted in the network of sea stations the required accuracy in determining salinity of ±0.02°/oo is unjustifiably high.

2. With the existing spatial positioning of sea coastal stations at considerable distances from one another the interpolation of salinity along the coast is impossible with an accuracy to ±0.02°/oo.

3. In the network of sea shore stations it is necessary to replace the argentometric method for determining the salinity of water by the areometric method, which makes it possible, using the tables in [3], to convert the specific gravity of water into salinity with an accuracy to 0.1°/oo or to determine salinity by electric salinometers with the very same accuracy [1].

4. The argentometric method can be retained at several "secular" stations in the sea located in water areas little subject to the influence of the fresh runoff of rivers.

BIBLIOGRAPHY

1. Ivanov, G. S., Ovsyannikov, A. N., "Variability of Sea Hydrological Elements and Computation of the Discreteness of Observations," METEOROLOGIYA I GIDROLOGIYA (Meteorology and Hydrology), No 11, 1973.

2. NABLYUDENIYA NA GIDROMETEOROLOGICHESKOY SETI SSSR (Observations in the Hydrometeorological Network USSR), edited by O. A. Gorodetskiy, Leningrad, 1970.

3. OKEANOGRAFICHESKIYE TABLITSY (Oceanographic Tables), Leningrad, Gidrometeoizdat, 1975.

UDC 551.466.2

COMPUTATION OF PARAMETERS OF RESONANCE FRONTAL WAVES

Moscow METEOROLOGIYA I GIDROLOGIYA in Russian No 9, Sep 79 pp 71-75

[Article by Candidate of Geographical Sciences G. G. Kuz'minskaya and T. I. Tsareva, Sochi Wave Research Station, submitted for publication 11 January 1979]

Abstract: Since atmospheric disturbances usually occur on tropospheric fronts, in a case when pressure gradients over the sea are weak there is basis for relating wave development directly to movement of a front. G. V. Ivankov, G. V. Matushevskiy and G. V. Rzheplinskiy have advanced the hypothesis of formation of such waves when the sea surface is affected by fluctuations of atmospheric pressure. The authors of this article have made computations using formulas proposed by the mentioned authors. The results of the computations coincided with field observations.

[Text] It is known that atmospheric disturbances in the temperate latitudes arise for the most part on main tropospheric fronts, that is, on the discontinuity between tropical and polar or polar and arctic air. Some cyclones arise under the direct influence of the underlying surface; usually its influence is an additional factor. Under the conditions prevailing in the eastern part of the Black Sea an additional front develops, passing parallel to the line of mountains and caused by their influence.

It is also known that the intensity of waves increases sharply in frontal zones. It is noted in [1, 4-6] that high (to hurricane force) wind velocities are associated more frequently with cold fronts -- primary and secondary, then with warm fronts, less frequently with occluded fronts. The slope of the atmospheric front to the horizon is very small: from 0.001 to 0.01. Therefore, although a frontal line is plotted on the chart of surface analysis of synoptic processes, in actuality this is not a line, but a region of separation of air masses. In this region there are strong turbulent air movements.

The authors of [3] analyzed the synoptic conditions causing one of the cases of waves in the Sochi region in March 1973. In the considered case the atmospheric pressure gradients over the sea were very small, the winds were weak and could not cause the waves with a height up to 4.4 m which were observed in nature. The authors postulated that these waves were caused by the passage of a cold front. In [2] such waves are caused by resonance waves because it was assumed that they were generated by fluctuations of atmospheric pressure during the passage of a cold front.

That same study gave a formula for the computation of the frequency σ of resonance waves

$$\sigma \approx \frac{g}{U}, \tag{1}$$

where U is the velocity of frontal movement and it was noted that spectral energy density increases with an increase in U; the value of the scaling factor a according to data for wind waves is

$$a \sim U^n, \quad n = 4 \div 6. \tag{2}$$

Now we will compare our field data on the wave elements during the passage of atmospheric fronts and weak winds over the sea ($\leqslant$ 5 m/sec) with the results of computations using these formulas.

The period of the waves for the maximum of spectral density is

$$\frac{2\pi}{\tau_{max}} \approx \frac{g}{U}, \quad \tau_{max},\ сек \approx \frac{6{,}28\ U,\ м/сек}{9{,}81} \approx \frac{6{,}28\ U,\ км/ч}{9{,}81 \cdot 3{,}6} \approx 0{,}18\ U \quad \text{km/hour.}$$

[cek = sec; km/ч = km/hour]

Using the dependence of the mean wave period $\bar{\tau}$ on τ_{max}, $\bar{\tau} = 0.85\tau_{max}$, we obtain

$$\bar{\tau},\ \text{sec} \approx 0.15U,\ \text{km/hour}. \tag{3}$$

Assuming the square of mean wave height $\bar{h}$ to be proportional to the maximum of the spectral density of energy, and the spectral width to be inversely proportional to U, in accordance with (3) we obtain

$$\bar{h} \approx cU^{\frac{n-1}{2}}, \tag{4}$$

$$h_{5\%} = 1{,}95\ \bar{h} \approx cU^{\frac{n-1}{2}} \cdot 1{,}95, \tag{5}$$

and the coefficient c must be determined using experimental data.

At our disposal we had six cases of the appearance of waves with the passage of a cold front in the region of Sochi and Novorossiysk (approaches to Sheskharis). One of these cases (the third in Table 1) is described in

[2, 3]. A comparison of the wave elements with the velocity of frontal movement for these cases is given in Table 1.

Table 1

Heights and Periods of Resonance Frontal Waves Arising During Movement of a Cold Front in the Black Sea

1 Место, дата и время наблюдения	U км/ч 2	$\bar{h}$ м	$h_{5\%}$ м	$\bar{\tau}$ сек 3
4 Сочи, 18 III 1970, 18 ч 30 мин	58	1,50	2,8	8,0
4 Сочи, 28 IX 1970, 12 ч 30 мин	35	0,50	1,0	6,0
4 Сочи, 05 III 1973, 18 ч 00 мин	65	1,76	3,4	9,4
5 Шесхарис, 08 XII 1975, 09 ч 00 мин	46	0,50	1,0	—
4 Сочи, 28 IV 1976, 17 ч 00 мин	35	0,46	0,9	4,6
4 Сочи, 27 IV 1977, 07 ч 00 мин	50	1,50	2,4	7,4

KEY:

1. Place, date and time of observation
2. km/hour
3. sec
4. Sochi...hours...minutes
5. Sheskharis...hours...minutes

For the third case in Table 1 $\bar{h}$ was assumed equal to $h_{max}/2.5$, and $h_{5\%}$ = $1.95/2.50\ h_{max}$ when h_{max} = 4.4 m in accordance with [2]. The mean period of the waves is assumed equal to $0.85\tau_{max}$ with τ_{max} = 10.5-11.4 sec.

Resonance frontal waves developed in those cases when the atmospheric pressure gradients were small or there was a wind from the shore.

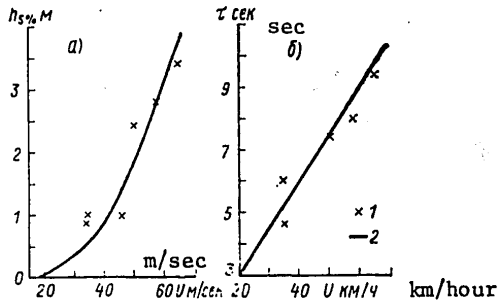

Fig. 1. Height (a) and periods (b) of waves arising during the movement of a cold front in the eastern part of the Black Sea. 1) according to field (experimental) data; 2) according to computations using formulas (1) and (6).

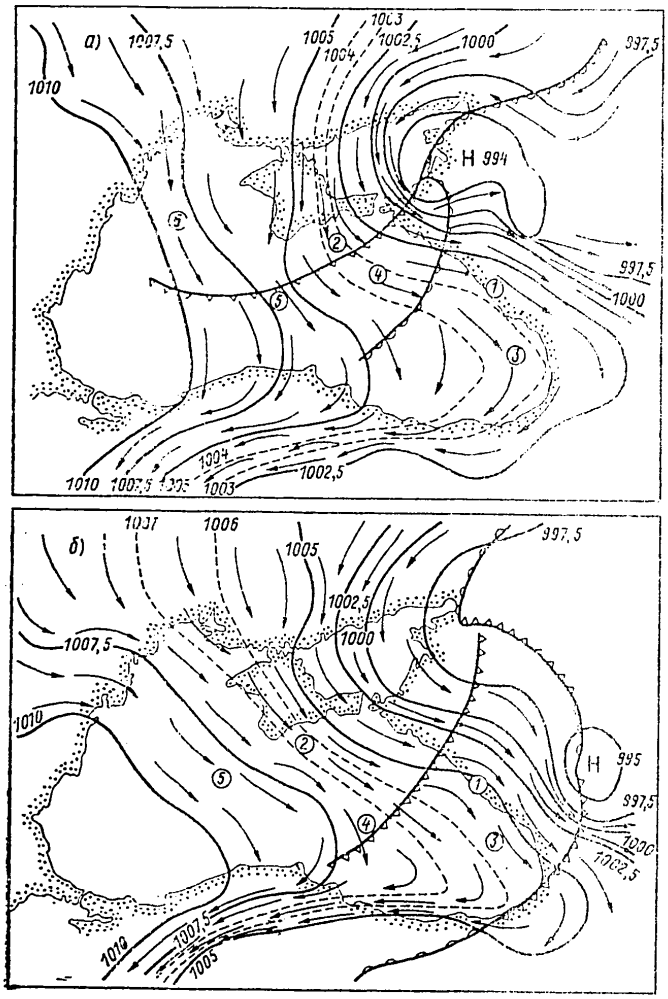

Fig. 2. Wind field on 18 March 1970 at 1200 (a) and 1500 (b) hours. The figures indicate computed points. H = low

The first case includes the observations of 18 March 1978, when computation of the waves from the wind, computed using the pressure gradient, gives $h_{5\%}$ = 1.0 m (2.8 m was observed) and the observations of 8 December 1975 when allowance for the pressure gradient leads to a wind velocity of 3 m/sec ($h_{5\%}$ = 1.0 m was observed).

The remaining observations belong to the second case (wind from the shore).

The data in Table 1 are plotted in Fig. 1, from which the empirical coefficients in formula (5) were selected. With these coefficients taken into account the following formula can be recommended for computing wave height

$$h_{5\%}\ M = 1{,}4 \cdot 10^{-5} U^3, \quad \text{km/hour.} \qquad (6)$$

Comparing (4) and (6), we obtain n - 1/2 = 3, that is, n = 7, which does not differ significantly from the n value obtained using formula (2).

Sometimes the frontal movement is associated with movement of a small cyclone on the periphery of a large cyclone. This case is a manifestation of the Fudziwara effect. The Fudziwara effect, named after the Japanese physicist who discovered this phenomenon, involves a change in the direction of movement of one cyclone under the influence of another cyclone or anticyclone. If two centers of action in the atmosphere are at such a distance from one another that the regions of their circulation intersect, each of them act on the other. Here three cases are possible:

a) if the intensity of both cyclones is identical, they begin to rotate one relative to the other in a counterclockwise direction and the center of rotation is situated in the middle between the centers of the cyclones;

b) if the intensity of one cyclone is small in comparison with the intensity of the other, the rotation will occur about the center situated near the large cyclone and accordingly the small cyclone will move more rapidly than the large one;

c) if the cyclone encounters a large anticyclone it will begin to move around this anticyclone in a clockwise direction.

The field of atmospheric pressure and the wind over the sea for a case determined by the influence of the Fudziwara effect are shown in Fig. 2. Under the influence of a large anticyclone situated to the west of the Black Sea the movement of the small cyclone began. At 1200 hours on 18 March 1970 its center was situated in the Sea of Azov region, and a clearly expressed atmospheric front passed in the central part of the Black Sea. The gradients of atmospheric pressure for the sea area were nonuniform: in the neighborhood of Kerch Strait -- 14 mb/degree of meridian, in the southeastern part of the sea -- 0.5 mb/degree. After 3 hours the situation had changed. The center of the cyclone and the region of high pressure gradients were displaced eastward from the Black Sea, to the Caucasus, and the cold front moved into the eastern part of the sea.

In this region the movement of a cyclone with a southerly component is unusual. It was caused by manifestation of the Fudziwara effect (case "c").

The quite good agreement of the results of computations of waves on the basis of frontal movement and observations is evidence in support of the considered computation method (see Fig. 1).

BIBLIOGRAPHY

1. Glazova, O. P., Bel'skaya, N. N., Kuznetsova, S. A., "Some Characteristics of Aerosynoptic Conditions of the Appearance of Hurricane-Force Winds," TRUDY GIDROMETTSENTRA SSSR (Transactions of the USSR Hydrometeorological Center), No 139, 1974.

2. Ivanenkov, G. V., Matushevskiy, G. V., Rzheplinskiy, G. V., "Resonance Excitation of Surface Waves in the Sea by Cold Atmospheric Fronts," IZVESTIYA AN SSSR, FIZIKA ATMOSFERY I OKEANA (News of the USSR Academy of Sciences, Physics of the Atmosphere and Ocean), Vol XIII, No 1, 1977.

3. Rzheplinskiy, G. V., Matushevskiy, G. V., Yeshchenko, L. A., "Unusual Swell Waves," METEOROLOGIYA I GIDROLOGIYA (Meteorology and Hydrology), No 3, 1975.

4. Sirotov, K. M., "On the Status and Development of Investigations of Waves in the Ocean," TRUDY GIDROMETTSENTRA SSSR, No 119, 1975.

5. Sirotov, K. M., Sett, L. S., "Curvature of Air Flows and Wind Waves in the Ocean," TRUDY GIDROMETTSENTRA SSSR, No 83, 1971.

6. Sirotov, K. M., Sett, L. S., "Evaluation of Forecasts of Waves in the Ocean," TRUDY GIDROMETTSENTRA SSSR, No 119, 1975.

7. Sitnikov, I. G., "BETSI," "KAMILLA" I DRUGIYE URAGANY ("Betsy," "Camille," and Other Hurricanes), Leningrad, 1975.

UDC 551.578.46

VARIABILITY IN SNOW DISTRIBUTION ON ICE IN THE ARCTIC OCEAN

Moscow METEOROLOGIYA I GIDROLOGIYA in Russian No 9, Sep 79 pp 76-85

[Article by Candidates of Geographical Sciences A. Ya. Buzuyev and I. P. Romanov, V. Ye. Fedyakov, Arctic and Antarctic Scientific Research Institute, submitted for publication 6 February 1979]

Abstract: On the basis of the results of statistical processing of data from measurements of snow depth a study was made of the variability of this element in dependence on hummocking and the age of ice.

[Text] The problem of how great a role is played by snow in formation of the ice cover has been repeatedly discussed [7, 11, 13].

It is also known that under definite circumstances the snow cover on Arctic ice exerts an important influence on navigation and the work of aviation and auto transportation.

An enormous amount of data has now been collected from measurements of snow depth on ice. Its generalization made it possible to obtain general ideas concerning the variation of snow accumulation on ice and to define regions with high and low snow accumulation [7, 13] and also to formulate procedures for taking snow depth into account in calculations of ice thickness [5, 10, 11]. In the mentioned studies reference is to mean snow depths.

Considerably fewer investigations have been made of the variability of depths and the peculiarities of the spatial distribution of snow on ice of different age and hummocking. And this is not accidental. Most of the measurements are data from standard snow surveys on shore ice, which are usually carried out at several points without taking into account the scale and nature of spatial changes of the considered element. Only the use of the results of special observations carried out sporadically made it possible to obtain information on the statistical structure of snow distribution (correlation functions, distribution law) for some age types of ice with different hummocking [1, 2], to estimate the variability of snow depth on the shore ice in the northeastern part of the Kara Sea [8].

The peculiarities of snow distribution on the ice in the Arctic Ocean can be considered in greater detail by using additional materials obtained during recent years.

It must be stated that measurements of snow depth are made by different methods. Therefore, before proceeding to an analysis of the results, we will briefly examine the sequence for obtaining initial data and their volume.

a) Profile observations on the shore ice of arctic seas. Five measurements are made each 100 m on two mutually perpendicular segments each with a length of 500 m [9].

The site for the profiles is usually selected at a distance of 100-300 m from the shore.

The analysis was made using data for 34 polar stations (14 in the Kara Sea, 12 in the Laptev Sea, 6 in the East Siberian Sea and 2 in the Chukchi Sea), a total of more than 5,000 profiles run during the period 1960-1975.

Profile observations are made during the entire snow accumulation cycle, from the moment of forming of the ice cover (September-November) to the total melting of the snow (May-July).

The shortcomings of this material are as follows:
-- the number of measuring points does not change with time, that is, has no dependence on the scales of variability of snow cover depth. Therefore, the problem of the representativeness of changes for this region remains open;
-- in many cases there is no detailed description of the survey routes and accordingly it is frequently impossible to ascertain where the snow depth was measured: on an even sector, slope of a hummock or its crest (in the presence of hummocking).

b) Data from special snow surveys are made:
-- optionally on the "Severnyy Polyus" drifting stations;
-- in support of operations for delivery of freight to Cape Kharasavey (February-April 1975-1977);
-- during expeditions on shore and drifting ice in arctic seas (March-June 1960-1977).

Special snow surveys as a rule had the objective of obtaining detailed information on the distribution of snow on ice, taking into account its age and hummocking. The measurements were made along routes with an extent from 100 to 10,000 m with intervals between measurements of 1.5 or 10 m and usually intersected all relief forms characteristic for the ice cover.

The carrying out of such detailed surveys is a time-consuming task; they have been carried out in different seasons and in different regions and do not take in the entire diversity in the distribution of snow on ice.

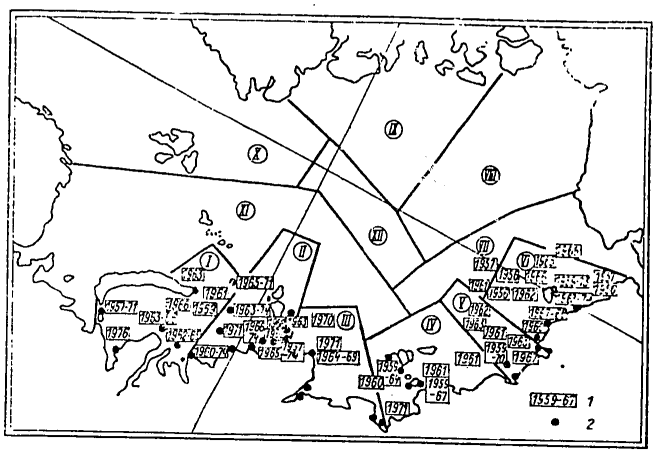

Fig. 1. Regions of the Arctic Ocean within whose limits the generalized characteristics of the variability of snow depth were obtained. 1) place and years of carrying out snow-measuring surveys on ice in sea; 2) polar stations for which data from profile snow surveys on the ice were used.

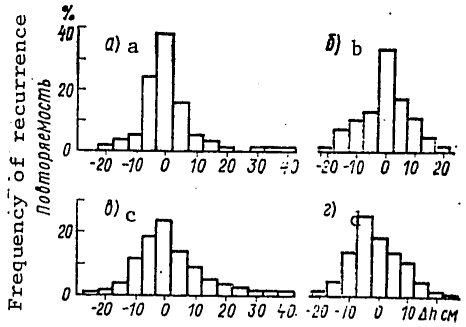

Fig. 2. Histograms of distribution of deviations of snow depth Δh from their mean value characteristic for two-year (d), one-year thin (c), one-year average thickness (b) and thin (a) ice in December-February. Along y-axis: Frequency of recurrence

c) Data from optional observations carried out at landing points on the ice on the "Sever" expedition (March-May 1974-1978). The method for these observations was developed by I. P. Romanov and involved the following.

The peculiarities of snow distribution are evaluated first from aboard an aircraft by visual means in the region of the proposed landing and the characteristic sectors in which measurements must be made are noted. After the landing of the aircraft 10-20 measurements of snow depth are made in each sector at arbitrarily selected points on different relief forms (even sector, freezing snowdrifts, ridges of hummocks, etc.).

The depth of snow in snow banks is measured at the base, in the middle and final parts; usually the measurements involved 10-12 snow banks.

The information, averaged using data from the enumerated measurements, served as the initial data for analysis.

The processing of observational data was preceded by the breakdown of the entire area of the Arctic Ocean into regions (Fig. 1).

In order to characterize the variability of snow depths in regions I-VI we used primarily materials from profile measurements; also given are data from numerous observations on the drifting ice.

Due to the low information content of individual series of profile measurements first for each series we computed the values

$$\overline{h} = \frac{\sum_{i=1}^{n} h_i}{n}; \quad \Delta h_i = h_i - \overline{h},$$

where h_i is the depth of the snow at the point, cm; $\overline{h}$ is the mean depth of the snow according to the particular series of measurements, cm.

Then the Δh_i values for 5-cm intervals were combined in dependence on the region, the intensity of snow accumulation, hummocking, mobility and age type of the ice. As a result of the grouping each set of observations was assigned an index (Table 1). For example, the index I-D-5 denotes that the particular set of observations includes available data from measurements of snow depth, carried out in region I on two-year shore ice, hummocking in class 1-2 during a period of "gradual" snow accumulation (December-February).

An analysis of the collected data (66 histograms were constructed on the basis of data from 14,000 measurements) indicated that the distribution of the Δh value has the following characteristics:
-- for all the periods of snow accumulation the center of the dispersion coincides with the center of the distribution; the histograms are somewhat asymmetric and are displaced in the direction of positive Δh;
-- with an increase in the ice thickness (an increase in "age") the probability $\Delta h = 0$ decreases.

On the basis of the results of processing of these data it was not possible to detect the influence of hummocking on the variability in snow distribution, which is completely understandable in the case of a low significance of individual observation series.

The histograms constructed for different conditions of formation of the snow cover differ extremely insignificantly (Fig. 2). Even on even ice of different age the histograms of the Δh distribution have much in common.

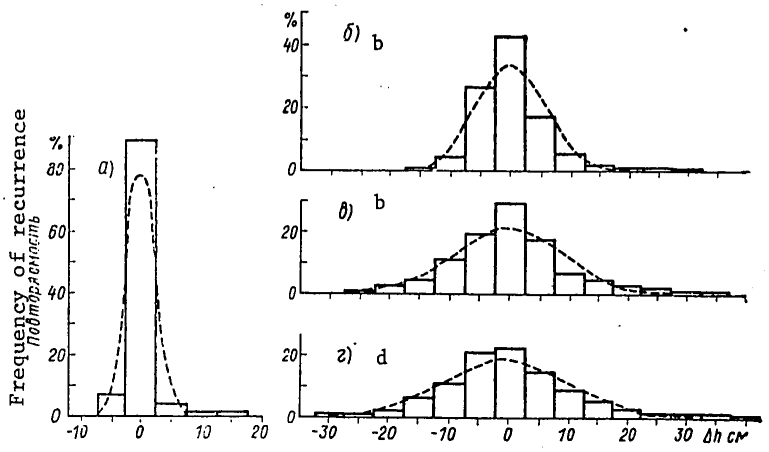

Fig. 3. Histograms of Δh distribution and their approximation (dashed curve) for mean snow depths 0-5 (a), 10-15 (b), 20-25 (c), 30-35 cm (d). Along y-axis: Frequency of recurrence

In addition, for the relatively even surface of the ice cover (hummocking $<$ 2b) the mean snow depths along the profiles vary in a wide range and differ little for ice of different age (Fig. 2). These changes are most conspicuous only with time, especially in regions I-II (Table 2).

In accordance with the above, a further analysis of the initial data was made on the assumption that the variability of snow depths in regions I-VI is determined by the background of snow accumulation (in other words, by the mean snow depth $\bar{h}$).

The processing of the data was accomplished in the following way:
-- series of measurements (to be more precise -- the values $\Delta h_i = h_i - \bar{h}$) were combined within the limits of each region by groups, in dependence on the level of mean snow depth ($\bar{h}$ = 0-5, 6-10, etc.),
-- histograms were constructed for the combined series and the distribution parameters were computed (Fig. 3).

For all the histograms the center of the distribution coincides with the center of the dispersion, the asymmetry coefficient rapidly decreases with an increase in $\bar{h}$ (Table 3), and the limitation of each distribution at the left is the $-\bar{h}$ value.

The presence of asymmetry, and also the nature of its changes with an increase in $\bar{h}$ (Table 3) reflects the peculiarities and distribution of snow on the ice and the method for making the measurements.

In actuality, with small $\bar{h}$ values individual significant deviations from the mean play a significant role in the "deformation" of the distribution. With an increase in $\bar{h}$ the influence of individual measurements is reflected to a lesser degree and the asymmetry tends to zero. This fact is confirmed by the positive asymmetry values computed from observational data (Table 3).

Table 1

Volume of Observations of Snow Depth for Each Group of Standard Conditions of Snow Accumulation in Region 1

Период снегонакопления 1		«Интенсивное» (сентябрь—ноябрь) 2				«Постепенное» (декабрь—февраль) 3				«Эпизодическое» (март—май) 4			
Характер ледяного покрова 5	подвижн. 6	припай 7		дрейф. лед 8		припай 7		дрейф. лед 8		припай 7		дрейф. лед 8	
	торосист. (баллы)	1—2	>2	1—2	>2	1—2	>2	1—2	>2	1—2	>2	1—2	>2
10 Возрастной вид льда	индекс 11	1	2	3	4	5	6	7	8	9	10	11	12
12 Многолетний	М 17	—	—	—	—	—	—	—	—	—	—	—	—
13 Двухлетний	Д 18	—	—	—	—	9	—	—	—	—	—	—	—
14 Однолетний толстый	О 19	—	—	—	—	333	—	—	—	361	514	—	—
15 Однолетний средней толщины	З 20	—	—	—	—	367	9	—	—	308	44	—	—
16 Однолетний тонкий (белый)	Б 21	—	—	—	—	269	—	—	—	62	—	—	—

KEY:

1. Snow accumulation period
2. "Intensive" (September-November)
3. "Gradual" (December-February)
4. "Sporadic" (March-May)
5. Nature of ice cover
6. Moving
7. Shore ice
8. Drifting ice
9. Hummocking (units)
10. Age type of ice
11. Index
12. Perennial (old)
13. Two-year
14. One-year, thick
15. One-year, average thickness
16. One-year, thin (white)
17. M
18. D (Д)
19. O
20. Z (З)
21. B (Б)

Table 2

Change in Mean Snow Depths (cm) With Time in Regions I-VI

Район 1	2 Диапазон средних высот снега		
	сентябрь—ноябрь 3	декабрь—февраль 4	март—май 5
I	6—9	16—22	29—36
II	5—8	17—22	29—36
III	4—10	10—16	13—23
IV	5—8	10—16	14—22
V	5—9	11—16	14—22
VI	4—12	11—16	16—22

KEY:
1. Region
2. Range of mean snow depths
3. September-November
4. December-February
5. March-May

Table 3

Value of Asymmetry Coefficient $S_k(\bar{h})$ in Distribution of Snow Depth Observed on One-Year Ice

	1 Диапазон средних высот снега $\bar{h}$, см						
	0—5	6—10	11—15	16—20	21—25	26—30	31—35
$S_k(h)$	2,314	1,222	0,875	0,863	0,574	0,488	0,540
2 Количество членов объединенных рядов	2145	2530	3100	2601	1922	1347	1007

KEY:
1. Range of mean snow depths $\bar{h}$, cm
2. Number of terms in combined series

Proceeding on the basis of what has been stated above, as a characteristic of the variability of snow depths on even ice we used a truncated normal distribution

$$\varphi(h) = \frac{C}{\sigma\sqrt{2\pi}} \exp\left[-\frac{(h_i-\bar{h})^2}{2\sigma^2}\right] \quad \text{when} \quad a \leq h \leq b, \qquad (1)$$

where C is a proportionality factor, $a = -\bar{h}$, $b = \infty$ (we recall that we are considering the Δh value).

Table 4

Values of Empirical Coefficients A, B

Возрастной вид льда (1)	Период наблюд. (2)	Число серий наблюд. (3)	A	B	$\frac{\sum_{i=1}^{n} h_i}{n}$ см	$\bar{h}_{min}$ см	$\bar{h}_{max}$ см
(4) Однолетний тонкий	(7) Сентябрь—ноябрь	199	0,422	0,835	7,4	0,8	24,4
(5) Однолетний средней толщины	(8) декабрь—февраль	349	0,489	0,863	16,0	1,8	63,2
(6) Однолетний толстый	(8) декабрь—февраль	315	0,687	0,743	15,4	1,3	55,1
(6) Однолетний толстый	(9) март—май	526	0,869	0,656	26,2	1,5	70,4

KEY:

1. Age type of ice
2. Observation period
3. Number of observation series
4. One-year thin
5. One-year, average thickness
6. One-year, thick
7. September-November
8. December-February
9. March-May

According to [12], if the general mean $\bar{h}_0$ is greater than double the general standard deviation σ_0, the coefficient C is close to 1 and the mathematical expectation M(h) and the standard deviation of the truncated normal distribution and the corresponding general values of the normal distribution are close in their values.

In the course of processing the material we obtained a dependence in the form $\sigma = f(\bar{h})$.

The approximation was made by the least squares method for the function $\sigma = A\bar{h}^B$ (Table 4). The results of the computations agree well with the initial data, and since in virtually all cases it was found that $\bar{h} > 2\sigma_h$, as the general characteristics in computations of the distribution of snow depths on one-year ice it is possible to use $\bar{h}$, σ_k assuming C = 1.

The results of the computations (Fig. 3) agree fairly well with the generalized observational data.

Thus, having information on the mean snow depths it is possible to compute the peculiarities of its distribution on even ice by using the expressions cited above. The situation is more complex with an evaluation of the influence of hummock formations on snow distribution. Up to the present time the method for carrying out snow surveys on ice with different degrees of hummocking has essentially remained undeveloped. This is attributable primarily to the complexity of measuring great snow depths in hummocked areas.

A generalization of the available measurements, made directly in hummocks (all the measurements were made at the end of the snow accumulation period) made it possible to obtain the dependence between the height H_{hum} of the hummocks and snow depth h. The dependence is fairly well approximated by the expression

$$h = 0{,}11\ H_T^{1{,}30}, \tag{2}$$

[$H_T = H_{hum}$] and the error in estimating the depth of the snow amidst the hummocks is 20%. The checking of dependence (2) using data from snow surveys on the shore ice at Cape Kharasavey in 1977 (these data were furnished through the courtesy of V. M. Klimovich) confirmed the correctness of this empirical expression.

The cited results agree with data from extremely representative observations of snow distribution in the vicinity of snow fences [3]. These observations, in particular, established that in regions with intensive blizzards snow fences cease to serve their purpose if the snow depth attains 2/3 of the height of the structure. As noted in [4], a great influence is exerted on snow accumulation by the "fetch" of the blizzard (in our case, the distance between the rows of hummocks) and the width of the snow-protecting structures (that is, the width of the hummock ridges). On the basis of theoretical investigations, field observations and modeling it was possible to obtain expressions making it possible to calculate the height of structures of a stipulated profile which will not be drifted over by snow, the width of snow accumulation zones. The use of these expressions is also justified in computations of the peculiarities of snow distribution on ice. In actuality, the computed relative "excess" of the structures (having a section similar to the section of a hummock ridge) above the snow surface is in the range 0.5-0.3 m. The "excesses" of the hummock ridges above the level of the snow surface vary precisely in such a range.

The influence of a barrier with the height H_{bar} on snow accumulation ceases to be felt, according to calculations, at a distance of about 20-30 H_{bar}.

The observational data indicate that the influence of hummock ridges on snow accumulation ceases to be felt precisely within these limits.

In zones of breaks in snow barrier structures there is formation of banks whose calculated height is approximately 2/3 H_{bar} and the predominant length is 20-30 H_{bar}.

According to the observations of I. P. Romanov, the snow depth in these banks attains 100 cm and their extent is about 14 m, which in general agrees with the data cited above. However, it must be taken into account that the broad use of the results of investigations [3, 4] in computations of the distribution of snow on ice is limited by the predominance of a random positioning of the hummock formations and rotation of the ice fields. These circumstances

do not make it possible to introduce into the computations such an important factor as the predominant direction of transfer. Accordingly, the peculiarities of snow distribution on ice with different degrees of hummocking are considered below as a random process.

On the basis of a generalization of the results of measurements of the heights of hummocks it was demonstrated that the collected data can be interpreted by a Maxwell distribution [6]. The probability density is determined by the expression

$$\varphi(x) = \frac{x^2}{\sigma_\tau^3}\sqrt{\frac{2}{\pi}}\,e^{-\frac{x^2}{2\sigma_\tau^2}}, \qquad (3)$$

where the σ_{hum} value is a parameter of the distribution and is expressed through the mathematical expectation $\bar{x}$ or the standard deviation σ

$$\sigma_\tau = \frac{\bar{x}}{1{,}596} = \frac{\sigma}{0{,}673}.$$

Substituting expression (2) into (3), after transformations we obtain an expression making it possible, in general form, to evaluate the distribution of snow in zones of hummock formations

$$\psi(h) = \frac{119{,}81\,h^{1{,}31}}{\sigma_\tau^3}\sqrt{\frac{2}{\pi}}\,e^{-\frac{28{,}94\,h^{1{,}64}}{2\sigma_\tau^2}}. \qquad (4)$$

Thus, for regions with different hummocking the distribution of snow depth on one-year ice is determined by the dependence

$$f(h) = \psi(h)S_\tau + \varphi(h)(1 - S_\tau), \qquad (5)$$

where S_{hum} is the area occupied by the hummocks; $\varphi(h)$ is the snow distribution on even sectors.

After knowing the general pattern of distribution of snow depths, it is possible to solve the problem of the necessary number of measurements n with which there is assurance of a stipulated accuracy in determining $\bar{h}$.

In conclusion, we will examine the variability of snow depths in the principal forms of snow relief: uniform cover on even one-year ice in frozen leads; zastrugi, banks, drifts on ice of different age; amidst hummock formations, etc.

The observational data used were the results of observations carried out on the "Sever" expeditions. The initial data were generalized for regions VII-XII (Fig. 1). It should be said at once that observations were made systematically for a total of five years, but for some elements, no more than two years.

Table 5

Mean Values and Limits of Changes in Snow Depths (cm) on Even Ice Sectors (h_{even}), in Hummocks (h_{hum}) and for Zastrugi (h_{zas})

Район 1	$h_р$ 2		$h_т$ 3		$h_з$ 4		2 $h_р$		3 $h_т$		4 $h_з$	
	ср.	пред.	ср.	пред.	ср.	пред.	ср.	пред.	ср.	пред.	ср.	пред.
	5	6	5	6	5	6						
	8 Толщина льда 30—70 *см*						8 Толщина льда 70—120 *см*					
VII	5	3—8	79	50—105	29	27—30	7	4—10	63	46—84	17	3—25
VIII	6	3—9	50	34—73	15	10—23	5	3—9	57	47—74	16	9—23
IX	5	3—9	129	88—170	29	10—40	4	2—6	125	65—167	27	8—45
X												
XI	4						4	3—5	62	42—80	17	7—30
XII	3	2—4	45	11—78	11	3—20	3	2—4	64	28—101	12	—
9 Среднее по всем районам	5	—	76	—	21	—	5	—	74	—	18	—
	Толщина льда 120—160 *см*						Толщина льда 160—200 *см*					
VII	6	4—11	58	36—76	23	19—30	12	3—30	89	58—170	41	20—85
VIII	6	5—8	64	58—75	20	14—32	9	6—14	85	55—150	30	19—60
IX	7	3—15	102	60—136	22	11—33	8	2—15	118	93—143	19	8—30
X	4	3—7	64	35—90	13	12—14	6	4—9	87	93—100	24	19—33
XI	5	3—7	73	63—89	21	13—25	6	3—8	73	60—102	22	15—30
XII	4	2—7	74	43—115	22	17—34	6	4—7	100	70—127	22	21—22
9 Среднее по всем районам	5	—	72	—	20	—	8	—	92	—	26	—

KEY:

1. Region
2. h_{even}
3. h_{hum}
4. h_{zas}
5. mean
6. limits
7. mean
8. Ice thickness...cm
9. Mean for all regions

The results of generalization of the data (Table 5) indicate that the mean value and amplitude in snow depths on even one-year ice of different thickness vary in a relatively narrow range through all the considered regions. One can only note a tendency to an increase in the mean depths with an increase in ice thickness. The mean values and variability of snow depths in zastrugi and amidst hummocked formations are considerably greater (Table 5).

The areas occupied by zastrugi and drifts vary in a wide range (Table 6), but due to the limited amount of initial data it was not possible to give a reliable characterization of this variability.

Nevertheless, the results given in Tables 5, 6 give a graphic idea concerning the principal peculiarities of the variability in the distribution of the snow cover on ice in the Central Arctic. These peculiarities supplement the quantitative characterization of the variability of snow depths which was formulated on the basis of the results of profile measurements and special snow surveys on ice of different age and hummocking.

Table 6

Generalized Characteristics for Zastrugi (Drifts) and Snow Banks in Frozen Lead

Район 1	2 Площадь, занятая застругами (надувами)				3 Характеристика снежных кос:			
	в замерзшем разводье 4		на основном льду 5		длина, м 6		высота снега в косах, см 7	
	средн. 8	пределы 9	средн.	пределы	средн. 8	пределы 9	средн.	пределы
VII	28	0—80	24	0—80	16	5—50	50	25—120
VIII	28	0—70	22	0—85	9	4—20	41	17—100
IX	24	0—60	19	0—40	15	6—55	50	35—100
X	32	0—40	18	0—60	12	—	50	—
XI	25	0—50	18	0—80	20	7—80	50	20—80
XII	24	9—40	20	0—60	12	7—20	46	20—75
10 Среднее по всем районам	27	—	20	—	14	—	48	—

KEY:

1. Region
2. Area occupied by zastrugi (drifts)
3. Characteristics of snow banks
4. In frozen lead
5. On main ice
6. Length, m
7. Snow depth in banks, cm
8. Mean
9. Limits
10. Mean for all regions

BIBLIOGRAPHY

1. Buzuyev, A. Ya., "Statistical Evaluation of the Spatial Distribution of the Principal Parameters of the Ice Cover," TRUDY AANII (Transactions of the Arctic and Antarctic Scientific Research Institute), Vol 326, 1975.

2. Buzuyev, A. Ya., Dubovtsev, V. F., "Statistical Characteristics of Some Ice Cover Parameters in the Arctic," TRUDY AANII, Vol 303, 1971.

3. Byalobzheskiy, G. V., et al., SNEGOZASHCHITNYYE SHCHITY I ZABORY (Snow Protection Panels and Fences), Moscow, Avtotransizdat, 1961.

4. Dyunin, A. K., MEKHANIKA METELEY (Mechanics of Blizzards), Novosibirsk, SO AN SSSR, 1963.

5. Kirillov, V. A., Spichkin, V. A., Belen'kaya, S. S., "Prediction of the Thickness of Shore Ice During Spring," TRUDY AANII, Vol 320, 1976.

6. Klimovich, V. M., "Characteristics of Hummocks on Shore Ice," METEOROLOGIYA I GIDROLOGIYA (Meteorology and Hydrology), No 5, 1972.

7. Loshchilov, V. S., "Snow Cover on Ice in the Central Arctic," PROBLEMY ARKTIKI I ANTARKTIKI (Problems of the Arctic and Antarctic), No 17, 1964.

8. Nazintsev, Yu. L., "Snow Accumulation on Ice in the Kara Sea," TRUDY AANII, Vol 303, 1971.

9. NASTAVLENIYE GIDROMETEOROLOGICHESKIM STANTSIYAM I POSTAM (Instructions for Hydrometeorological Stations and Posts), No 9, Part I, Gidrometeoizdat, 1968.

10. Sabinin, K. D., "On the Problem of the Influence of the Snow Cover and Water Heat on Ice Growth," OKEANOLOGIYA (Oceanology), Vol 3, No 1, 1963.

11. Tsurikov, V. L., "Analysis of Growth of Sea Ice Under a Snow Cover," OKEANOLOGIYA, Vol 3, No 3, 1963.

12. Shor, Ya. B., STATISTICHESKIYE METODY ANALIZA I KONTROLYA KACHESTVA I NADEZHNOSTI (Statistical Methods for Analysis and Monitoring of Quality and Reliability), Moscow, Sovetskoye Radio, 1962.

13. Yakovlev, G. I., "Snow Cover on the Drifting Ice of the Central Arctic," PROBLEMY ARKTIKI I ANTARKTIKI, No 3, 1960.

UDC 556.048

CHECKING OF STATISTICAL HYPOTHESES IN COMPUTATIONS OF MAXIMUM WATER DISCHARGES WITH A LOW GUARANTEED PROBABILITY OF OCCURRENCE

Moscow METEOROLOGIYA I GIDROLOGIYA in Russian No 9, Sep 79 pp 86-92

[Article by Candidate of Geographical Sciences A. V. Khristoforov, Moscow State University, submitted for publication 14 December 1978]

Abstract: The computation of maximum discharges is usually reduced to extrapolation of the guaranteed probability curves. The hypotheses on the form of the law of distribution of probabilities used in this case can serve as additional sources of computations. It is shown in this article that even great deviations of the true guaranteed probability curves from the hypothetical curves if they occur only in the region of extremal values, cannot be reliably detected by any statistical means. The author determined the range of the guaranteed probability values within whose limits the obtaining of any reliable evaluations is impossible without drawing upon additional information. The conclusions drawn are applied to a case when spatial-temporal generalizations are used in the computations

[Text] The determination of maximum water discharges with an annual excess probability from 0.1 to 0.0001, necessary for different water management computations, is usually reduced to extrapolation of the empirical guaranteed probability curves by the methods of the theory of random values and mathematical statistics [1, 3, 6].

The general scheme consists of three stages:
1. Adoption of the H_0 hypothesis concerning the form of the distribution law.
2. Evaluation of the unknown parameters determining the hypothetical distribution in the series of observations.
3. Checking of the correspondence between the adopted hypothesis and the sample.

The adopted hypothesis stipulates the approximating parametric family of distributions (Pearson family, three-parameter gamma distribution, etc.) or determines the rule of use of spatial-temporal generalizations, for example, by means of generalized guaranteed probability curves [1, 2].

Each drainage basin and each hydrological station is characterized by its own laws of fluctuations of runoff, dependent on the conditions for water supply to the river and movement of the flow along the channel; therefore, the deviation of the true distribution law from the hypothetical law always exists.

As a result, the total error in computing the maximum discharges with a low guaranteed probability consists of the errors caused by instability of the sample evaluations of the distribution parameters and the errors as a result of deviation of the true distribution from the hypothetical value [3]. The problems involved in the accuracy of determination of the parameters on the assumption of correctness of the adopted hypothesis at the present time have been investigated in considerable detail [1, 8]. However, the results of the erroneousness of the hypothesis, which can be particularly significant in computations of values with a rare frequency of occurrence, for the time being have been studied poorly. This article is devoted to an evaluation of the possibilities of checking the results from the adoption of hypotheses in computations of maximum runoff.

The principal difficulty in studying the total error in determining the guaranteed probability curves for runoff in the range of rare frequency of occurrence is as follows: even a very large deviation of the true guaranteed probability curve from the hypothetical curve, if it occurs only in the region of extremal values, cannot be reliably detected by any statistical means.

As a confirmation we will examine first the case of checking of the hypothesis on the particular form of distribution law obtained using an individual sample.

Assume that the hypothesis H_0, lying at the basis of the computation scheme, stipulates the guaranteed probability curve in the form $x_0(p; \theta_1, \ldots, \theta_s)$, where $\theta_1, \ldots, \theta_s$ are unknown parameters subject to evaluation using the sample $x_1, \ldots, x_N$. With any values of the parameters the function $x_0(p; \theta_1, \ldots, \theta_s)$ decreases with an increase in p and its curve has a convexity downwards with small values of the argument.

We will represent the true guaranteed probability curve in the form

$$x(p; \theta_1, \ldots, \theta_s, \theta_{s+1}, \ldots, \theta_{s+r}) = x_0(p; \theta_1, \ldots, \theta_s) + \sum_{i=1}^{r} \theta_{s+i} \varphi_i(p), \quad (1)$$

where the functions $\varphi_1(p),\ldots,\varphi_r(p)$ are equal to zero with $p \geqslant p_0$ and are monotonically decreasing convex downward in the segment $[0, p_0]$. The greater the r value, the more possibilities there are for describing different deviations from the H_0 hypothesis. In this particular case the H_0 hypothesis can be represented as

$$H_0: \theta_{s+1} = \ldots = \theta_{s+r} = 0. \tag{2}$$

The deviation of the true distribution from the hypothetical distribution occurs only in the region of small guaranteed probabilities p and will be the greater the greater are the parameters $\theta_{s+1},\ldots,\theta_{s+r}$ which are not taken into account.

The question arises as to the maximum admissible deviations of the true distribution from the H_0 hypothesis with which the methods of mathematical statistics still cannot exhibit a contradiction between the hypothesis and the true distribution of elements of the sample $x_1,\ldots,x_N$.

Extremely widespread and with optimality properties is the criterion of the probability ratio [5, 7], which refutes H_0 in the case of high values of the statistics τ:

$$\tau = -2 \ln \frac{\prod_{i=1}^{N} f(x_i; \theta_1^{**}, \ldots, \theta_s^{**}; \theta_{s+1}=0, \ldots, \theta_{s+r}=0)}{\prod_{i=1}^{N} f(x_i; \theta_1^{*}, \ldots, \theta_s^{*}, \theta_{s+1}^{*}, \ldots, \theta_{s+r}^{*})}, \tag{3}$$

where $f(x; \theta_1,\ldots,\theta_{s+r})$ is the probability density function, corresponding to the guaranteed probability curve (1), $\theta_1^*,\ldots,\theta_{s+r}^*$ are evaluations of the parameters of the true distribution by the maximum probability method. $\theta_1^{**},\ldots,\theta_s^{**}$ are evaluations of the parameters by the maximum probability method on assumption (2) of the H_0 hypothesis.

If the H_0 hypothesis is correct, the statistics τ has an asymptotically χ^2 distribution with r degrees of freedom. Otherwise the τ statistics has an approximately noncentral χ^2 distribution with r degrees of freedom and the noncentrality parameter ε.

$$\varepsilon = N \sum_{i,j=1}^{r} \theta_{s+i}\, \theta_{s+j}\, M\left\{ \frac{\partial \ln f}{\partial \theta_{s+i}} \frac{\partial \ln f}{\partial \theta_{s+j}} \right\}, \tag{4}$$

where M is the mathematical expectation symbol [5].

The following ratio follows from formulas (1), (4)

$$\varepsilon = N \int_0^{p_0} \left[1 + \frac{x_0'(p; \theta_1, \ldots, \theta_s)}{\sum_{i=1}^{r} \theta_{s+i}\, \varphi_i'(p)} \right]^{-2} dp \leqslant p_0 N, \tag{5}$$

since the derivatives x_0', φ_1',..., φ'_r are negative in the segment [0, p_0].

Table 1

Maximum Values of Probability Ratio Criterion

r	Уровень значимости α			
	0,01	0,05	0,10	0,20
1	0,03	0,11	0,18	0,30
16	0,08	0,19	0,30	0,45
50	0,05	0,16	0,27	0,42
500	0,02	0,06	0,11	0,21

KEY:
1. Significance level

If the random value $\chi^2(r, \varepsilon)$ has a noncentral χ^2 distribution with the parameters (r, ε), the random value $r + \varepsilon/r + 2\varepsilon\ \chi^2(r, \varepsilon)$ has an approximately χ^2 distribution with $r + \varepsilon^2/r + 2\varepsilon$ degrees of freedom [5]. With ε values not exceeding $\sqrt{r}$, the validity of this μ criterion differs little from the significance level α, that is, the probability of refuting the incorrect hypothesis H_0 is only a little greater than the probability of refuting H_0 when it is correct.

Table 1 gives the maximum $\mu(\alpha)$ values for the probability ratio criterion corresponding to the case $\varepsilon = \sqrt{r}$.

Accordingly, if the true distribution function differs from the hypothetical function only in the field of extremely high values, whose guaranteed probabilities do not exceed p_0, and the critical p_0 value satisfies the inequality

$$p_0 \leqslant \frac{\sqrt{r}}{N};\ r \geqslant 1, \tag{6}$$

then this criterion, despite its optimum properties, is unable to reveal even the largest possible errors in computing the guaranteed probability curve in the zone [0, p_0].

The complex H_0 hypothesis can be checked using the Pearson (χ^2) test [5, 7]. In this case there is stipulation of $k > s + 1$ intervals $A_1,\ldots,A_k$ and from the sample it is possible to determine the frequencies $p_1^*,\ldots,p_k^*$ of entry into the corresponding intervals; evaluations of the parameters $\theta_1^*,\ldots,\theta_s^*$ are found from the minimum of the function $\chi^2(\theta_1,\ldots,\theta_s)$.

$$\chi^2(\theta_1,\ldots,\theta_s) = N \sum_{i=1}^{k} \frac{[p_i^* - p_{0i}(\theta_1,\ldots,\theta_s)]^2}{p_{0i}(\theta_1,\ldots,\theta_s)}. \tag{7}$$

where $p_{0i}(\theta_1,\ldots,\theta_s)$ are the hypothetical probabilities of falling into the intervals A_i; i = 1,...,k.

The H_0 hypothesis is refuted in the case of high values of the statistics $\chi^2(\theta_1^*,\ldots,\theta_s^*)$. If the checked hypothesis is true, the statistics of the criterion has an asymptotically χ^2 distribution with k-s-1 degrees of freedom. Otherwise the $\chi^2(\theta_1^*,\ldots,\theta_s^*)$ value has an approximately noncentral χ^2 distribution with k-s-1 degrees of freedom and the noncentrality parameter δ [5, 7],

$$\delta \leq \delta_0 = N\sum_{i=1}^{k}\frac{[p_i - p_{0i}(\overline{\theta}_1,\ldots,\overline{\theta}_s)]^2}{p_{0i}(\overline{\theta}_1,\ldots,\overline{\theta}_s)}, \tag{8}$$

where $\overline{\theta}_1,\ldots,\overline{\theta}_s$ are the true values of the first s parameters in formula (1), and

$$p_i = p_i(\overline{\theta}_1,\ldots,\overline{\theta}_s,\overline{\theta}_{s+1},\ldots,\overline{\theta}_{s+r})$$

are the true probabilities of falling into A_i; i = 1,...,k, which coincide with $p_{0i}(\overline{\theta}_1,\ldots,\overline{\theta}_s)$ for all the intervals lying to the left of the point x_0, the guaranteed probability p_0.

The parameter δ_0 will be maximum when the end of one of the intervals coincides with the point x_0.

The (χ^2) criterion is oriented on detection of the discrepancies between the probability density functions and not the guaranteed probability curves. If we limit ourselves only to those breakdowns $A_1,\ldots,A_k$ for which large deviations of the hypothetical guaranteed probability curve from the true curve correspond to a high significance of the test, that is, for which the noncentrality δ is an increasing function of the parameters $\theta_{s+1},\ldots,\theta_{s+r}$ not taken into account, the significance of this criterion will be maximum with a tendency of the parameters $\theta_{s+1},\ldots,\theta_{s+r}$ to infinity. In this case the true probabilities of falling into intervals lying to the right of x0 tend to zero and accordingly, in this class of breakdowns $A_1,\ldots,A_k$ the noncentrality parameter satisfies the inequality

$$\delta \leq \delta_0 \leq p_0 N. \tag{9}$$

Thus, with r = k - s - 1 formula (6), as for the Pearson (χ^2) test, ensures the impossibility of checking the airs in computing the guaranteed probability curve in the region of high values.

As an illustration we will examine a three-parameter gamma distribution, determined by the mathematical expectation $\overline{X}$, the variation coefficients C_v and the asymmetry coefficients C_s. We will denote the values $\overline{X}$; C_v; $C_s/C_v - 2$ by θ_1; θ_2; θ_3. The guaranteed probability curves, corresponding to the values of the parameter θ_3 = 0; 1; 2 differ substantially from one another in the region of low guaranteed probabilities only in the segment [0, p_0], with p_0 equal to 0.02. Thus, this case from the practice of hydrological computations can be conditionally assigned to the situation described by the theoretical example (1), with s equal to 2 and r equal to 1.

The hypothesis of an ordinary gamma distribution ($C_s/C_v = 2$) corresponds to the H_0 hypothesis of equality of the θ_3 parameter to zero.

In [4] the statistical tests method was used in determining the validity of the (χ^2) test for checking the H_0 hypothesis against the alternative $\theta_3 = 1;2$.

It was found that with $N \leqslant 50$ the validity of the μ criterion differs little from the significance level α (by not more than 0.06-0.20). With N = 100 and breakdown into 20 equivalent intervals the significance functions become maximum.

Table 2

Significance of (χ^2) Test With N = 100; k = 20

θ_3	1 Уровень значимости α			
0	0,01	0,05	0,10	0,25
1	0,03	0,14	0,24	0,40
2	0,17	0,40	0,59	0,70

KEY:
1. Significance level

It follows from Table 2 that only with series of observations of 100 terms is it possible to reject the untrue H_0 hypothesis with $\theta_3 = 2$. With 1/N values greater than the critical guaranteed probability $p_0 = 0.02$ a reliable statistical checking is impossible, which precisely corresponds to formula (6), since in this case r = 1. The conclusions drawn can also be applied to a case when spatial-temporal generalizations are used for extrapolation of the guaranteed probability curves.

Assume that there are m samples representing runoff observations at different stations in a definite region. For the entire set of investigated random values we will use the hypothesis $\tilde{H}_0$ that the elements of the i-th sample conform to the distribution function $F_0(x; \theta_{i1},\ldots, \theta_{is})$, where the parameters $\theta_{i1},\ldots, \theta_{is}$ are subject to evaluation using the sample $x_{i1},\ldots,x_{iN_i}$.

In this case the very form of the function $F_0(x; \theta_1,\ldots, \theta_s)$ can first be determined using spatial-temporal generalizations, as in the case of construction of generalized guaranteed probability curves.

The criteria described above are also applicable for checking the hypothesis $\tilde{H}_0$. If τ_i and ε_i are determined using formulas (3), (4) for the i-th sample, the H_0 hypothesis with respect to the general form of the distribution law for the entire region must be refuted with large $\tilde{\tau}$ values, where

$$\tilde{\tau} = \sum_{i=1}^{m} \tau_i. \tag{10}$$

The $\tilde{\tau}$ statistics has an approximately noncentral χ^2 distribution with the noncentrality parameter $\tilde{\varepsilon}$,

$$\tilde{\varepsilon} = \sum_{i=1}^{m} \varepsilon_i. \tag{11}$$

Thus, if the region $[0, p_0]$ of deviation of the hypothetical guaranteed probability curves from the true values is quite small,

$$p_0 \leqslant \frac{1}{\sqrt{m\,\bar{N}}}, \tag{12}$$

where $\bar{N}$ is the mean arithmetical value of the lengths of the samples for the region, the validity of this criterion will again be inadequate.

Similarly, if χ_i^2 and δ_i are determined using formulas (7), (8), the hypothesis $\tilde{H}_0$ must be refuted with high values of the statistics $\tilde{\chi}^2$ [2, 4, 6],

$$\tilde{\chi}^2 = \sum_{i=1}^{m} \chi_i^2. \tag{13}$$

The $\tilde{\chi}^2$ statistics has a noncentral χ^2 distribution with m(k-s-1) degrees of freedom and the noncentrality parameter $\tilde{\delta}$,

$$\tilde{\delta} = \sum_{i=1}^{m} \delta_i. \tag{14}$$

Since $k-s-1 \geqslant 1$, expression (12) guarantees the impossibility of checking the erroneousness of the $\tilde{H}_0$ hypothesis in the field of low guaranteed probabilities $[0, p_0]$.

If the lengths of all the series are equal and the $\tilde{H}_0$ hypothesis is simple, for its checking we use the "guaranteed probability of guaranteed probabilities" method [2; 4; 6]. This method is used in determining the maximum terms in each sample $x_{i(N)}$ and the η_i values are computed

$$\eta_i = F_{0i}(x_{i(N)}); \quad i = 1, \ldots, m. \tag{15}$$

If the $\tilde{H}_0$ hypothesis is correct, the elements of the sample $\eta_1, \ldots, \eta_m$ have a distribution function equal to x^N in the segment [0; 1]. The correspondence of this sample to the particular distribution can be checked, for example, using the Kolmogorov λ-test.

The hypothetical distribution functions coincide with the true functions for all values of the random parameters whose guaranteed probabilities exceed p_0 and therefore the probability of rejecting the untrue hypothesis $\tilde{H}_0$ will be maximum in the limiting case when the deviations of the true guaranteed probability curves from the hypothetical curves tend to infinity

in the segment [0, p_0]. In this situation the law of distribution of random values η_i has the form

$$P\{\eta_i < x\} = x^N; \quad P\{\eta_i = 1\} = 1 - q_0^N, \quad \text{when } 0 \leqslant x \leqslant q_0, \tag{16}$$

where P is the probability sign, $q_0 = 1 - p_0$.

Table 3

Values of Function $\psi(m, \alpha)$

Уровень значимости α [1]	Число пунктов m [2]			
	9	25	49	100
0,01	2,8	4,5	6,0	8,5
0,10	4,8	7,1	8,3	12,2
0,27	6,1	9,8	11,0	16,2

KEY:
1. Significance level
2. Number of points

The maximum significance of the particular criterion, corresponding to the limiting case, is determined by the expression

$$\mu(\alpha) \leqslant \alpha + 0{,}25 + P\left\{1 - \nu \geqslant \frac{\lambda(\alpha)}{\sqrt{m}}\right\}, \tag{17}$$

where ν is the frequency of the probability event q_0^N, determined from m tests, $\lambda(\alpha)$ is the quantile of guaranteed probability of α statistics of the Kolmogorov λ-test.

The computations show that with $N \geqslant 10$ in order for the significance of the $\mu(\alpha)$ criterion to exceed the significance level α by not more than 0.35 it is sufficient that the limit p_0 of the region of discrepancy of the hypothetical and true guaranteed probability curves satisfy the inequality

$$p_0 \leqslant \frac{1}{N\psi(m, \alpha)}. \tag{18}$$

The values of the $\psi(m, \alpha)$ function are given in Table 3.

The function $\psi(m, \alpha)$ was close to $\sqrt{m}$ and accordingly it can be concluded that expression (12) also for the "guaranteed probability of guaranteed probabilities" method leads to an inadequately great difference between the significance of this criterion and the significance level. In a case when the hypothesis $\tilde{H}_0$ is complex the necessary statistical evaluation of the unknown parameters makes the significance of the criterion still less [2, 4].

It must be noted that the presence of a correlation between the samples, possible deviations from stationarity and other deviations from the classical formulation of the problem favor a decrease in significance of the

criteria [4] and accordingly broaden the limits of the zone of total indeterminancy [0, p_0].

If the critical value of the guaranteed probability p_0 satisfies inequality (12), even the use of spatial-temporal generalizations does not make it possible to check the results of adoption of hypotheses on the form of the distribution using standard statistical means.

Thus, we have found the limits of the zone of guaranteed probability within which there can be some reliable extrapolation of the guaranteed probability curves for computations of maximum runoff.

BIBLIOGRAPHY

1. Blokhinov, Ye. G., RASPREDELENIYE VEROYATNOSTEY VELICHIN RECHNOGO STOKA (Distribution of Probabilities of River Runoff Values), Moscow, Nauka, 1974.

2. Yevstigneyev, V. M., Zhuk, V. A., Kalinin, G. P., Nikol'skaya, N. V., RASCHET RECHNOGO STOKA PO OBOBSHCHENNYM KRIVYM OBESPECHENNOSTI (Computation of River Runoff Using Generalized Guaranteed Probability Curves), Moscow, Izd-vo MGU, 1975.

3. Yevstigneyev, V. M., Zhuk, V. A., Khristoforov, A. V., "Accuracy of Computations of Maximum Water Discharges With a Rare Frequency of Recurrence," EKSPRESS-INFORMATSIYA VNIIGMI-MTsD (Express Information, VNIIGMI-MTsD (All-Union Scientific Research Institute of Hydrometeorological Information-World Data Center)), No 3(47), 1976.

4. Zhuk, V. A., Yevstigneyev, V. M., Chutkina, L. P., "Peculiarities of Use of Agreement Criteria in the Checking of Hypotheses on the Laws of Distribution of Characteristic Runoff Values," PROBLEMY GIDROLOGII (Problems in Hydrology), Moscow, Nauka, 1978.

5. Kendall, M. J., Stewart, A., STATISTICHESKIYE VYVODY I SVYAZI (Statistical Conclusions and Correlations), Moscow, Nauka, 1973.

6. Kritskiy, S. N., Menkel', M. R., "Evaluation of Probabilities of Frequency of Recurrence of Rarely Observed Hydrological Phenomena," PROBLEMY REGULIROVANIYA RECHNOGO STOKA (Problems in Regulation of River Runoff), No 6, Moscow, Izd-vo AN SSSR, 1956.

7. Leman, E., PROVERKA STATISTICHESKIKH GIPOTEZ (Checking of Statistical Hypotheses), Moscow, Nauka, 1964.

8. Rozhdestvenskaya, A. V., OTSENKA TOCHNOSTI KRIVYKH RASPREDELENIYA GIDROLOGICHESKIKH KHARAKTERISTIK (Evaluation of Accuracy of Distribution Curves for Hydrological Characteristics), Leningrad, Gidrometeoizdat, 1977.

UDC 551.515.3(47+57)

FREQUENCY OF RECURRENCE OF DUST STORMS IN THE TERRITORY OF THE USSR

Moscow METEOROLOGIYA I GIDROLOGIYA in Russian No 9, Sep 79 pp 93-97

[Article by Candidate of Geographical Sciences L. V. Klimenko and L. A. Moskaleva, Moscow State University, submitted for publication 16 February 1979]

Abstract: The distribution and frequency of recurrence of dust storms in the territory of the USSR are discussed. The article gives a map and description of the regional peculiarities of the appearance of dust storms and defines the role of economic activity in their appearance. The annual variation of dust storms in the places with their greatest frequency of recurrence is discussed.

[Text] The literature has repeatedly touched upon the problem of the reasons and conditions for the appearance of dust storms, their geographical distribution [2] and measures for contending with them; descriptions have been given for individual catastrophic cases and territories have been regionalized on the basis of the degree to which they are subject to dust storms [1]. Some studies give an analysis of the frequency of recurrence of this phenomenon for individual regions [3, 4, 6].

For example, a study by N. N. Romanov [4] contains statistical material on the frequency of recurrence of dust storms over the territory of Central Asia for a five-year period (1951-1955), maps were prepared showing total five-year values, and the annual and diurnal variation of dust storms; their genesis in dependence on different synoptic situations is analyzed. Yu. I. Chirkov and M. M. Agafonova [6] prepared a map of the mean long-term number of days with dust storms in the territory of the main agricultural regions of the USSR (except for Central Asia).

However, the available literature on dust storms does not give a sufficiently complete idea concerning their frequency of recurrence and distribution over the entire territory of the USSR where they are observed. Accordingly, an attempt has been made to bring together the available materials for the purpose of compiling a generalized map of the frequency of recurrence of

dust storms over the territory of the USSR (Fig. 1). The map was compiled using data from the HANDBOOK ON USSR CLIMATE [5] on the mean annual number of days with dust storms during a 25-year period, for the most part from 1936 through the beginning of the 1960's. For revealing greater detail concerning the phenomenon we initially prepared maps of the frequency of recurrence of the dust storms in individual regions for all meteorological stations listed in the corresponding handbook. Then the regional maps were reduced to a common scale of 1:10,000,000 on which we drew isolines with the values of the mean number of days with dust storms -- 1, 5, 10, 20 or more days. To the north, where the dust storms do not occur annually, their frequency of recurrence is small and irregular, it was not possible to draw continuous isolines of their mean annual number.

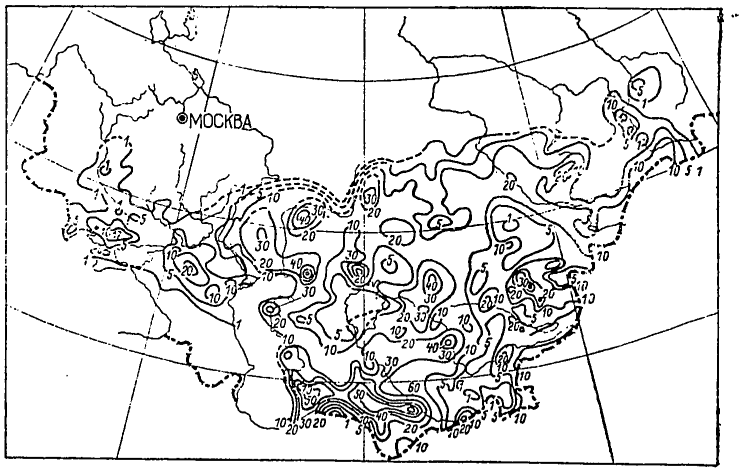

Fig. 1. Mean annual number of dust storms in the territory of the Soviet Union.

In the European part of the USSR, within the limits of the steppe zone, it is possible to discriminate two regions with an increased frequency of recurrence and duration of dust storms -- southern Ukraine and southeastern European USSR.

In the Ukrainian SSR there are three clearly expressed maxima of the frequency of recurrence of dust storms: first, in the Kherson-Kakhovka region, where the number of days with dust storms attains an annual average of 17.3 (Nizhniye Serogozy), second, in the Voroshilovgrad region and third, in the southwestern part of Odesskaya Oblast with its center in the neighborhood of Saratа.

In the southeastern European USSR an increase in the number of dust storms is observed within the Kumo-Manychskaya depression and the Sal'skiye steppes, where on the average there are up to 20-23 days annually with dust storms (populated places Gigant, Zavetnoye).

In the delta and floodplain of the Volga strong southeasterly and southerly winds cause salt storms in the spring and autumn when there is dessication of the lake: in spring -- to high water, and in autumn -- after the waters drop off [6].

In the remaining territory of the USSR dust storms are propagated in the southern part of Western Siberia, southwestern Central Siberia, in Kazakhstan and Central Asia.

In the southern part of Western Siberia dust storms occur in Tyumenskaya, Omskaya (Ishimskaya Steppe) and Novosibirskaya (Barabinskaya Steppe) Oblasts and Altayskiy Kray (Kulundinskaya Steppe).

In the southern part of Tyumenskaya Oblast the mean annual number of days with dust storms varies from 0.2 to 4, and in Omskaya Oblast -- from 0.3 to 12-13 days, gradually increasing southward. In the example of this region one can clearly see the influence of man's economic activity on the environment and the processes transpiring in it. After being plowed in the 1950's in the southern part of Omskaya Oblast the frequency of occurrence of dust storms on the average increased by a factor of 2.5, and according to data from Bol'sherech'ye and Pokrovo-Irtyshskoye stations -- by a factor of 5-6. In Novosibirskaya Oblast and Altayskiy Kray the mean annual number of days with dust storms reaches 20-28.

In the southern part of Krasnoyarskiy Kray and in the Tuvinskaya ASSR dust storms are observed most frequently in May-June, but also occur in winter when there is a small snow cover or when there is none. The greatest mean annual number of days with dust storms (up to 10-12) is observed in the Minusinskaya Basin and in the northeastern part of the Khakasskaya Autonomous Oblast.

Kazakhstan and Central Asia, with their extensive expanses of dry steppes, semideserts and deserts, are characterized by the greatest frequency of recurrence of dust storms.

The distribution of the mean annual number of days with dust storms in the extensive territory of Kazakhstan is nonuniform and to a considerable degree is local, which is associated not only with the wind velocity, but also the character of the underlying surface. In steppe regions with light sandy soils as an average for the year there are 20-30 days with dust storms. In the regions of sandy deserts of the Bol'shiye Barsuki sands and to the south of Balkhash, the Sary-Ishikotrau sands, the number of sand storms increases from 30-40 to 50-60 days. In territories with a heavy mechanical composition of the soils, and also in mountainous regions,

the number of days with dust storms decreases to 2 days per year [5].

In Central Asia the greatest frequency of recurrence of dust storms is noted in Turkmenia; this is attributable to the broad occurrence of poorly bound sands, gray desert soils and an exceedingly small quantity of precipitation (100-200 mm annually). Under such conditions dust storms can arise not only when there are considerable wind velocities (7-10 m/sec), but also when there are moderate winds (4-6 m/sec).

In the Tsentral'nyye and Zaunguzskiye Karakum and in the southwestern part of the republic in summer dust storms are observed on the average during the course of 6-8 days per month. Due to the great dryness of the soil and the absence of a snow cover dust storms also occur in Turkmenia in winter when their number attains up to 4-6 days per month [5].

Dust storms are also observed in the mountainous regions of Central Asia where their distribution, to a still greater degree than in the lowland territories, has a nonuniform, local character. In Kirgizia the greatest mean annual numbers of days with dust storms (14-16 days) are noted in the western part of the Issyk-Kul'skaya Basin and in the lowland part of the Chuyskaya Valley; in the Kochkorskaya Valley and in the neighborhood of Novorossiysk -- 12-13 days; in Daraut-Kurgan -- 10 days. At the remaining stations -- from 4 to 8 days per year. In Tadzhikistan the greatest frequency of recurrence of dust storms, from 20 days or more, is noted in the southern part of the republic, and in the Eastern and Southern Pamir -- on the average 8-14 days.

Thus, the map shows that the number of days with dust storms increases from the zone of the wooded steppes and steppes to the deserts of Central Asia. The focus of the maximum frequency of occurrence of dust storms for the USSR is situated in Turkmenia, where they are observed on the average not less than 40-50 days per year, with a maximum in individual places up to 80 or more days. The general pattern of frequency of recurrence of dust storms conforms to the geographic zonality. However, against this background there is a clearly expressed focal nature of the distribution of dust storms, which is caused both by the local natural peculiarities of the territories -- meteorological conditions, character of relief, soil-vegetation cover, mechanical composition of the ground -- and also man's economic activity. For example, plowing in regions with a relatively regular appearance of dust storms leads to the formation of their new centers with a high frequency of recurrence.

In addition to the mean annual number of days with dust storms, Table 1 gives the annual variation of the frequency of recurrence of dust storms for the regions most subject to these processes. In the regions of occurrence of sandy deserts dust storms can be observed throughout the year with a small variability in their frequency of recurrence from month to month and with a maximum falling in the hottest summer months (Repetek).

Table 1

Frequency of Recurrence (%) of Number of Days With Dust Storms

	Метеорологическая станция 1	2 Месяц I	II	III	IV	V	VI	VII	VIII	IX	X	XI	XII	3 Год, %	Среднее годовое число дней с пыльными бурями 4
5	Нижние Серогозы (Херсонская обл.)	—	0,6	5,8	17,3	7,5	8,7	15,0	17,3	19,1	6,9	1,2	0,6	100	17,3
6	Павлоград (Днепропетровская обл.)	—	0,7	3,4	18,9	24,0	12,0	17,1	12,0	5,1	1,7	1,7	3,4	100	5,84
7	Верхнеднепровск (Днепропетровская обл.)	—	3,1	0,9	12,4	14,1	12,4	17,1	17,1	17,1	4,7	1,1	—	100	6,43
8	Заветное (Ростовская обл.)	—	—	0,4	8,2	10,3	16,7	19,3	22,3	15,5	5,2	2,1	—	100	23,3
9	Гигант (Ростовская обл.)	—	—	3,9	15,0	10,2	13,6	15,0	19,0	15,0	4,4	2,9	1,0	100	20,6
10	Капустин Яр (Астраханская обл.)	—	—	—	7,4	16,9	18,2	19,6	16,9	13,5	6,8	0,7	—	100	14,8
11	Покрово—Иртышское (Омская обл.), 1936—1950 гг.	—	—	—	5,3	52,6	10,5	13,2	15,8	—	2,6	—	—	100	3,8
12	То же, 1951—1962 гг.	—	—	—	4,1	27,4	18,3	9,1	13,7	18,3	9,1	—	—	100	21,9
13	Алейская ж/д. ст. (Алтайский край)	—	—	0,1	6,0	19,1	20,5	17,0	15,6	12,8	7,1	1,4	0,4	100	28,2
14	Рубцовск (Алтайский край)	—	—	—	6,8	24,4	18,3	15,1	15,1	12,7	6,8	0,8	—	100	25,1
15	Буденовская (Хакасская АО)	1,0	2,0	5,9	16,6	31,3	11,8	1,0	3,9	5,9	7,8	10,8	2,0	100	10,2
16	Кызыл (Тувинская АССР)	—	—	—	8,6	29,7	28,9	12,5	7,0	5,5	5,5	2,3	—	100	12,8
17	Джамбейты (Уральская обл.)	—	—	—	4,4	17,0	19,2	18,7	19,2	13,9	6,8	0,4	0,4	100	45,9
18	Джалтыр (Целиноградская обл.)	—	—	—	4,2	21,5	18,8	18,1	14,0	13,2	9,4	0,8	—	100	26,5
19	Баканас (Алма-Атинская обл.)	0,2	0,2	2,7	11,5	14,7	16,8	17,3	14,7	11,3	7,1	2,7	0,8	100	47,7
20	Небит-Даг (Туркменская ССР)	4,2	3,7	8,0	8,8	9,8	11,2	10,5	11,5	12,2	9,8	7,3	3,0	100	60,0
21	Репетек (Туркменская ССР)	6,9	9,1	11,1	10,4	10,4	10,6	13,7	10,4	4,9	4,3	3,8	4,4	100	65,6

FOR OFFICIAL USE ONLY

APPROVED FOR RELEASE: 2007/02/08: CIA-RDP82-00850R000200030039-4

KEY TO TABLE 1

1. Meteorological station
2. Month
3. Year, %
4. Mean annual number of days with dust storms
5. Nizhniye Serogozy (Khersonskaya Oblast)
6. Pavlograd (Dnepropetrovskaya Oblast)
7. Verkhnedneprovsk (Dnepropetrovskaya Oblast)
8. Zavetnoye (Rostovskaya Oblast)
9. Gigant (Rostovskaya Oblast)
10. Kapustin Yar (Astrakhanskaya Oblast)
11. Pokrovo-Irtyshskoye (Omskaya Oblast) 1936-1950
12. Same, 1951-1962
13. Aleyskaya Railroad Station (Altayskaya Kray)
14. Rubtsovsk (Altayskiy Kray)
15. Budenovskaya (Khakasskaya Autonomous Oblast)
16. Kyzyl (Tuvinskaya ASSR)
17. Dzhambeyty (Ural'skaya Oblast)
18. Dzhaltyr (Tselinogradskaya Oblast)
19. Bakanas (Alma-Atinskaya Oblast)
20. Nebit-Dag (Turkmenskaya SSR)
21. Repetek (Turkmenskaya SSR)

In the more northerly, steppe regions dust storms arise for the most part in the warm season of the year. Frequently there are two maxima of their frequency of occurrence: in spring, when the fields are plowed, the vegetation cover is absent and strong winds blow, and at the end of summer-early autumn when the soils are dessicated and the fields are again plowed.

The plowing of some virgin lands in our country in the 1950's resulted not only in an increase in the number of dust storms, but also a change in the annual variation of their frequency of recurrence. Thus, in the example of the data for Pokrovo-Irtyshskoye station it can be seen clearly that after plowing there was a marked increase in the mean annual number of days with dust storms (Table 1). The dust storm maximum in this case does not fall in any one month (May), as was the case before plowing, but there is a smoother variation of the frequency of occurrence of dust storms in the course of the warm season of the year with a decrease in the spring maximum, an increase in the number of dust storms in the remaining months and the appearance of a second, autumn maximum approaching that of spring.

BIBLIOGRAPHY

1. Buchinskiy, I. Ye., ZASUKHI I SUKHOVEI (Droughts and Searing Winds), Leningrad, Gidrometeoizdat, 1976.

2. Zakharov, P. S., PYL'NYYE BURI (Dust Storms), Leningrad, Gidrometeoizdat, 1965.

3. PYL'NYYE BURI I IKH PREDOTVRASHCHENIYE (Dust Storms and Their Prevention), Moscow, Izd-vo AN SSSR, 1963.

4. Romanov, N. N., "Dust Storms in Central Asia," TRUDY SAGU (Transactions of Central Asian State University), NOVAYA SERIYA (New Series), No 174, FIZ-ICHESKIYE NAUKI (Physical Sciences), Kn 20, 1960.

5. SPRAVOCHNIK PO KLIMATU SSSR (Handbook of USSR Climate), No 10, Part 5, 1969; No 13, 17, 18, Part 3, 1967; No 19, 20, Part 3, 1966; No 21, Part 3, 1967; No 30, 31, Part 3, 1968; No 32, Part 3, 1967.

6. Chirkov, Yu. I., "Frequency of Recurrence of Dust Storms in the Territory of the USSR and the Possibility of Predicting Their Formation," TRUDY GIDROMETEOROL. NAUCHNO-ISSLED. TSENTRA SSSR (Transactions of the USSR Hydrometeorological Scientific Research Center), No 69, 1970.

UDC 551.50:633.11

MODELING OF THE PROCESS OF FORMING OF THE YIELD OF WINTER WHEAT

Moscow METEOROLOGIYA I GIDROLOGIYA in Russian No 9, 1979 pp 98-106

[Article by Candidates of Geographical Sciences M. S. Kulik, A. N. Polevoy and I. Ye. Vol'vach, All-Union Scientific Research Institute of Agricultural Meteorology, submitted for publication 3 April 1979]

Abstract: This article gives a dynamic model of formation of the yield of winter wheat describing the principal processes of vital activity of a plant (respiration, photosynthesis, growth of individual organs) and the influence of environmental factors on their intensity.

[Text] Yield formation is the complex totality of a whole series of physiological processes whose intensity is determined by the biological peculiarities of the plants, environmental factors and the interrelationship among the processes themselves.

However, the principal role in yield formation is played by photosynthesis. In grain ear crops the photosynthesis process can take place not only in the leaves, but also in the other above-ground organs -- leaf sheaths, stems and ears. The data given in [15] show that different plant organs assimilate with different intensities.

The ears have a relatively high intensity of photosynthesis. At the onset of the milky ripeness phase the intensity of photosynthesis of the awns, spikelet and flowering glumes of the ear is as great as for the leaves of the two upper levels and is considerably greater than for the leaves of the third level from above [11].

The photosynthesis of each of the photosynthesizing organs (leaves -- l, stems -- s, ears -- p) can be represented by the formula [19, 22]

$$\Phi_{0i}^{j} = \frac{\Phi_{\max i}\, b\, I^{j}}{[(b\, I^{j})^2 + \Phi_{\max i}^2]^{1/2}}, \tag{1}$$

where Φ_{0i} is the intensity of photosynthesis of the i-th organ under optimum conditions of heat and moisture supply and real illumination conditions (mg CO_2/(dm^2·hour)); $\Phi_{\max i}$ is the intensity of photosynthesis of the i-th organ in the case of light saturation and a normal CO_2 concentration (mg CO_2/(dm^2·hour)); b is the initial slope of the light curve of photosynthesis (mg $CO_2 \cdot dm^{-2} hour^{-2}$/(cal·$cm^{-2}$·$min^{-1}$)); I is the intensity of photosynthetically active radiation within the sown area (cal/(cm^2·min)). When determining the intensity of photosynthesis of ears I is assumed equal to the intensity of photosynthetically active radiation at the upper boundary of the sown area; j is the number of days in the computation period.

In ontogenesis the photosynthetic activity of the leaves and other photosynthesizing organs is determined by their age and change in internal structure. In the sprouting phase in spring crops and at the time of renewal of the growing season of winter crops only the forming leaves are not characterized by a high intensity of photosynthesis. Such a structure of the leaf (especially middle-level leaves) is formed by the "earing-flowering" phase which is optimum for their photosynthetic activity.

For computing the photosynthesis in ontogenesis under real environmental conditions different from the biological optimum, we write the expression

$$\Phi_{\tau}^{j} = \Phi_{0}^{j}\, \alpha_{\Phi}^{j}\, \Psi_{\Phi}^{j}\, \gamma_{\Phi}^{j} \tag{2}$$

[Ф = ph] where Φ_{τ} is the intensity of photosynthesis under real environmental conditions (mg CO_2/(dm^2·hour)), α_{ph} is the ontogenetic photosynthesis curve, ψ_{ph} and γ_{ph} are functions of the effect of environmental factors (air temperature and soil moisture content), representing single-peak curves approximated by the expressions

$$\Psi_{\Phi} = 0{,}2\, \frac{T_{\text{д}}^{j} - T_{\text{дп}}}{T_{\text{д опт}} - T_{\text{дп}}} \left[6 - \left(\frac{T_{\text{д}}^{j} - T_{\text{дп}}}{T_{\text{д опт}} - T_{\text{дп}}}\right)^5\right], \tag{3}$$

and

$$\gamma_{\Phi}^{j} = A_1 \exp\left(A_2 \frac{W^{j}}{W_{\text{нпв}}}\right) - A_3 \exp\left(-A_4 \frac{W^{j}}{W_{\text{нпв}}}\right), \tag{4}$$

[д = d; пр = thr; опт = op(timum); нпв = mfmc = minimum field moisture capacity] where T_d is the mean daily air temperature, T_{thr} and $T_{d\ opt}$ are the threshold and optimum air temperatures for photosynthesis, W are the reserves of productive moisture in the half-meter soil layer (mm), W_{mfmc} is the minimum field moisture capacity of the half-meter soil layer (mm).

The approximation of the temperature curve for photosynthesis in the form of expression (3) is given in [14].

The curve characterizing the influence of soil moisture content on photosynthesis was constructed, adhering to [16], separately for sandy loam and clayey loam soils.

The functions α_{ph}, ψ_{ph} and γ_{ph}, entering into expression (2), were normalized and vary from 0 to 1.

The photosynthesis of each organ during the light time of day can be computed using the formula

$$\Phi_i^l = E\Phi_{\bar{i}}^l L_i^l \tau_{\text{д}}^l , \tag{5}$$

where $\bar{\Phi}_i$ is the daily photosynthesis of the i-th organ per unit area (g/(m^2·day)), E is the coefficient of efficiency of photosynthesis, L_i is the area of the assimilating surface of the i-th organ (m^2/m^2), τ_d is length of day.

The photosynthesis of the sown area during the 24 hours is

$$\Phi^l = \sum_i^{l,s,p} \Phi_i^l. \tag{6}$$

In contrast to the photosynthesis process all plant organs have the capacity for respiratory gas exchange.

Expenditures on respiration are subdivided into respiration associated with maintenance of the structural organization of the tissues and respiration associated with movement of substances, photosynthesis and creation of new structural units [12, 18, 20].

The increment of biomass of the i-th plant organ during the day is determined by the difference between the receipt of "fresh" products of photosynthesis in the organ, respiration and redistribution of "old" assimilates.

Taking into account the equations of growth proposed in [8], their modification as in [4] and the inclusion of the diurnal gas exchange of the sown area [12] in them, we will write the biomass balance equation of the i-th organ in the form

$$\begin{cases} \dfrac{\Delta m_i^l}{\Delta t} = \dfrac{1}{1+\alpha_{R_i}^l c_1}\beta_i^l \Phi^l - \dfrac{1}{1+\alpha_{R_i}^l c_2}(\alpha_{R_i}^l c_1 \varphi_R^l + v_i^l)\ \tilde{m}_i^l; \\ \dfrac{\Delta m_p^l}{\Delta t} = \dfrac{1}{1+\alpha_{R_p}^l c_2}\beta_p^l \Phi^l - \dfrac{1}{1+\alpha_{R_p}^l c_2}\left(\alpha_{R_p}^l c_1 \varphi_R^l - \sum_i^{i,s,r} v_i^l \tilde{m}_i^l\right) \end{cases} \tag{7}$$

where m_i is the total dry biomass of individual $i \in l$, s, r (r are the roots) of the organs (g/m^2), $\tilde{m}_i$ is the living biomass of the i-th organ, β_i is the redistribution function for "fresh" assimilates, v_i is the redistribution function for "old" assimilates, α_{R_i} is the ontogenetic respiration curve, c_i is a coefficient characterizing the expenditures on maintaining the structure, c_2 is a coefficient characterizing the expenditures associated with movement of substances, photosynthesis and creation of new structural units, φ_R is the temperature coefficient of respiration, which, in accordance with [18], is determined using the formula

$$\varphi_R^l = 2^{0.1\,(T_A^l - T_0)}, \tag{8}$$

where T_0 is the cardinal temperature of respiration.

The increment in the total biomass of the sown area is

$$\frac{\Delta \tilde{M}^{l+1}}{\Delta t} = \sum_{i}^{i,\,s,\,r,\,p} \frac{\Delta m_i^{l+1}}{\Delta t}, \tag{9}$$

where M is the total biomass of the sown area (g/m^2).

With $\Delta m_i^j \geqslant 0$ the increment of living biomass of the i-th organ then will be equal to the increment of its total biomass.

$$\frac{\Delta m_i^l}{\Delta t} = \frac{\Delta m_i^l}{\Delta t}. \tag{10}$$

If it is assumed that the decrease in the living biomass of the vegetative organs can proceed only to an entirely definite critical value, in such a case when $\Delta m_i^j/\Delta t < 0$ the decrease in the total biomass of the vegetative organ by some value results in the dying out of a considerably greater part of the living biomass, which will be determined by the expression

$$\frac{\Delta \tilde{m}_i^l}{\Delta t} = \frac{\Delta m_i^l}{\Delta t} \frac{1}{K_c}, \tag{11}$$

where K_c is a parameter characterizing the critical value of decrease in the living biomass of the i-th organ with which its dying-out begins.

The equations for describing the growth of living and general biomass of the i-th plant organ will have the form

$$\begin{cases} m_i^{l+1} = m_i^l + \dfrac{\Delta m_i^l}{\Delta t}; \\ \qquad i \in l, s, r, p \\ \tilde{m}_i^{l+1} = \tilde{m}_i^l + \dfrac{\Delta \tilde{m}_i^l}{\Delta t}. \\ \qquad i \in l, s, r, p \end{cases} \tag{12}$$

In equation (7) the expression $\Delta m_p^j/\Delta t$ is the increment of total dry biomass of the entire reproductive organ (stem of ear, spikelets and grains).

The dynamics of accumulation of dry matter of grain can be determined using a formula in the form

$$m_g^{l+1} = m_g^l + \frac{1}{\frac{1}{K_m}\frac{\Delta m_{g\max}^l}{\Delta t} + \frac{\Delta m_p^l}{\Delta t}} \frac{\Delta m_{g\max}^l}{\Delta t} \frac{\Delta m_p^l}{\Delta t}. \tag{13}$$

where m_g is the dry biomass of the grain (g/m^2), K_m is the initial slope of the curve, characterizing the rate of growth of the grain in dependence on the level of inflow of the assimilates into the ear, $m_{g\ max}$ is the maximum possible increment of grain weight (g/m^2) with the real relationship of the elements determining the productive plant stand per unit area and the size of the ear, which can be obtained using the formula

$$\frac{\Delta m_{g\max}^l}{\Delta t} = \frac{-2{,}3\, A_5 m_{g\max} \cdot 10^{A_6+t}}{(1+10^{A_6+t})^2}, \tag{14}$$

where $m_{g\ max}$ is the maximum possible weight of the grain (g/m^2).

For its estimate we use the expression

$$m_{g\max} = N_s S_p n_p n_g m_{gv}, \tag{15}$$

where N_s is the density of plant stands in different development phases; S_p is the productive bushiness, n_p is the number of spikelets in an ear, n_g is the number of grains in a spikelet, m_{gv} is the maximum possible weight of 1,000 grains characterizing this variety.

Computations of the surface area of the assimilating organs in the case of a positive balance of their biomass can be accomplished using the formulas proposed in [4, 12]

$$L_i^{l+1} = L_i^l + \frac{\Delta m_i^l}{\Delta t}\frac{1}{m_{t_i}^l},$$

$$\text{when} \quad \frac{\Delta m_i^l}{\Delta t} \geqslant 0, \quad i \in l, s, p, \tag{16}$$

where m_t is the specific surface density of the i-th organ (g/m^2).

With a negative increment in the biomass of leaves and stems for description of the increase in their assimilating surface we use an expression in the form

$$L_i^{l+1} = L_i^l - \frac{\Delta \tilde{m}_i^l}{\Delta t}\frac{1}{m_{t_i}},$$

$$\text{when } \frac{\Delta m_i^j}{\Delta t} < 0,\ i \in l,\ s. \tag{17}$$

Under conditions of a stressed water regime there is an impairment in the basic processes of vital functioning of plants. The dynamics of the relationship between photosynthesis, respiration and the increment of biomass can be represented [6] in the form of the following scheme. It is possible to discriminate three phases in the state of plants: positive, zero and negative balance of organic matter. From the moment of onset of drought the values of the parameters characterizing the intensity of the processes of photosynthesis, respiration and increment of biomass undeviatingly decrease. The above-ground part of the plants is not capable of assimilating the carbohydrates forming in the process of photosynthesis. The root system, being oriented along the soil moisture content gradient, is situated under more favorable conditions and it is possible to use the carbohydrate "excesses" for the exploitation of new soil volumes.

The tendency to an increase in the fraction of underground plant organs under moisture deficit conditions can be regarded as a specific adaptive reaction of the plant directed to the maintenance of the highest possible water potential in the photosynthesizing centers by the more intensive supply of underground organs with the products of photosynthesis [6, 7, 17, 21].

With a further intensification of drought as a result of decrease in the intensity of photosynthesis and deterioration of conditions for growth the mass exchange decreases to the compensation level. Such a state can be maintained for some time and then the products of photosynthesis cease to cover the expenditures on respiration, there is cessation of photosynthesis -- the maintenance of structural intactness of the system is ensured only due to the earlier stored energy.

We will assume that under the influence of unfavorable conditions during the period of vegetative growth the changes in the nature of growth of the above-ground part of the plant occur with

$$\frac{\Delta M^{j+1}}{\Delta t} < \frac{\Delta M^j}{\Delta t},\ \text{if}\ \frac{\Delta M^{j+1}}{\Delta t} \neq 0.$$

We will assume that the increment of the biomass of the roots is maintained at the same level or that it is equal to the increment of biomass of the entire plant:

$$\frac{\Delta m_r^{j+1}}{\Delta t} = \begin{cases} \dfrac{\Delta m_r^j}{\Delta t}, & \text{if}\ \dfrac{\Delta M^{j+1}}{\Delta t} > \dfrac{\Delta m_r^j}{\Delta t} \\ \dfrac{\Delta M^{j+1}}{\Delta t}, & \text{if}\ \dfrac{\Delta M^{j+1}}{\Delta t} < \dfrac{\Delta m_r^j}{\Delta t}, \end{cases} \tag{18}$$

then the increment of the above-ground biomass is determined from the expression

$$\frac{\Delta m_{\text{над}}^{j+1}}{\Delta t} = \begin{cases} \frac{\Delta M^{j+1}}{\Delta t} - \frac{\Delta m_r^{j+1}}{\Delta t}, & \text{if } \frac{\Delta m_r^{j+1}}{\Delta t} < \frac{\Delta M^{j+1}}{\Delta t} \\ 0, & \text{if } \frac{\Delta m_r^{j+1}}{\Delta t} = \frac{\Delta M^{j+1}}{\Delta t}, \end{cases} \tag{19}$$

where m_{above} is the biomass of the above-ground organs (g/m^2).

The growth functions of the above-ground plant organs are determined similarly [5].

The dynamics of increments of total biomass of the sown area is examined here as an internal "switch" for the adabktive increase in the fraction of underground organs when the plant is exposed to unfavorable conditions.

In order to compute photosynthesis (1) it is necessary to have the intensities of photosynthetically active radiation (PAR) in the sown crop. This value is computed using the formula

$$I^j = \frac{I_0^j}{1 + cL^j}, \tag{20}$$

where I_0 is the intensity of PAR at the upper boundary of the sown area ($cal/(cm^2 \cdot min)$), c is an empirical constant.

For computing the flux of PAR at the upper boundary of the sown area we use the formula

$$I_0^j = 0{,}5 \frac{Q^j}{\tau_{\text{день}}}, \tag{21}$$

[день = day] where Q is total radiation ($cal/(cm^2 \cdot day)$), τ_{day} is the length of day.

The total radiation is computed using the Sivkov formula [10]

[сред = mid(day)]
$$Q^j = 12{,}66\,(SS^j)^{1.31} + 315\,(\sin h_n)^{2.1}, \tag{22}$$

where SS is the duration of sunshine during the day (hours), where h_{mid} is midday solar altitude, which is determined using the formula

$$\sin h_n = A + B, \tag{23}$$

where $A = \sin\varphi \sin\delta$, $B = \cos\varphi \cos\delta$, φ is geographic latitude, δ is solar declination.

The table of solar declinations for the spring and autumn months was approximated by the polynomial [1]:

$$\delta = [0{,}473\,(t_0 + j) - 0{,}196 \cdot 10^{-2}\,(t_0 + j)^2 - \\ - 0{,}407 \cdot 10^{-5}\,(t_0 + j)^3 - 0{,}616] \cdot 0{,}017453, \tag{24}$$

where t_0 is the number of the day from the beginning of the computation period, reckoned from 20 March, j is the number of the day of the computation period (j = 0, 1,...,N).

In the case of absence of observational data on sunshine, total radiation can be computed using information on lower and total cloud cover using the formula [2]

$$Q = Q_0 [1 - C_н n_н - C_{св} (n - n_н)], \tag{25}$$

[H = low(er); CB = m-l = middle-lower] where Q_0 is the total radiation in the clear sky (cal/(cm^{2}day)), C_{low} is the coefficient for lower-level clouds, C_{m-l} is the coefficient for clouds of the middle and upper levels, n_{low}, n is the quantity of clouds in fractions of unity of the lower level and total cloud cover.

The length of day is determined using the formula

$$\tau_д^j = \tau_з^j - \tau_в^j, \tag{26}$$

[Д = d; З = ss = sunset; B = sr = sunrise]

where the time of sunrise (τ_{sr}) and sunset (τ_{ss}) is determined using the formulas

$$\begin{cases} \tau_{з.} = 12 + \frac{12}{\pi} \arccos\left(-\frac{A}{B}\right), \\ \tau_в = 24 - \tau_{з.} \end{cases} \tag{27}$$

Formula (4) includes the reserves of productive soil moisture in the half-meter soil layer; change in moisture supplies during the course of the 10-day period (between the times of observations) can be determined using the expression

$$W^{j+1} = W^j + \theta^j + V^j - E^j - C^j, \tag{28}$$

where θ is the precipitation sum in 24 hours (mm), V is the movement of ground water into the aeration zone per day (mm), E is total evaporation per day (mm), C is the infiltration of atmospheric precipitation (mm).

The flow of ground water into the aeration zone is computed using the formula

$$V^j = \frac{E_0^j}{f^H}, \tag{29}$$

where E_0 is evaporability per day (mm), computed using the mean daily dew-point spread, f is a parameter dependent on the hydrophysical properties of the soil, H is the depth of the ground water (m).

The diurnal evaporation values can be obtained using the formula proposed in [13]

$$E^j = \frac{2\,W^j + Q^j + V^j}{1 + \frac{2\,W_{\text{нпв}}}{\eta\,E_0^j}}, \tag{30}$$

[НПВ = mfmc = minimum field moisture capacity] is the minimum field moisture capacity in the half-meter soil layer (mm), η is a parameter dependent on the type and phase of development of the plants.

For computing the infiltration of atmospheric precipitation we use the expression

$$C^j = W^j + \Theta^j - E^j - W^{\cdot}_{\text{нпв}}. \tag{31}$$

[НПВ = mfmc]

The ground water level between observation times entering into formula (29) is found using the formula

$$H^{j+1} = H^j + \Delta H^j, \tag{32}$$

and the change in the ground water level during a day (m) -- using the formulas

$$\begin{aligned} \Delta H^j &= -\frac{C^j}{100}\frac{1}{\mu}, && \text{when } C > 0; \\ \Delta H^j &= \frac{V^j}{100}\frac{1}{\mu}, && \text{when } C \leqslant 0, \end{aligned} \tag{33}$$

where μ is the coefficient of ground water yield.

In order to carry out computations using the proposed model of formation of the yield of winter wheat during the spring-summer period it is necessary to have the following agrometeorological information:
-- maximum air temperature;
-- mean daily air temperature;
-- mean daily dew-point spread;
-- number of hours of sunshine daily (or information on cloud cover);
-- sum of precipitation per 24 hours;
-- reserves of productive moisture in the half-meter soil layer;
-- ground water level.

The dynamics of biomass of individual organs of winter wheat and the grain yield is computed from the moment of renewal of the growing season (j = 0).

The described method also makes it possible to evaluate the influence of environmental factors on the increment of the vegetation mass for different combinations of different parameters characterizing the agrometeorological conditions.

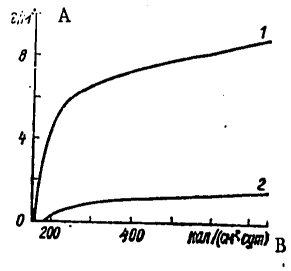

Fig. 1. Light curves of productivity of winter wheat against a background of different soil moistening. 1) $W/W_{mfmc} = 0.8$; 2) $W/W_{mfmc} = 0.2$.

KEY:
A) g/m^2
B) $cal/(cm^2 \cdot day)$

Some results of such numerical experiments are given in Fig. 1. It can be seen that the productivity light curve obtained against a background of different moistening has some peculiarities. With an increase in the density of the light flux in the entire considered range the plant productivity increases, but the biomass increment increases rapidly and attains considerable values only against a background of optimum moistening (80% of the maximum soil moisture content). In the case of an inadequacy of moisture (20% of the maximum soil moisture content) the productivity maximum is almost four times less than under good conditions. We also note that deterioration of moisture supply conditions leads to some displacement of the compensation point in the direction of high light flux density values.

One of the possible ways to apply a model of the production process for winter wheat in actual practice can be the development, on its basis, of a method for a quantitative evaluation of the conditions for growth of the crop during the spring-summer period.

The numerous reviews published by operational agencies of the State Committee on Hydrometeorology are based on a detailed evaluation of the existing and anticipated weather conditions. The latter is carried out using relatively simple and accessible criteria which make it possible to evaluate the degree of favorability of existing agrometeorological conditions for the growth, development and formation of the yield of a crop in comparison with the optimum mean long-term conditions or the conditions for any year taken as a standard [9].

An evaluation of the conditions is carried out for 10-day periods, months and periods during the growing cycle; the values of the meteorological elements used in the evaluation are averaged for the corresponding time interval. Naturally, in this case the evaluations themselves are smoothed. In [3] K. S. Veselovskiy already wrote that "in the mean values the extremes

disappear, but the higher and lower temperatures characterize climate better in that these exert a special infuence on organic life."

The computations of such evaluations using a model make it possible to make them more complete and thorough; in evaluating each successive period it is possible to take the prehistory into account, that is, the consequence of the preceding period, and also take into account the extremal values of the environmental elements during the course of any evaluated period.

BIBLIOGRAPHY

1. Abashina, Ye. V., Prosvirkina, A. G., Sirotenko, O. D., "Simplified Dynamic Model of Formation of the Yield of Spring Barley," TRUDY IEM (Transactions of the Institute of Experimental Meteorology), No 8(67), 1977.

2. Berlyand, T. G., RASPREDELENIYE SOLNECHNOY RADIATSII NA KONTINENTAKH (Distribution of Solar Radiation on the Continents), Leningrad, Gidrometeoizdat, 1961.

3. Veselovskiy, K. S., O KLIMATE ROSSII (Climate of Russia), St. Peterburg, Izd-vo AN, 1857.

4. Galyamin, Ye. P., "Construction of a Dynamic Model of Formation of Yields of Agrocoenoses," BIOLOGICHESKIYE SISTEMY V ZEMLEDELII I LESOVODSTVE (Biological Systems in Agriculture and Forestry), Moscow, Nauka, 1974.

5. Galyamin, Ye. P., Siptits, S. O., Milyutin, N. N., "Model of Formation of the Yield of an Agrobiocoenosis and its Identification," MODELIROVANIYE PRODUKTSIONNYKH PROTSESSOV V AGROEKOSISTEMAKH (Modeling of Production Processes in Agroecosystems), Moscow, Nauka, 1976.

6. Kuperman, I. A., Khitrovo, Ye. V., "Dynamics of Some Components of Mass Exchange of Wheat During a Progressive Soil Drought," FIZIOLOGIYA PRISPOSOBLENIYA RASTENIY K POCHVENNYM USLOVIYAM (Physiology of Adaptation of Plants to Soil Conditions), Novosibirsk, Nauka, 1973.

7. Moldau, --, "Influence of Water Deficit on Plant Increment," IZV. AN ESSR (News of the Estonian Academy of Sciences), Biologiya (Biology), Vol 23, No 4, 1974.

8. Ross, Yu., "System of Equations for the Quantitative Growth of Plants," FITOAKTINOMETRICHESKIYE ISSLEDOVANIYA RASTITEL'NOGO POKROVA (Phytoactinometric Investigations of the Plant Cover), Tallin, Valgus, 1971.

9. RUKOVODSTVO PO SOSTAVLENIYU AGROMETEOROLOGICHESKIKH PROGNOZOV (Manual on Compilation of Agrometeorological Forecasts), Leningrad, Gidrometeoizdat, 1962.

10. Sivkov, S. I., METODY RASCHETA KHARAKTERISTIK SOLNECHNOY RADIATSII (Methods for Computing the Characteristics of Solar Radiation), Leningrad, Gidrometeoizdat, 1968.

11. Tarchevskiy, I. A., FOTOSINTEZ PSHENITSY. FIZIOLOGIYA SEL'SKOKHOZYAYSTVENNYKH RASTENIY (Photosynthesis of Wheat. Physiology of Agricultural Plants), Moscow, Izd-vo MGU, Vol IV, 1969.

12. Tooming, Kh. G., SOLNECHNAYA RADIATSIYA I FORMIROVANIYE UROZHAYA (Solar Radiation and Yield Formation), Leningrad, Gidrometeoizdat, 1977.

13. Kharchenko, S. I., GIDROLOGIYA OROSHAYEMYKH ZEMEL' (Hydrology of Irrigated Lands), Leningrad, Gidrometeoizdat, 1975.

14. Chmora, S. N., Oya, V. M., "Study of the Temperature Dependence of Leaf Photosynthesis," FIZIOLOGIYA RASTENIY (Plant Physiology), 14, No 4, 1967.

15. Shatilov, I. S., Vaulin, A. V., "Dynamics of an Assimilating Surface and the Role of Individual Plant Organs in Formation of Barley Yield," IZVESTIYA TSKhA (News of the Academy of Agricultural Sciences), No 1, 1972.

16. Baker, D. N., Musgrave, R. B., "The Effect of Low-Level Moisture Stresses on the Rate of Apparent Photosynthesis in Corn," CROP SCIENCE, Vol 4, No 3, 1964.

17. Brouwer, R., "Morphological and Physiological Adaptations to External Conditions," ACTA BOT. NEDERL., Vol 17, No 1, 1968.

18. Curry, R. B., "Dynamic Simulation of Plant Growth. Development of a Model," TRANS. ASAE, Vol 14, No 5, 1971.

19. Horie, T. "Simulation of Sunflower Growth. I. Formulation and Parameterization of Dry Matter Production, Leaf Photosynthesis, Respiration and Partitioning of Photosynthesis," BULL. NAT. INST. AGRIC. SCI., JAPAN, SER. A-24, 1977.

20. McCree, K. J., "An Equation for the Rate of Respiration of White Clover Plants Grown Under Controlled Conditions," PREDICTION AND MEASUREMENT OF PHOTOSYNTHETIC PRODUCTIVITY, Wageningen, Pudoc, 1970.

21. Struik, G. J., Bray, J. R., "Root-Shoot Ratios of Native Forest Herbs and Zea mays at Different Soil-Moisture Levels," ECOLOGY, Vol 51, No 5, 1970.

22. Thornley, J. H. M., MATHEMATICAL MODELS IN PLANT PHYSIOLOGY, Acad. Press, London, New York, 1976.

UDC 551.(524+55)

TIME VALIDITY OF METEOROLOGICAL INFORMATION

Moscow METEOROLOGIYA I GIDROLOGIYA in Russian No 9, Sep 79 pp 107-109

[Article by G. P. Lutsenko and Candidate of Technical Sciences V. D. Nikolayev, submitted for publication 24 November 1978]

Abstract: The authors carried out investigations and an analysis of the temporal variability of the wind and temperature fields under conditions of different thermodynamic and circulation states of the atmosphere. The article gives quantitative estimates of the time validity of data on wind and air temperature in cyclones and anticyclones, for different wind velocities, in stable and unstable air masses.

[Text] By the term "time validity" of meteorological information is meant the time interval during which this information can be used in solving different classes of problems. In a general case, the time validity of meteorological data is determined by the following principal factors:
-- the scale of atmospheric processes elucidated in time;
-- the required degree of informativeness (detail);
-- the nature of the specific problems providing for the use of meteorological data.

The time validity can differ substantially in dependence on each of these factors. In actuality, in solving the problem of the time interval during which, for example, a definite type of atmospheric circulation will persist in some region and the required informativeness is reduced only to a quantitative evaluation (zonal circulation, arctic intrusion, etc.), it is only possible to deal with 24-hour intervals [2] (Table 1).

From the point of view of implementation of specific tasks, the time validities of meteorological information are usually more rigorous. In the system of the USSR Hydrometeorological Service such time periods are intradiurnal intervals and in particular, 6-hour intervals.

These times have been established on the basis of an analysis of definite relationships between the mean square error in meteorological data, which leads to errors in prediction above the norm σ_d, and the temporal variability of meteorological elements.

Fundamentally the analytical expression for the validity times for meteorological information t_k in a general case has the form [6]

$$t_k = 6\left[\frac{\sigma_1}{\sigma(6\ ч)}\right]^2, \quad (1)$$

[ч = d] where σ(6 hours) is the mean square variability of the meteorological element in the course of 6 hours.

Investigations of the statistical variability of meteorological elements in the intradiurnal interval indicated that the mean square differences in the values of the meteorological elements increase in conformity to the "first-order law" [6]

$$\sigma(t) = \sigma_1\sqrt{t}, \quad (2)$$

where σ_1 = 0.4σ(6 hours).

However, it must be noted that this law was established (theoretically and experimentally) for the entire diversity of synoptic processes without allowance for specific weather conditions.

At the same time, already from purely physical considerations it can be postulated that σ(t) for different thermodynamic and circulation states of the atmosphere are substantially different, which, in turn, leads to a difference in the validity times for meteorological information under these conditions from those existing at the present time.

In actuality, the physical nature of the variability of atmospheric characteristics is such that in the process of turbulent mixing of air particles in the atmosphere there is transport of the main substances of these particles. The intensity of this transport (in the last analysis, the intensity of variability) is usually characterized, as is well known, by the Richardson number Re, which is a function of the velocity v of movement of air particles v:

$$\mathrm{Re} = \frac{vL}{\nu}, \quad (3)$$

where L is the characteristic scale of the flow; ν is the kinematic viscosity of air.

Naturally, with small v values Re itself is also insignificant, that is, the flow is laminar in nature, which also predetermines the relatively low variability of the meteorological elements.

With respect to the relationship between the variability of atmospheric characteristics and the nature of the pressure field, here it is necessary to take into account the limitation of the pressure gradient from above in anticyclonic formations [4].

Table 1

Duration of Types of Atmospheric Circulation for European USSR

Тип циркуляции 1	Продолжительность, ч 2		
	Минимальная 3	Средняя 4	Максимальная 5
6 Зональная	48	109	210
7 Циклоническая деятельность	48	105	192
8 Арктическое вторжение	48	101	210

KEY:

1. Type of circulation
2. Duration, hours
3. Minimum
4. Mean
5. Maximum
6. Zonal
7. Cyclonic activity
8. Arctic intrusion

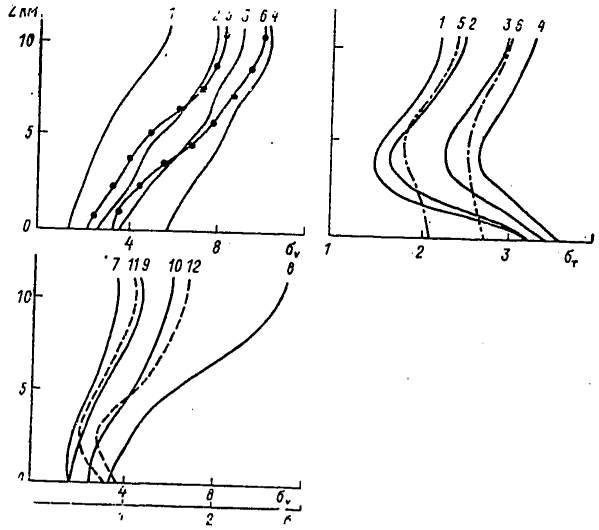

Fig. 1. Mean square variability of wind velocity and air temperature as a function of thermodynamic and circulation states of atmosphere. 1) v = 0-3 m/sec; 2) v = 3-8 m/sec; 3) v = 8-16 m/sec; 4) v = 16-24 m/sec; 5) stable air mass; 6) unstable air mass; 7) cyclone with wind velocities 0-3 m/sec; 8) cyclone with wind velocities 16-24 m/sec; 9) anticyclone with wind velocities 0-3 m/sec; 10) anticyclone with wind velocities 16-24 m/sec; 11) cyclone; 12) anticyclone.

The value of the Re parameter, all other conditions being equal, in cyclones on the average is greater than in anticyclones because the variability of meteorological elements in cyclones is greater than in anticyclones.

In this study we investigated the variability of the wind characteristics (direction α_v and velocity v) and air temperature T for specific states of the atmosphere and conclusions were drawn concerning the validity times for data on wind and temperature under these conditions. It was taken into account that the time differences of wind and temperature adhere to a normal distribution law [5].

As the thermodynamic and circulation characteristics of the state of the atmosphere, in the investigation we used: the deviations of atmospheric pressure from the norm (as the norm within the limits of the European USSR we used p = 1005 mb); wind velocity (by gradations); degree of thermal stability of air masses ($\gamma \leqslant 0.7°$C/100 m -- stable air mass -- SAM; $\gamma > 0.7°$ C/100 m -- unstable air mass -- UAM, pressure trend, nature of pressure field (cyclone - anticyclone), and also the wind regime of pressure systems. In addition, the seasonal states of the atmosphere were taken into account.

Computations of the characteristics of variability were made for several atmospheric sounding stations within the limits of the European USSR. The data are given to the altitudes of the middle troposphere.

The principal results of the investigations can be summarized as follows (Fig. 1).

The variability of wind velocity and air temperature to a considerable degree is dependent on the atmospheric wind regime. For example, on the average, within the limits of the troposphere when there is a weak wind (not more than 6-8 m/sec) the variability of wind velocity and temperature is 2-2.5 times less than when there are considerable wind velocities (more than 15-20 m/sec).

The dependence of the variability of wind velocity on the thermal state of air masses is somewhat smoothed, although here also in stable air masses the variability of wind velocity is 1.3-1.5 times greater than in unstable air masses.

The dependence of air temperature variability both on wind velocity and on the nature of the thermal stability of air masses is smoothed. However, it is easy to note that in unstable air masses and when there is a strong wind the variability of temperature is 1.3-1.5 times greater than in stable air masses and when there is a weak wind.

The dependence of the variability of wind velocity and air temperature on the nature of the pressure field is considerable; this dependence is manifested most clearly under conditions of a different wind regime of the

pressure systems. For example, the variability of wind velocity in the case of its high values in cyclonic eddies is three times greater than in an anticyclone with a weak wind. The variability of air temperature in a cyclone is also almost twice as great as in an anticyclone.

With respect to the variability of wind direction, with one and the same wind velocities the variability of wind in the cyclone is 1.5-2 times greater than in an anticyclone. With different wind velocities the variability of its direction conforms to the general patterns obtained by different authors [1, 3, 6]: it decreases with an increase in wind velocity and vice versa (Table 2).

Table 2

Mean Square Variability of Wind Direction (Degrees) in Six Hours for Different Velocities*

z км	1 v м/сек			
	0—3	3—8	8—16	16—24
0	51	36	28	—
1,5	83	48	26	—
7	82	49	32	24
9	97	61	40	30

2 * Значения σ_{α_v} рассчитывались на середину каждой градации.

KEY:

1. v m/sec
2. *The σ_{α_v} values were computed in the middle of each gradation

It was impossible to establish any significant correlation between wind variability and air temperature with the deviation of atmospheric pressure and the pressure tendency from the norm in the process of the investigations.

Thus, our investigations demonstrated that the variability of the wind characteristics and air temperature is essentially dependent on the specific state of the atmosphere. This, in turn, leads to the following: the "validity times" for the mentioned meteorological elements with different states of the atmosphere are also different. Already on the basis of preliminary evaluations it can be concluded that the "validity times" for data on the wind and air temperature, and at the same time, the regime of wind and temperature sounding of the atmosphere in cyclones and anticyclones with high and low wind velocities within the limits of the troposphere, differ from those now existing by a factor of 2-2.5.

Further investigations of the temporal structure of the fields of meteorological elements as a function of thermodynamic and circulation states of the atmosphere make possible a more specific solution of problems relating

to the "validity times" for meteorological information, atmospheric sounding regimes and the principles for control of operation of atmospheric sounding stations under these conditions.

BIBLIOGRAPHY

1. Garifulin, K. K., IZMENCHIVOST' VETRA V SVOBODNOY ATMOSFERE (Wind Variability in the Free Atmosphere), Leningrad, Gidrometeoizdat, 1967.

2. Dzerdzeyevskiy, B. L., Kurganskaya, V. M., Vitvitskaya, Z. M., "Classification of Circulation Mechanisms in the Northern Hemisphere and Characteristics of Synoptic Seasons," TRUDY NIU GUGMS (Transactions of Scientific Research Institutes of the Main Administration of the Hydrometeorological Service), Ser 2, No 21, 1946.

3. Kovalenko, V. V., Zelenoy, I. K., "Wind and Temperature Variability in the Atmosphere With Time and Distance," SBORNIK RABOT LENINGRADSKOY GIDROMETEOROLOGICHESKOY OBSERVATORII (Collection of Papers of the Leningrad Hydrometeorological Observatory), 1962.

4. Laykhtman, D. L., DINAMICHESKAYA METEOROLOGIYA (Dynamic Meteorology), Leningrad, Gidrometeoizdat, 1976.

5. Lutsenko, G. P., Nikolayev, V. D., "Variability of the Temperature and Wind Fields in Different Forms of Atmospheric Circulation," METEOROLOGIYA I GIDROLOGIYA (Meteorology and Hydrology), No 11, 1976.

6. Reshetov, V. D., IZMENICHIVOST' METEOROLOGICHESKIKH ELEMENTOV V ATMOSFERE (Variability of Meteorological Elements in the Atmosphere), Leningrad, Gidrometeoizdat, 1973.

UDC 551.(557.5:578.42:509.323)

RELATIONSHIP BETWEEN THE PLANETARY HIGH-ALTITUDE FRONTAL ZONE AND THE POSITION OF THE SNOW COVER BOUNDARY DURING THE AUTUMN AND SPRING PERIODS

Moscow METEOROLOGIYA I GIDROLOGIYA in Russian No 9, Sep 79, pp 110-112

[Article by Candidate of Geographical Sciences V. B. Afanas'yeva, Candidate of Physical and Mathematical Sciences N. P. Yesakova and R. V. Klimentova, Main Geophysical Observatory, submitted for publication 29 September 1978]

Abstract: A study was made of the relationship between the planetary high-altitude frontal zone (PHAFZ) and the position of the snow cover boundary in spring and autumn. It was established that both in spring and autumn in the territory of Eurasia the PHAFZ has a definite relationship to the position of the snow cover boundary. The correlation coefficients are given. The results obtained make it possible to use data on the position of the PHAFZ for determining the boundary of the snow cover, being an important predictor in the prediction of mean 10-day temperature.

[Text] The snow cover, having singular radiation and thermal properties, forms a surface differing sharply from the snowless underlying surface. This circumstance exerts a strong influence on climate and must be taken into account when preparing long-range weather forecasts.

In the Dynamic Meteorology Section of the Main Geophysical Observatory, in the development of the hydrodynamic-statistical method for predicting mean 10-day temperature, in addition to the circulation factors presently used in the forecasts, an allowance was made for cloud cover, ice content of northern seas and snow cover. At the same time it was established that the snow cover is one of the principal predictors in temperature forecasting. However, the collection of data on the position of its boundary frequently involves definite difficulties. The presently accumulated extensive observational data made it possible to construct mean 10-day maps of these elements, in particular, of the snow cover, on which were plotted isolines

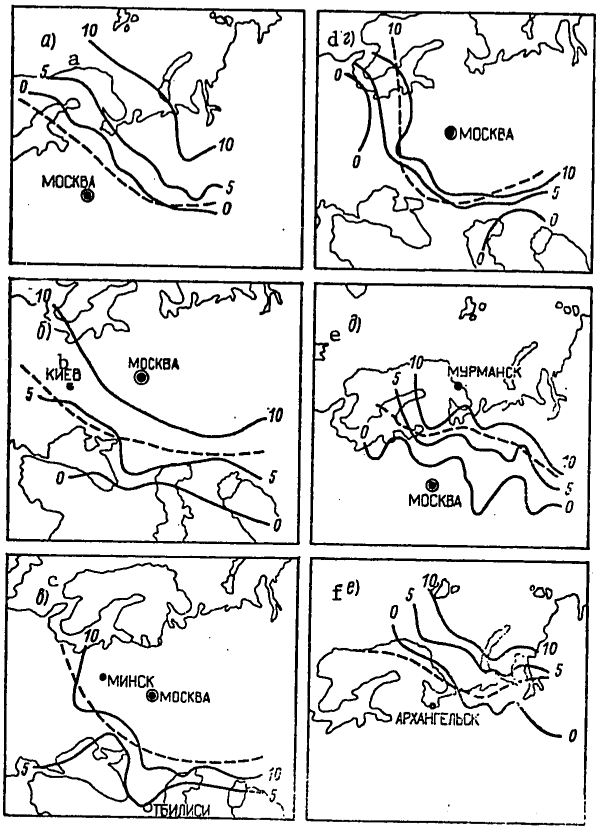

Fig. 1. Maps of distribution of the snow cover, 1956, second 10-day period. a) October, b) November, c) December, d) March, e) April, f) May

of 0, 5 and 10 days with presence of a snow cover in a 10-day period during the autumn and spring periods (October-December, March-May). The method for preparing these maps has been described in considerable detail in published studies. An analysis of the maps indicated that the position of the snow cover boundary varies in different years in a considerable range [1].

In order to take into account the position of the snow cover boundary in the preparation of statistical forecasts it was necessary to establish its statistical correlations with different meteorological elements. In this study an attempt is made to establish statistical correlations between the position of the snow cover and the planetary high-altitude frontal zone (PHAFZ), and if a sufficiently close correlation is obtained, use the position of the PHAFZ for determining the boundary of the snow cover, since in itself a determination of the position of the PHAFZ does not constitute significant difficulties.

In studies by V. A. Bugayev and V. A. Dzhordzhio [2], V. I. Vorob'yev [4], and V. A. Bugayev [3] it is pointed out that the PHAFZ is most sharply expressed at the surface 300-200 mb. However, it is also quite clearly expressed on AT_{500} pressure pattern charts. In our study the position of the PHAFZ was determined extremely approximately as the position of the isohypse 536 gp dam on AT_{500} charts. The position of the 536 gp dam isohypse, averaged for a 10-day period, was plotted on mean 10-day maps of the snow cover for the autumn and spring periods (October-December and March-May). It was possible to construct a great number of maps for the period from 1949 through 1968. As an example we have given the maps for 1956 (Fig. 1). It should be noted that for the autumn period such work had been done earlier [5], and then supplemented for spring.

As a result of examination of the maps it became obvious that in autumn the position of the snow cover boundary has a definite relationship to the PHAFZ (Fig. 1).

In October, when the snow cover boundary runs along the northern part of the continent, the position of the PHAFZ (dashed line) coincides quite well with the isoline 0 days with snow in the 10-day period (Fig. 1a), which separates the territory free of a snow cover. In mid-November, when the snow cover boundary is displaced to the south, the PHAFZ (Fig. 1b) is displaced in the direction of an increase in the values of the isolines representing the distribution of the snow cover and in the second 10-day period approaches the isoline for 5 days with snow.

In mid-December, when the snow cover boundary is situated in the southern European USSR the PHAFZ is displaced still more southward and in the third 10-day period in December (Fig. 1c) approaches the isoline 10 days with snow. A more detailed examination of the correlation between the PHAFZ and the snow cover boundary in the autumn is given in [5].

During the spring period the relationship between the position of the snow cover boundary and the PHAFZ is also obvious. As might be expected, in mid-March, when the snow cover boundary passes through the southern part of the European USSR (Fig. 1e), the PHAFZ is situated closer to the isoline for 10 days with snow during the 10-day period. By mid-April, when the snow cover boundary (Fig. 1b) is displaced northward, the PHAFZ is shifted in the direction of a decrease in the values of the isolines for the distribution of snow cover and is situated closest to the 5-day isoline, and finally, in mid-May, when the snow cover boundary passes through the northern part of the European USSR, the PHAFZ approaches the isoline for 0 days with snow (Fig. 1f).

Thus, the PHAFZ is displaced in the same direction as the snow cover boundary, lagging somewhat within the limits of the region with an unstable snow cover, which is situated between the isolines for 0 and 10 days with snow in the 10-day period, which is confirmed below by computations.

Table 1

Correlation Coefficients Between PHAFZ and Position of Isolines for 0, 5 and 10 Days With Snow in 10-Day Period

0	5	10	0	5	10	0	5	10
			1 Осень					
3 Октябрь			4 Ноябрь			5 Декабрь		
0,78	0,55	0,56	0,43	0,63	0,58	0,52	0,53	0,73
			2 Весна					
6 Март			7 Апрель			8 Май		
41,4	50,4	66,0	62,0	65,2	64,1	67,0	52,1	56,2

KEY:

1. Autumn
2. Spring
3. October
4. November
5. December
6. March
7. April
8. May

Table 1 gives the results of the correlation coefficients between the PHAFZ and the position of the isolines for 0, 5 and 10 days with snow in the 10-day period for autumn and spring, averaged by months for 8 years (1949-1956). The table shows that for the autumn the highest correlation coefficients in October (0.78) are observed between the PHAFZ and the isoline for 0 days with snow, in November -- with the isoline for 5 days and in December -- with the isoline for 10 days with snow, as is indicated graphically in the figures. In spring the reverse picture is observed. In March the highest correlation coefficient is observed between the PHAFZ and the isoline for 10 days with snow, in April -- with the isoline for 5 days and in May -- with the isoline for 0 days with snow.

The physical relationship between the PHAFZ and the snow cover boundary is entirely explicable since on the snow cover boundary there is a break between albedo and heat flows and a zone of maximum contrasts arises near it. The ascertained dependence can evidently be of prognostic importance since on the basis of the position of the PHAFZ to a certain degree it is possible to judge the position of the snow cover boundary.

In the future plans call for checking the computations of the correlation coefficients for a longer series of years.

BIBLIOGRAPHY

1. Afanas'yeva, V. B., Yesakova, N. P., "Correlation Between the Planetary High-Altitude Frontal Zone and Position of the Snow Cover Boundary," TRUDY GGO (Transactions of the Main Geophysical Observatory), No 236, 1960.

2. Bugayev, V. A., Dzhordzhio, V. A., "Planetary High-Altitude Frontal Zone," TRUDY TsIP (Transactions of the Central Institute of Forecasts), No 25, 1951.

3. Bugayev, V. A., "Planetary High-Altitude Frontal Zone and Cyclogenesis," METEOROLOGIYA I GIDROLOGIYA V UZBEKISTAN (Meteorology and Hydrology in Uzbekistan), Izd-vo AN Uzb. SSR, 1955.

4. Vorob'ye, V. I., STRUYNYYE TECHENIYE V VYSOKIKH I UMERENNYKH SHIROTAKH (Jet Streams in the High and Middle Latitudes), Leningrad, Gidrometeoizdat, 1960.

5. Yesakova, N. P., Afanas'yeva, V. B., "Methods for Characterizing Anomalies of Cloud Cover, Snow Cover and Radiation Fluxes," TRUDY GGO, No 143, 1962.

UDC 551.46.086

COASTAL STATIONARY WAVE-MEASURING COMPLEX

Moscow METEOROLOGIYA I GIDROLOGIYA in Russian No 9, Sep 79 pp 113-116

[Article by Candidate of Technical Sciences V. B. Vaysband and V. N. Shanin, Institute of Oceanology USSR Academy of Sciences, submitted for publication 18 September 1978]

Abstract: The article describes an operating wave-measuring complex located in the coastal zone of the Black Sea. The authors give the technical specifications of a base of rigid construction on which the wave sensors are placed. There is a description of these sensors and also the circuit diagram of a three-string wave recorder, making it possible to obtain all the basic wave elements. The experience of prolonged operation of the complex demonstrated its effectiveness when making long-term wave measurements.

[Text] At the present time in our country and abroad there has been a considerable increase in interest in long-term instrumental wave observations. The organization of such observations is complicated by the fact that they are impossible without a specially fabricated and technically outfitted wave-measuring complex.

There is a substantial increase in the requirements on the reliability of operation of the measuring apparatus and on the stable accuracy of measurement of wave parameters. However, the satisfaction of these requirements and conditions when creating a wave-measuring complex considerably increases material expenditures. And nevertheless, great material and technical expenditures in the organization of long-term wave measurements in the long run are justified.

A stationary wave-measuring complex is now operating in the coastal zone in the Southern Division of the Institute of Oceanology imeni P. P. Shirshov USSR Academy of Sciences. The above-mentioned requirements were taken into account in its creation. The wave-measuring complex is situated in the

coastal zone and consists of two instruments, one of which is installed in a sector with a depth of 5 m, whereas the other is in a sector with a depth of 7.5 m. The first wave meter measures the waves at one point, whereas the other is a three-point wave meter by means of which it is possible to determine all the principal wave elements: height, period, velocity, length and direction of their movement. The spatial positioning of the instruments makes it possible to take into account the transformation of a number of wave elements.

The wave-measuring complex consists of the following technological elements: 1) A system for the placement (carrier) of the measurement instrumentation, 2) Sensors of the wave process, 3) Underwater lines for supplying electric current to the sensors and for transmitting information to the recorder, 4) Recording instrumentation, 5) Measurement circuit.

The site of placement of these wave meters is characterized by an intensive hydrodynamic process. This necessitated the creation and development of some solid and stable systems for the placement of sensors capable of withstanding, over a long period, of high wave loads and active corrosion processes. In addition, these carriers must be easily transportable and be installed in the coastal zone by means of unspecialized ships. The bases constructed and installed with these requirements taken into account are identical in design, although with respect to size they differ somewhat from one another. As an example we will consider the construction of the base of a three-point wave recorder (Fig. 1a).

A vertical steel pipe 2 with a diameter of 150 mm and a height of 6.0 m is rigidly mounted on a metal platform measuring 2.5 x 2.5 m. Four cast iron weights are placed on the platform in special nests. Each weight has a mass of 250 kg. In order to impart rigidity the central pipe is connected to the platform with steel tie rods 4. Attached within the pipe is a telescopic hollow shaft 5 with a diameter of 85 mm and a height of 6.0 m, which by means of the collar 6 and the helical stopper 7 can be rigidly fixed at any level within the limits of water body depths from 7.0 to 8.5 m. Three horizontal supports 8 with a length of 1.0 m are welded on a telescopic shaft at two levels at an angle of 120° from one another. Metal braces are attached for making the supports rigid. At the ends the lower supports have metal funnels 9 designed for attachment of the base for the wave sensor body 10. The ends of the upper supports have tightening collars for attachment of the body of the wave sensors 11.

The base of the wave recorder, except for the platform, is fabricated from stainless steel. The total mass of the entire base with the weights is about 1.5 tons. The base of the single-point wave recorder is somewhat less in its dimensions and accordingly also in mass. As the sensors in both wave recorders use is made of a calibrated Nichrome string supplied a-c current with a sonic frequency. Experience in use of sensors of such a type in sea water has indicated that their metrological characteristics are sufficiently precise and stable with time. However, the use of strings unprotected

from the external mechanical effect of the medium leads to their frequent damage, and accordingly, cessation of measurements. In order to preclude such damage the strings were enclosed in light perforated tubes (Fig. 1b).

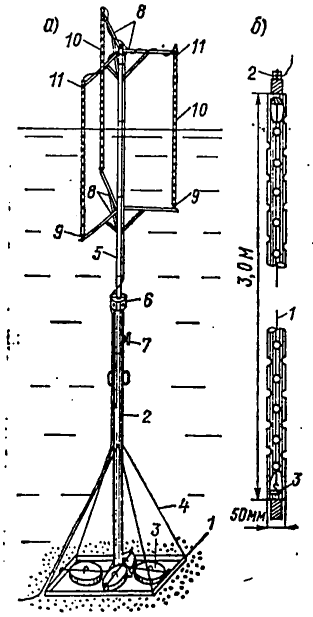

Fig. 1. General view of three-string wave recorder (a) and external appearance of body of string sensor of wave height (b).

In the upper part of the tube the string 1 was attached in a screw clamp 2, to which electric current was carried through an underwater cable. At the bottom of the tube the string was attached on the lower current-insulating sleeve. The latter was simultaneously the base of the sensor body, entering into the nest of the guide funnel on the lower support. The total area of the perforated openings in the sensor body was approximately half the total area of the entire body, which ensures free escape of water from the tube or its filling during oscillation of the wave-covered water surface, whose level within and outside the body is virtually identical. Such a design solution for the sensor ensures not only protection of the string against damage, but also its rapid replacement, which in the practice of wave measurements is a circumstance of more than a little importance. The body of the

sensors was fabricated from stainless steel. The standard dimensions of the sensor bodies ensured their interchangeability. A multistrand cable of the KVD type with internal shielding is used for supplying electric current to the sensors. This type of cable has not only a high mechanical strength but also a high internal water-insulating capacity.

By virtue of intensive movements of entrained sediments and their mechanical effect most often cases of damage to cables occurs in those zones of a water body affected by surf or near the water line. In order to exclude such an effect all the cable lines were enclosed in metal tubes intersecting the dangerous zone along the bottom of the water body. A significant circumstance having great importance for the preservation of the tubes themselves is that they are fabricated from stainless steel. The tubes, made of carbon steel, fail after 1-2 years of operation. The removal of the damaged tubes, the extraction of the cables (if they have remained intact) and the laying of new tubes each 1-2 years is far more expensive than laying of stainless steel tubes.

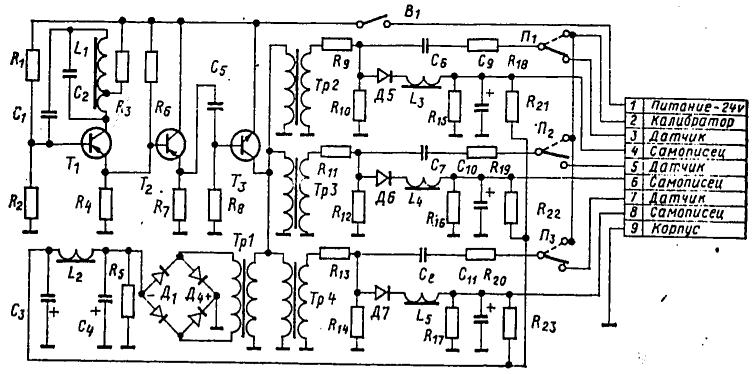

Fig. 2. Circuit diagram of three-string wave recorder.

KEY:

1. Current - 24 V
2. Calibrator
3. Sensor
4. Automatic recorder
5. Sensor
6. Automatic recorder
7. Sensor
8. Automatic recorder
9. Body

As already noted, the sensors used in the wave recorder are strings with a high resistance. This principle for measuring waves is relatively successfully embodied in the GM-61 instrument [1]. However, for a number of technical reasons we could not use the electric power units from the GM-61

instrument for a multipoint wave recorder. It was necessary to develop and construct a special unit differing somewhat from the unit for a standard wave recorder.

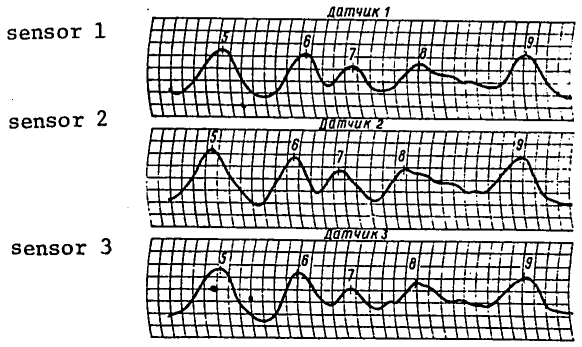

Fig. 3. Fragment of synchronous record of wave profiles on tape of N 327/3 recorder.

The special measuring unit consists of the following main parts: one GNCh low-frequency generator with a power of 5 W, three decoupled identical IS measurement circuits and an AC autocompensator.

The low-frequency generator ensures the feeding of current to the wave recorder strings through a decoupling circuit with a frequency of 4 KHz. It includes three transistors, in the collector of one of them, T3KT802A, four transformers Tr 1, Tr 2, Tr 3, Tr 4 are cut in in-parallel as decoupling circuits. These ensure supply of electric current to the detector strings and to the autocompensator (Fig. 2). Such a decoupling method eliminates harmful potential connections between the sensors and the measuring circuits and also their mutual influence.

The resistors R9 R_{10}, R_{11} R12 and R_{13} R_{14} are for regulating the working current and voltage across the sensors. The condensers C_6, C_7, C_8 prevent the penetration of constant current interference from the string to the measuring circuits. The latter can be created from polarization of the strings, from stray earth currents and network interference. The measured current, by means of the diodes D_{5-7}, forms a positive voltage across the load resistors; this consists of the constant component V_{const} and the useful signal V_{use}. At the same time, a negative voltage of the same strength as V_{const} is fed from the autocompensator through the resistors R_{21-23} to the resistors R_{15-17}. This ensures in R_{15-17} the discrimination of a useful signal from the change in current as a result of wave oscillations.

Since the autocompensator is fed from the low-frequency generator (a-c current) through the decoupling transformer Tr 1, because of this connection the change in the output voltage of the low-frequency generator leads to a proportional change in the current in the measuring and compensating circuits. In this case the zero level of the current at the output of the measuring circuit does not change. Such an autocompensation circuit makes it possible to couple the signal zero level with the recorder zero and to the static level of the sea, which in case of necessity makes it possible to restore the latter on the automatic recorder tape.

The instrument measuring circuit provides for the possibility of checking and routinely changing the scale of the record of wave heights in the process of measuring them. Usually in the course of measuring wave heights the scale of their registry on the recorder tape is determined in the process of calibrating the sensor at sea. In this case a relationship is established between the depth of submergence of the sensor in the water ΔH and the signal level ΔS on the recorder tape.

If for any reasons in the course of instrument operation there is a change in the characteristics of the measuring circuit, it is possible to discover this deviation only with subsequent calibration. In order to exclude the uncertainty element, in the circuit of the three-string wave recorder provision must be made for the possibility of current checking. This can be done because the linear calibration of the sensors is related not only to the registry of the signal on the recorder tape, but also to the change in resistance ΔI of the string. The operation of determining this relationship is accomplished using a precise resistance box which is connected through the switch $П_1$- $П_3$ to the measuring circuit in place of the string sensors. Then from the recorder tape, using the resistance box, a resistance is selected which causes an amplitude of the recorder pen identical with ΔS.

After determining ΔI in the entire range ΔS a calibration curve in the form $I = f(\Delta H, \Delta S)$ is constructed which in the process of operation of the wave recorder makes it possible to detect the presence of distortions at the scale of the wave record. In addition, the presence of such a dependence makes it possible to change the scale of the wave record in dependence on wave strength. This was particularly important for us because the channels of the N 327/3 recorder have a relatively narrow dynamic range (Fig. 3).

The width of the working part of each record channel is 40 mm. It must be mentioned that in this recorder the record of the readings is by pen on a tape in a curvilinear coordinate system. However, with a rate of movement of the recorder tape 10 mm/sec or more the error in determining the wave profile as a result of the curvilinear form of the record is practically minimum. At the same time the N 327/3 recorder has a number of technical qualities which distinguish it advantageously from other types of recorders with a linear form of registry.

The N 327/3 recorder is an instrument making it possible with a high accuracy to register rapidly transpiring processes in the range from 0 to 50 Hz. With adherence to normal operating conditions the maximum error in signal registry does not exceed the limits 5%. A great convenience in making the measurements is that each measuring channel in the recorder is in the form of an individual measurement unit, including a measurement mechanism, recording device and amplifier.

The experience in operation of the wave-measuring complex over a period of years has shown that its design characteristics and technical elements correspond to the requirements of long-term wave observations in the coastal zone of the sea.

BIBLIOGRAPHY

1. PRIBREZHNYY VOLNOGRAF GM-61: METODICHESKIYE UKAZANIYA (GM-61 Coastal Wave Recorder: Systematic Instructions), No 38, GUGMS, GOIN, 1974.

UDC 551.46:621.396.969

INVESTIGATION OF CORRELATION BETWEEN THE NATURE OF A RADAR SIGNAL ENVELOPE AND THE FORM OF THE SEA SURFACE REFLECTING SURFACE

Moscow METEOROLOGIYA I GIDROLOGIYA in Russian No 9, Sep 79 pp 116-119

[Article by Candidate of Technical Sciences I. V. Kirejev and A. V. Svechnikov, State Oceanographic Institute, submitted for publication 28 August 1978]

Abstract: It is demonstrated that anomalous reflection occurs from the crests of waves which are in a stage prior to collapse; the principal contribution to the reflected signal in the case of wind waves is from sectors of the slope situated closer to the crest, whereas for swell -- those situated closer to its middle; the surface sectors covered with foam reflect more weakly; on the basis of the nature of the envelope of the reflected signal it is possible to judge the state of individual wave elements.

[Text] In developing radar methods for measuring sea waves the emphasis is usually on determining the correlations between the statistical characteristics of sea waves and the radar signal. To a lesser degree the correlations of their fine structures were investigated. An example of determination of such correlations is source [3], in which it was shown that wave crests prior to collapse cause stable bursts of a horizontally polarized radar signal which fluctuate little. The determination of such correlations already makes it possible to study not only the statistical characteristics but also individual phenomena.

The study of the correlation of fine structures of waves and the radar signal is, indeed, the only direction in study and investigation of the deviations, observed in a number of cases, of the quantitative characteristics of the reflected signal from the characteristics determined by the principal backscattering patterns. For example, in the centimeter range of radio waves there was found to be an excess of the specific effective scattering area in the case of horizontal polarization (σ^0_{hh}) over the ESA for vertical polarization (σ^0_{vv}) in the case of waves higher than class 2-3 and irradiation

of sea waves from the leeward side in the case of small glancing angles. In the case of irradiation from the windward side this anomalous phenomenon is not observed. This effect can be explained only on the basis of a study of the differences in reflectivities of the leeward and windward slopes of a sea wave.

Research Method

An experiment, whose essence is described below, was carried out on the 18th voyage of the scientific research ship "Akademik Korolev."

A buoy with corner reflectors was lowered on a cable into the water from the drifting vessel. The cable was let out to a length which ensured that the buoy would move 150-200 m away from the ship. A weight with a mass of 25 kg was suspended on a cable 50 m in length to the end of a pipe which passed through the center of a foam plastic circle in order to stabilize the buoy.

Buoy position was determined from the circular scan display of a "Don" radar on a scale of 0.8 mile. Then the radar antenna was directed toward the buoy. The signal received from the reflector was fed from the radar receiver output to the input of a wave-measuring device created at the Radioelectronics Institute Ukrainian Academy of Sciences. It operated in a moving strobe regime. The signal from the output of the peak detector is fed to an HO-41 light-ray oscillograph.

First only the signal from a corner reflector was recorded, and then, when the buoy moved beyond the range of the radar ray, during approach of a wave of any type to the buoy, a command was fed for registry of the signal on the oscillograph and there was simultaneous photographing of the sea surface by a camera with a teleobjective of the "MTO-500 A" type. By comparing the results of registry of the radar signal envelope on a phototape with a photograph of the sea surface in the neighborhood of the buoy and with its visual description, prepared at the same time, a correlation is established between the nature of the envelope and the form of the reflecting sector of the sea surface.

In the experiment it was possible to define the following types of surfaces: waves without foaming crests, waves with foaming crests, wave slopes covered with foam.

It is known [4] that at one and the same moment in time the input of the radar receiver receives signals from the reflectors, which are situated in an area with a length $0.5\ c\tau$. This value determines the radar range resolution.

Since range selection was accomplished by strobing the input of the device, during the time interval equal to the strobe pulse duration (τ_{sec}) the radio pulses moved along the direction of propagation of electromagnetic energy by a finite value. As a result, a signal passes through the device

which will be dependent on the nature and parameters of the reflectors, situated in an area with the length 0.5 $(\tau + \tau_{sec})c$. The peak detector discriminates the maximum of the signals arriving from this area.

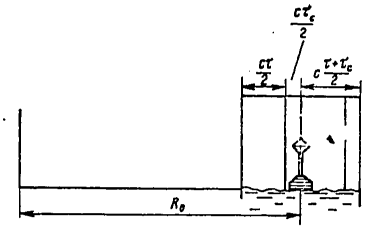

$\tau_c = \tau_{sec}$

Fig. 1. Diagram explaining the nature of the signal envelope.

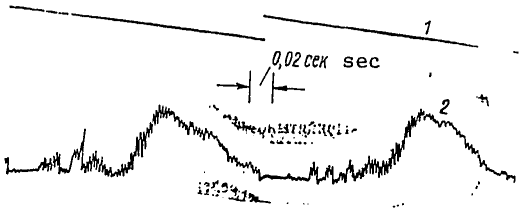

Fig. 2. Oscillogram of envelope of signal reflected from corner reflector. 1) voltage of range scanning; 2) oscillogram

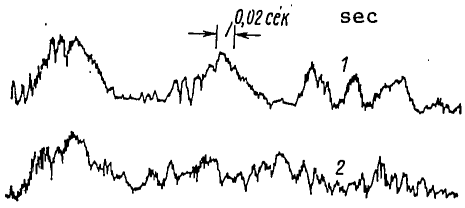

Fig. 3. Oscillogram of envelope of signal reflected from sea surface. 1) during first period of range scanning; 2) during subsequent period

Now we will proceed to an examination of the process of reflection of radio pulses from the corner reflector mounted on the buoy and the nature of the oscillograms of the envelope of a radar signal with a moving strobe, that is, when the time during which the input of the wave-measuring device is "open" is constant and equal to τ_{sec} and the distance to the area from which the signal is received continuously changes.

The radar operating regime during this experiment was as follows: duration of radio pulse -- 0.12 μsec, pulse repetition rate -- 3200 pulses/sec, strobe duration -- 0.03 μsec, intermediate frequency amplification -- 18 MHz, rate of movement of strobing sector of sea surface -- 600 m/sec.

The reader should note the absence of a dependence of readings of the wave-measuring device on the shape of the pulse passing through the radar intermediate frequency amplifier. The fact is that in the device there is discrimination of the envelope of video pulses and for its normal operation it is only necessary that no pulses be present in the receiving channel. Special investigations carried out by Siforov [1] demonstrated that the optimum passband of the receiving channel at the 0.7-level falls in the range $(1\text{-}1.3)/\tau$, since in this band the voltage amplitude of the radio pulse at the detector input attains values close to the steady value.

In the considered case the optimum band is 8.5-11 MHz, and accordingly the amplitude of pulse voltage does not encumber the radar receiving channel.

The initial prerequisites for explaining the oscillograms will be examined using Fig. 1. We will assume that the distance to the buoy with the reflector is equal to R_0. A signal begins to arrive at the input of the wave-measuring device from the reflector at the time when the strobe delay is equal to

$$2\frac{R_0}{c}-2\frac{\tau_c}{2},$$

[c = sec] that is, when by the end of strobe action there is arrival of a signal caused by approach of the leading edge of the radio pulse to the reflector. The distance to the area from which the signal arrives at this time will be equal to

$$R_0-0{,}5\,(\tau+\tau_c)\,c.$$

[c = sec]

Since the leading edge of the radio pulse has only approached the reflector, the nature of the signal will be determined by the parameters of the sea surface situated in front of the buoy. With advance of the strobe an ever-greater part of the energy reradiated by the reflector will be fed to the input of the radar receiver, and accordingly, also the attachment. Some of the electromagnetic energy scattered by the nonideal reflector in the direction of the sea surface is reradiated by the latter and is partially fed to the radar input, causing an amplification of fluctuations of the signal envelope (Fig. 2). [An inaccuracy in maintaining a right angle by only 1° leads to a decrease in the maximum value σ of the corner reflector by a factor of 2-5 due to the scattering of electromagnetic energy.] However, it can be postulated that the corner reflector is also reached by electromagnetic waves reflected from the sea surface, which, being scattered by the reflector, are fed to the radar input or are reradiated in the direction of arrival of electromagnetic waves from the sea surface. In the latter case the maximum difference in the path in one direction must be half as great as in the first (22 and 11 m).

The maximum of the envelope of the reflected signal appears with movement of the strobe in the time interval 0.25τ and with a shift into the interval $0.5\ (\tau + \tau_{sec})$ the arrival of the signal from the reflector in that time segment when the input is open will end.

Since after shifting of the strobe by 0.25τ or more the signal scattered by the reflector and reradiated by the sea surface no longer arrives at the input, the envelope fluctuations decrease considerably (the trailing edge of the pulse on the oscillogram).

The total length of the surface participating in the shaping of the signal, together with the corner reflector, is equal to $c(\tau + \tau_{sec})$.

Figure 3 shows oscillograms of the reflected signal envelope. In the course of the first period of spatial scanning there is reflection from two waves with a length of about 85 m and three shorter waves. In its form the considered oscillogram is very similar to the oscillogram received from the corner reflector (Fig. 2). This gives basis for postulating that on the front slope of sea waves there is some intensively reflecting sector whose extent under experimental conditions was considerably less than the length of the slope of the sea wave. The reflections from other sectors of the slope lead only to fluctuations of the reflected signal envelope.

As a result of carrying out a series of experiments it was established that rather intensive radar signals are registered from the wind waves, even in the case of small glancing angles (less than 1°), whereas from swell we registered a reflection only in the case of glancing angles greater than 5°, and then only from the slope of the one nearest-lying wave. Accordingly, the strongly reflecting sector of wind waves is situated at the crest of the wave, whereas in the case of surf -- closer to the middle of the slope.

This same phenomenon was noted in [3] in measurements with a fixed strobe, that is, in a study of the temporal invariability of the reflected signal. As we see, the two methods ("temporal" and "spatial") gave one and the same result on the position of the sector of the sea wave slope determining the strength and nature of the reflected signal.

At the peak of the envelope for the signal caused by the first wave and initially in the envelope characterizing the reflection from the second wave it is possible to see sharp dips with an extent of 3-6 m. By comparing the nature of the signal with the corresponding photograph we conclude that they arise with reflection from sectors of waves covered with foam.

The region of the maximum of the oscillogram for the second wave differs substantially from the similar region of the preceding wave, since it almost does not fluctuate. As indicated by an analysis of the oscillogram shown in Fig. 3, and the corresponding photograph of the sea surface, such a signal arises with reflection from waves near the collapse stage. The

characteristic dimension of such a sector of the sea surface is 4-5 m.

On the oscillogram corresponding to the second spatial period (Fig. 3), each sector of which has a time shift of 0.5 sec from the preceding one, the signal from the first wave almost retained its characteristic form and was displaced to the left by one interval between the time marks (approximately 6 m in space). However, the shape of the envelope associated with the second wave changed sharply. It was established that such an envelope shape is typical for reflections from a collapsing wave with considerable surface sectors covered with foam.

Thus, confirmation is obtained for observations of bursts of a signal [3] when working with a fixed strobe. Allowance for the characteristics of bursts can increase the accuracy in measurement of the principal wave parameters [2].

The established correlation of the spatial oscillograms of a radio signal reflected from the wave-covered sea surface makes it possible to develop a method for determining the degree of coverage of the sea surface with foam and also study the physical processes transpiring on the wave-covered sea surface.

Summary

1. It has been established that the spatial positioning of the bursts coincides with the crests of waves in the stage prior to collapse. This confirms the qualitative conclusions drawn in [3] on the nature of these bursts.

2. Spatial observations of the signal indicated that the maximum reflection for wind waves is observed from the sector of the slope situated closer to the crest, whereas with reflection from swell covered with ripples these sectors are situated closer to the middle of the slope.

3. The level of the signal reflected from surface sectors covered with foam is below the level of the signals reflected from the slopes of noncollapsing waves.

BIBLIOGRAPHY

1. Gutkin, L. S., Lebedev, V. L., Siforov, V. I., RADIOPRIYEMNYYE USTROYSTVA (Radio Receivers), Part II, Moscow, Sovetskoye Radio, 1963.

2. Zamarayev, B. D., Kalmykov, A. I., Kireyev, I. V., et al., "Methods for Determining the Characteristics of Waves by the Radar Method," NEKONTAKTNYYE METODY IZMERENIYA OKEANOGRAFICHESKIKH PARAMETROV (Noncontact Methods for Measuring Oceanographic Parameters), Moscow, Gidrometeoizdat, 1975.

3. Kalmykov, A. I., Kurekin, A. S., Lementa, Yu. A., et al., "Some Peculiarities of Backscattering of Radio Waves in the Superhigh Frequency Range at the Sea Surface in the Case of Small Glancing Angles," Preprint Ukrainian Academy of Sciences, Institute of Radioelectronics, No 40, Khar'kov, 1974.

4. SOVREMENNAYA RADIOLOKATSIYA. ANALIZ, RASCHET I PROYEKTIROVANIYE SISTEM (Modern Radar. Analysis, Computation and Designing of Systems), translated from English, edited by Yu. B. Kobzarev, Moscow, Sovetskoye Radio, 1969.

REVIEW OF "GENERAL CIRCULATION MODELS OF THE ATMOSPHERE. METHODS IN COMPUTATIONAL PHYSICS." ACADEMIC PRESS, NEW YORK - SAN FRANCISCO - LONDON, VOL 17, 1977

Moscow METEOROLOGIYA I GIDROLOGIYA in Russian No 9, Sep 79 pp 120-121

[Review by Professor S. A. Mashkovich]

[Text] A volume devoted to models of general circulation of the atmosphere has been published in the series METHODS IN COMPUTATIONAL PHYSICS. The preceding volumes of this publication were devoted to the status of investigations and applications in different fields of physics (statistical physics, quantum mechanics, hydrodynamics, nuclear physics, astrophysics, seismology, radioastronomy, etc.).

The fact that the publishers of the mentioned series have turned to the problem of modeling of general circulation of the atmosphere is entirely legitimate. In actuality, numerical modeling of general circulation of the atmosphere is one of the complex, important and interesting problems of physics. For its solution it is necessary to use the most powerful electronic computers and the most effective numerical methods. Moreover, further progress in the modeling of general circulation of the atmosphere (improvement in spatial resolution in models, detailed allowance for different physical processes, broadening the sphere of applications of such models, etc.) is essentially dependent on the creation of still more productive electronic computers. In the investigations of this problem there has been graphic manifestation of both the potential and the limitations associated with computational apparatus. Therefore, the experience in modeling of general circulation of the atmosphere can be used by specialists working in other fields. For example, as mentioned in the foreword to the book, it can be interesting for everyone carrying out computations with three-dimensional models of complex physical systems.

However, the significance of the book goes beyond this. Recently models of general circulation of the atmosphere have been used more and more extensively for solution of a number of practical problems relating to the environment. We can mention their use for study and prediction of changes in climate, for analysis of anthropogenic influences on climate, for the development of

numerical methods for long-range weather forecasting, etc. The familiarization of a wide range of readers with approaches to solution of such problems seems useful. Finally, this book is also important for meteorologists. The concise exposition of the range of problems associated with the formulation of numerical models of general circulation of the atmosphere, the description of specific models of general circulation of the atmosphere and some results obtained on their basis, all this will unquestionably attract the attention of both specialists directly concerned with this problem and those desiring to familiarize themselves with it.

The book consists of five articles.

The first of these (A. Kasahara -- "Computational Aspects of Numerical Models for Weather Forecasting and the Reproduction of Climate") gives general information on the modeling of general circulation of the atmosphere (fundamental equations, choice of schemes for taking into account different physical processes, numerical solution methods, etc.). This is far from a complete list of the problems dealt with in the article: radiation processes, prediction of cloud cover and precipitation, atmospheric boundary layer, influence of the oceans, parameterization of movements of a subgrid scale, boundary condition effect at the upper boundary of the atmosphere, difference approximation, scheme with retention of quadratic invariants, implicit integration methods, nonlinear instability, initial conditions, initialization, four-dimensional analysis, atmospheric predictability. However, it should be noted that some subjects are dealt with extremely briefly.

The three subsequent articles are devoted to a description of specific finite-difference models: five-level model of the British Meteorological Service (G. A. Corby, A. Gilchrist, P. R. Roventree), the model of the National Atmospheric Research Center in the United States (W. Washington, D. Williamson) and a 12-layer model of the University of California at Los Angeles (A. Arakawa and W. Lamb). The first two models differ appreciably with respect to the degree of detail in taking physical processes into account. The British model is more economical, whereas the more detailed allowance for physical processes in the Washington-Williams model makes it more flexible. Here there is a graphic manifestation of the dependence of the practical realization of the model on the compromise between the detail of the physical description and the reasonable choice of duration of calculations.

This can be illustrated by the following figures. The integration of the British model for 24 hours requires 10 minutes time with an "IBM 360/195" electronic computer. The National Atmospheric Research Center model (six-layer variant, latitude-longitude grid with an interval 2.5°) requires 2 hours time with a "Suveg 7600" electronic computer and a doubling of the horizontal resolution leads to an eightfold increase in expenditures of computer time.

The article by Corby, et al. described in detail a five-level variant of a model with a Kurihara grid (4626 points on a sphere) in which allowance for radiation has been parameterized and the scheme for the computation of

exchange at the surface operates with a restriction on the number of types of underlying surface. Nevertheless, the model gives realistic results for different seasons, as is illustrated by data on the reproduction of meteorological fields for January and July. More complex variants of the model are also mentioned: a 13-layer variant (with 8 levels in the stratosphere) for computing changes in the ozone layer; a variant with a detailed description of radiation taking into account the temporal changes in cloud cover, computed within the framework of the model, intended for evaluation of the sensitivity of climatic computations to the cloud cover parameters.

The description of the National Atmospheric Research Center model contains information on the system of equations, boundary conditions and physical processes taken into account in solving the problem and numerical approximation of the equations. The article enumerates various applications of the model (reproduction of climate and general circulation of the atmosphere, numerical forecasting, initialization, four-dimensional analysis, etc.).

The article by Arakawa and Lamb devotes much attention to a thorough analysis of the computational aspects of the problem. There is a detailed description of the problem of such spatial-finite-difference schemes which would ensure maintenance of discrete analogues of some physically important integral relationships for the continuous atmosphere. The extremely rich physical content of the model is set forth very concisely.

The last article is devoted to modeling of general circulation of the atmosphere and numerical forecasting with the use of the spectral method. The last decade has been characterized by intensive development and use of nonlinear spectral models of the atmosphere. Effective methods for numerical solution of prognostic equations have been developed and tested. These make possible a considerable reduction in the volume of computations. The testing of spectral models demonstrated not only their capacity for competing with finite-difference models, but also definite advantages in comparison with the latter. In this connection, at a number of prognostic and research centers at the present time spectral models of forecasting, general circulation of the atmosphere and climate are either used together with traditional finite-difference models or have replaced them. Therefore, there is complete justification for including in the book the timely article by W. Burke, B. Macavaney, and others on the modeling of global atmospheric currents by spectral methods.

The article describes a variant of a spectral model developed by W. Burke which has come into rather broad use abroad. The solution of the problem is sought in the form of series of spherical functions. For computing the nonlinear terms in the equations use is made of the spectral-grid transformation method. Time integration is carried out using a "semi-implicit" scheme, especially effective in combination with the spectral method. Also described are schemes for including topography of the earth's surface, radiation processes, condensation, horizontal and vertical diffusion, surface friction in

the model, and also a method for stipulating temperature at the ocean surface. The article gives the results of operational use of the model for computing two-day forecasts for the earth's southern hemisphere, and also preliminary information on computation of global circulation of the atmosphere (reproduction of January circulation). Thirteen minutes of operation of the "Suveg 7600" electronic computer are expended for calculating global circulation for 24 hours.

The content of the article illustrates well the great possibilities of the spectral models. However, one must view critically certain statements made by the author: "The development of spectral methods for numerical integration of the equations of atmospheric motion can be traced from the study by Silberman (1954)," "the pioneering application of spectral methods by Silberman in 1954." It is fitting to recall that the spectral approach to solution of prognostic problems and problems in the theory of general circulation of the atmosphere and climate was proposed by Ye. N. Blinova (1943), and on this basis a number of linear prognostic schemes and models of general circulation of the atmosphere and climate were created. The successive approximations method is used at the Central Institute of Forecasts for solution of nonlinear spectral equations. A solution was obtained in two variants. In the first (1952-1953) it was expressed through definite integrals of the product of Legendre polynomials and their derivatives (these integrals are called interaction coefficients by Silberman). In the second variant (1954) the nonlinear terms are computed by conversion from a spectral representation of meteorological fields to the values at the points of intersection of a regular grid.

Thus, the method for use of spectral methods for solution of prognostic problems must be sought earlier than indicated by the authors of the article.

Other comments can be made concerning the book's contents. For example, it is hard to understand why the book does not include a description of the model of general circulation of the atmosphere created in the United States Laboratory of Geophysical Hydrodynamics, which is best developed and which is widely used for different purposes. Also left out are the problems relating to modeling of joint circulation of the atmosphere and ocean.

However, these comments do not detract from the importance of this publication. In conclusion it must be pointed out that the book has an extensive bibliography on numerical modeling of general circulation of the atmosphere and climate.

REVIEW OF MONOGRAPH BY KH. G. TOOMING: SOLNECHNAYA RADIATSIYA I FORMIROVANIYE UROZHAYA (SOLAR RADIATION AND YIELD FORMATION), LENINGRAD, GIDROMETEOIZDAT, 1977

Moscow METEOROLOGIYA I GIDROLOGIYA in Russian No 9, Sep 79 pp 122-123

[Review by I. A. Shul'gin and I. A. Murey]

[Text] In a series of books on agrometeorology which have been published during recent years in the USSR and abroad special and proper attention has been given to a monograph by Kh. G. Tooming, published by the Gidrometeoizdat and entitled SOLNECHNAYA RADIATSIYA I FORMIROVANIYE UROZHAYA (Solar Radiation and Yield Formation). The book is devoted to the theory of photosynthetic productivity of plants and quantitative determination of hydrometeorological factors in the processes of biological and economic productivity of sown crops.

The monograph examines an exceedingly important problem: the possibility of most effective use of the highly important factor of productivity and the main energy factor, solar radiation, in the process of formation of biological production with the participation of diverse processes transpiring in the plant itself.

This problem, by virtue of its exceptional theoretical and practical significance, has attracted the attention of many scientific workers in their examination of different aspects of activity of the plant cover, natural and artificial phytocoenoses and the production process itself.

The intensive development of the theory of photosynthetic activity of coenoses has led to the formulation of ideas concerning a sown crop as a complex, but at the same time, an integrated opticobiological system with characteristic regularities of formation, distribution of photosynthetically active radiation, photosynthesis, respiration, growth of the assimilation surface, and redistribution of the products in the storing or reproductive organs.

Within the framework of this theory there was validation of the position of the practical possibility of effective use of solar radiation by means of formation of a sown area with definite architectonics and leaf area, on the one hand, and the harmonious nutrition of plants with mineral elements and

moisture supply in accordance with the receipt of radiation, on the other hand.

In his monograph Kh. G. Tooming took an extremely original approach to solution of the problem. It is possible to agree with the editor of the book, Yu. K. Ross, who notes in the foreword that the author, being a Candidate of Physical and Mathematical Sciences and Doctor of Biological Sciences, being a master of the approaches and methods of the precise sciences and having a good knowledge of the physiology of the production process, has aptly selected the mathematical modeling and numerical experiments approach for solution of this problem.

Kh. G. Tooming has mathematically formulated the concept that during the period of growth of the vegetative organs the sown area "tends" to maximize its productivity (CO_2 gas exchange), and accordingly, efficiency as well. Applying this principle relative to the radiation regime and the architectonics of the sown area and solving the corresponding variational problem, he established the quantitative interrelationships between photosynthesis, respiration and architectonics of plants, on the one hand, and the radiation regime, on the other. This enabled the author to evaluate the role of the considered parameters in maximizing productivity, to formulate a number of general principles useful for the practical work of seed-selection stations.

The book consists of an introduction, five chapters and a conclusion. The bibliography contains 501 items, among them 264 in the Russian language.

It is emphasized in the introduction that the main task of agrometeorology, in connection with the programming of yield, is determination of the upper limit of productivity of the principal agricultural crops in different geographical regions on the basis of the receipts of photosynthetically active radiation and efficiency and development of the agrometeorological principles for lessening the gap between the theoretically possible and real yields. This can be achieved: 1) by creating, by means of melioration and agrotechnology, of those environmental conditions which would best correspond to the needs of the plants in sown areas; 2) by optimum regionalization of existing varieties in accordance with the climate and microclimate; 3) by producing and using varieties best corresponding to the environmental conditions in this region.

The first chapter characterizes the patterns of receipt of solar energy, including photosynthetically active radiation, per unit of horizontal surface.

The second, and in essence, the main theoretical chapter, is devoted to an exposition of the mathematical model of the dependence of the production process and yield of phytocoenoses on the regime of photosynthetically active radiation. Mathematical models of the radiation regime in sown crops and photosynthesis as the principal component in the production process and in the growth of plants are described in a concise form, but in a form which is clear and accessible for agrometeorologists. Also given are the principal

theoretical concepts of the author and their mathematical realization. As we have already noted, the principal scientific merit of the author is the formulation (mathematically -- in the form of the variational problem) of the concept of maximum productivity of a phytocoenosis, the solution of which made it possible to determine the correlations between the radiation regime, light curves of photosynthesis and respiration (in the darkness), under given environmental conditions resulting in maximum productivity and revealing the nature of adaptation of the phytocoenosis to different regimes of photosynthetically active radiation at its different levels. Although the physiological mechanisms of such light adaptation are not examined by the author, however the conclusions themselves unambiguously indicate the fundamentally important role of the studied processes in the effective use of photosynthetically active radiation and the conclusions themselves agree with the existing concepts. It is important that the Kh. G. Tooming concept makes it possible, from unified points of view, to explain much diverse experimental data on adaptation of plants to light and on the interrelationship between photosynthesis and the architectonics of plants. True, the book does not adequately explain (for the most part due to the lack of experimental data at the time of writing of the book) relaxation times and the rates of adaptation of plants to the regime of photosynthetically active radiation, which we did only in 1977-1978.

This same chapter also presents the author's own results on study of the radiation regime of phytocoenoses. The new concept of "intensity of adaptation radiation" (IAR) is introduced. This determines the intensity of photosynthetically active radiation with which this phytocoenosis or its layer have a maximum efficiency of PAR in the production process. It must be emphasized that the IAR value corresponds under plant habitat conditions to the diurnal dose of PAR (Shul'gin, 1973). The relationships between IAR and the anatomical criteria of leaves following from the computations are interesting and promising.

The third chapter gives the results of numerical experiments for the purposes of explaining the dependence between the productivity of phytocoenoses and their geometrical structure and the regime of photosynthetically active radiation, the ideal geometrical structure of the phytocoenosis and the geographical change in productivity and efficiency of a phytocoenosis in relation to the change in receipts of PAR. The results make a valuable contribution to theoretical ecology, make possible a more detailed and deeper understanding of the complex interrelationships between the radiation regime, architectonics and productivity of plants under different environmental conditions. These investigations emphasize still more that the role of radiation in the production process is more complex and multisided than was assumed earlier by agrometeorologists. Radiation is not only an energy source for photosynthesis as such (substrate role), but also exerts an influence on photomorphogenesis of a coenosis or plant and their architectonics. On the other hand, the intactness of a plant as a system, with its numerous and interrelated processes, is manifested more clearly.

The fourth chapter, which is brief, is devoted to an analysis of the effectiveness of use of photosynthetically active radiation by phytocoenoses (efficiency).

The last, fifth chapter has the most practical character and is closely related to modern agrometeorology and the theory of programming of high yields, the development of which in our country is related to the studies of I. S. Shatilov. Proceeding on the basis of his theoretical concepts and the results of numerical experiments, the author in quantitative form formulates a series of principles and requirements for the optimization of the growth of leaf area in a sown crop, optimization of the light curves for productivity and growth of plants, develops a series of recommendations for seed selection specialists for obtaining new varieties and making more effective use of PAR in a coenosis. It should be noted that some of these principles were formulated earlier only qualitatively. Among the author's conclusions the most important, possibly, is the conclusion that a change in any of the plant parameters can lead to an increase in yield only in a case if there is retention of the optimum extent of the leaf surface in the sown crop and the optimum area of leaves is not constant. A new variety with modified indices of photosynthetic activity can give a higher yield only in a case if it is possible to create a highly productive (that is, well-organized) sown crop.

To be sure, models of the Tooming production process to a certain degree are characterized by the shortcomings of all such models. This is well recognized by the author himself, emphasizing that on the basis of his computations he formulates only the general principles of processes and evaluates the relative role of any factor in the process of yield formation. But today this is more important than dozens of scattered experimental studies. At the same time, on the basis of many investigations, including also our investigations under "factorostatic" conditions for study of the photosynthetic activity of coenoses of different density, it can be asserted that the Kh. G. Tooming models fundamentally correctly take into account the role of the radiation regime and architectonics in the production process.

In general, the book by Kh. G. Tooming has been written on a high theoretical level. The author has good intuition as a natural scientist. Being current with the entire world literature in the field of the production process of phytocoenoses and having the mathematical techniques at his command, he was able to write, in compressed form, a book with a very substantial content which is valuable for theoretical ecology and physiology of plants on the basis of an analysis of the interrelationships between the receipts of photosynthetically active radiation and processes in phytocoenoses, on the one hand, and for agrometeorology and seed selection for increasing the yield of agricultural sown crops, on the other.

The book has high-quality printing and binding.

The publication of this book by Kh. G. Tooming, "Solar Radiation and Yield Formation," is an event in the entire world literature on biogeophysics and agrometeorology.

SIXTIETH BIRTHDAY OF SEMEN PAVLOVICH KOZNOV

Moscow METEOROLOGIYA I GIDROLOGIYA in Russian No 9, Sep 79 pp 124-125

[Article by the Board of the USSR State Committee on Hydrometeorology and Environmental Monitoring]

[Text] Semen Pavlovich Koznov, head of the Northwestern Territorial Administration on Hydrometeorology and Environmental Monitoring, marked his 60th birthday on 19 September 1979.

Semen Pavlovich began his work activity in the Hydrometeorological Service in 1940 after graduating from the Moscow Hydrometeorological Technical School. During the years of the Great Fatherland War he was in the active army on the Leningrad front. He was presented government awards for participation in battles with the German-Fascist invaders. Semen Pavlovich entered the ranks of the CPSU in 1945.

After demobilization, from January 1946 through September 1947, S. P. Koznov worked in the hydrometeorological service of the Baltic fleet, and from October 1947 to the present time all his activity has been associated with the Northwestern Territorial Administration on Hydrometeorology and Environmental Monitoring.

During the period from 1947 through 1949 S. P. Koznov worked as a weather forecasting engineer. Then he was head of the aviation meteorological station at the Leningrad airport. During the years 1951-1959 he was head of the section on the servicing of aviation and the national economy and deputy head of the forecasting service. During these years he devoted many efforts to the organization of meteorological support of aviation. During 1949-1951, by direction of the Main Administration of the Hydrometeorological Service, he worked as head of the Forecasting Division of the Hydrometeorological Bureau in the Mongolian People's Republic. In 1956, while continuing on the job, he graduated from the university.

In the years which followed, while working as head of the forecasting service and head of the Leningrad Weather Bureau, he devoted great attention to study of the specifics of productive activity of national economic organizations, the organization of specialized hydrometeorological support, an increase in the quality of forecasting of weather and hydrological conditions, investigation, development and introduction of new forecasting and information methods.

Since May 1963 S. P. Koznov has headed one of the largest territorial administrations of the State Committee on Hydrometeorology and Environmental Monitoring.

Being the director of a major body of specialists, having rich work experience, high skills and good organizational capabilities, Semen Pavlovich carries out much work for strengthening operational and observational agencies, the organization of a higher quality, specialized hydrometeorological support of the most important branches of the national economy, such as the sea and river fleet, civil aviation, and especially agriculture and water management.

Being a member of the Lengorispolkom commission for contending with disasters, S. P. Koznov directly participates in the support of Party and Soviet agencies for forecasts and warnings of Leningrad floods. He is working on study and introduction of new forecasting methods.

He has done much for shifting the processing of the results of hydrometeorological observations to computer, for the introduction of new technology in the network of stations, the compilation and publication of regime and reference materials.

Semen Pavlovich has been repeatedly commended by the directors of the State Committee on Hydrometeorology and the Central Committee of the Trade Union of Aviation Workers for his initiative and practical introduction of new observational methods, increasing the effectiveness of hydrometeorological support of the national economy. In 1957 he was awarded the emblem "Distinguished Worker of the USSR Hydrometeorological Service" and in 1970, the silver medal of the USSR Exhibition of Achievements in the National Economy.

His activity has been directed to carrying out the new tasks assigned by resolutions of the Party and government to the State Committee on Hydrometeorology. Under his direction and with his direct participation there has been successful organization of a national service for observations and monitoring of preservation of the environment and automated systems for monitoring the quality of atmospheric air and surface waters in Leningrad are being introduced.

Semen Pavlovich is the chairman of the basin section "Atlantic Ocean and Baltic Sea" of the USSR State Committee on Science and Technology. He coordinates hydrometeorological investigations of the Baltic Sea.

S. P. Koznov, with great operational-productive and organizational activity, is actively participating in public life. The businesslike and personal qualities of Semen Pavlovich, his demanding and sensitive relationship to the workers, have earned him merited authority in the organizations of the State Committee on Hydrometeorology, among the chiefs of its subdivisions and rank-and-file workers.

Semen Pavlovich Koznov meets his 60th birthday full of creative forces. Congratulating him on his birthday, we wish him good health, personal happiness and new creative successes.

SIXTIETH BIRTHDAY OF NIKOLAY YEFIMOVICH ZAKHARCHENKO

Moscow METEOROLOGIYA I GIDROLOGIYA in Russian No 9, Sep 79 pp 125-126

[Article by the Board of the USSR State Committee on Hydrometeorology and Environmental Monitoring]

[Text] Nikolay Yefimovich Zakharchenko, head of the Latvian Republic Administration on Hydrometeorology and Environmental Monitoring, Meritorious Worker in Preservation of Nature Latvian SSR, noted his 60th birthday and 40 years of productive-scientific activity on 24 September 1979.

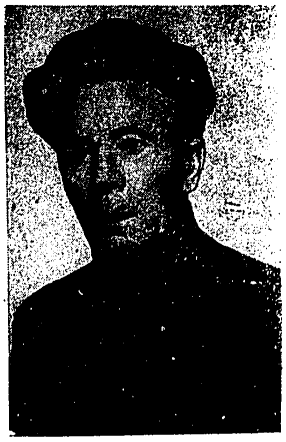

Nikolay Yefimovich began his work activity in the mid 1930's as an apprentice metal craftsman in a factory and as a kolkhoz shepherd. After graduating from the Feodosiya Hydrometeorological Technical School Nikolay Yefimovich Zakharchenko was designated head of the hydrometeorological station Ostrov Svinoy of the Azerbaydzhan Administration of the Hydrometeorological Service.

During the years of the Great Fatherland War Nikolay Yefimovich served in tank units, and after the War, in the Administration of the Hydrometeorological Service of the Black Sea Fleet. Advancing from senior technician to

head of the technical inspection section, in 1950 he was sent to work at the Administration of the Hydrometeorological Service Estonian SSR as head of the section on study of the hydrometeorological regime of the sea.

In February 1953 he was designated deputy head of the Administration of the Hydrometeorological Service Latvian SSR. Being in this responsible post, Nikolay Yefimovich was constantly studying and in 1963 graduated from the Leningrad Hydrometeorological Institute in the field of specialization "oceanology." During this period he carried out a number of research studies, writing, in particular, "Transparency of Waters in the Gulf of Riga," "Currents in the Gulf of Riga and Methods for Their Investigation," "Horizontal Turbulent Exchange and its Relationship to the Resultant Current Direction," "Heat Balance of the Gulf of Riga and the Role of Convection" and others.

With the designation of N. Ye. Zakharchenko to the post of head of this administration he displayed his organizational capabilities. He is devoting considerable attention to improving the forms and methods for hydrometeorological support of Party and soviet agencies in Latvia, which is considerably increasing the effectiveness of use of service data in the national economy. During recent years Nikolay Yefimovich has been doing much work in the field of preservation of nature. Under his direction and with his direct participation a service has been established in the republic for observing and monitoring contamination of the environment.

Taking into account the exceptional timeliness and to a large extent the newness of the problem of preserving the environment, Nikolay Yefimovich is personally directing research work in this field. For example, studies have been carried out for evaluating contamination of the southern part of the Gulf of Riga for the planning of purification structures, evaluation of contamination of the Liyelupe River for the purpose of issuance of recommendations on further use of the river and its preservation as a natural water body. A multisided program has been drawn up for the preservation of nature and effective use of the natural resources of the Latvian SSR during 1976-1990.

A fundamental scheme of interdepartmental information on environmental contamination in the Latvian SSR was drawn up with his direct participation and has been adopted. This work, which was awarded a gold medal and a first-degree diploma of the USSR Exhibition of Achievements in the National Economy, has been recommended by the USSR State Committee on Hydrometeorology and Environmental Monitoring for introduction by other administrations in the country.

Nikolay Yefimovich Zakharchenko is taking an active part in the public life of the city and republic, being a deputy of the Oktyabr'skiy Rayon Soviet of Peoples Deputies in Riga where he heads the commission on the preservation of nature. He is a member of the expert commission in the Gosplan

Lithuanian SSR on the problems involved in the dumping of waste water. He is a member of the scientific council of the USSR State Committee on Science and Technology on the problem "Study of the Oceans and Seas and Use of Their Resources" and also a member of the basin section "Atlantic Ocean and the Baltic Sea."

From the day of organization of the All-Union Society of Inventors and Rationalizers he for many years headed the branch council of the All-Union Society of Inventors and Rationalizers of Aviation Workers of Latvia; for more than 20 years he has been a propagandist, director of political and economic education of the higher echelon of the administration.

For his merits in developing the hydrometeorological service and active participation in public life he has a number of government awards and twice has been given diplomas of honor by the Presidium Supreme Soviet Latvian SSR.

Nikolay Yefimovich is reaching his 60th birthday at the height of his creative forces.

Warmly congratulating this veteran of the Hydrometeorological Service on his noteworthy anniversary, we wish him long and productive years of life, excellent health and new successes in public activity.

CONFERENCES, MEETINGS AND SEMINARS

Moscow METEOROLOGIYA I GIDROLOGIYA in Russian No 9, Sep 79 pp 126-127

[Article by Ts. I. Bobovnikova]

[Text] The Second All-Union Conference "Migration of Contaminating Substances in the Soil, in Soil-Water, Soil-Plant Systems" was held at the Institute of Experimental Meteorology. The work of the conference was attended by 80 specialists from institutes of the USSR State Committee on Hydrometeorology and Environmental Monitoring, USSR Agriculture Ministry, USSR Health Ministry, USSR Academy of Sciences, USSR Geology Ministry, USSR Ministry of Higher Education, USSR Water Management Ministry and others. Fifty-seven reports were presented and discussed, covering the following scientific directions: physicomathematical modeling; migration and transformation of contaminating substances in soils and on the boundaries of the soil with contiguous media; study of the migration of pesticides, metals, carcinogenic substances, petroleum products and biogenous substances in soils and in contiguous media; hygienic evaluation of soil contamination; influence of anthropogenic contaminating substances on the physicochemical and biological indices of soils.

A report by Ya. I. Gaziyev (Institute of Experimental Meteorology) examined the problems involved in formulating prognostic models of soil contamination by the smoke effluent of state regional electric power stations and gave some evaluations obtained using a model, developed by the author, of fractional transport in the atmosphere and fallout onto the earth's surface of the smoke effluent of state regional electric power stations.

A report by Ye. I. Spyn and R. Ye. Sova (VNIIGINTOKS, Kiev) was devoted to new approaches to the principles for norm-setting for pesticides in the soil. The authors proposed a method for the validation of norms by computations -- the approximate admissible concentration (AAC) of pesticides in the soil.

A report by V. A. Borzilov and N. B. Senilov was a review of work by the Institute of Experimental Meteorology in creating physicomathematical models of the behavior of contaminating substances in the environment,

in particular, their falling onto the soil surface, behavior in the water and entry into plants.

V. V. Yermakov (VNIIVS, Moscow), in his communication, entitled "Biogenous Migration of Mercury Under Conditions of Technogenesis in the Biosphere," gave particular attention to the detection of mercury alkyl in different objects in the biosphere, to the transformation of mercury compounds in organisms and the peculiarities of migration of this toxic element in the biosphere.

N. G. Zyrin, et al. (Moscow State University) examined the influence of a major lead and zinc combine on the contamination of soils, defined zones with different degrees of contamination and demonstrated that the compounds of heavy metals, entering the soil due to atmospheric contamination, have a greater solubility and are more accessible to plants than compounds of metals from the soils of natural landscapes.

N. F. Beloborodov, L. V. Gavrilov and I. A. Orlik (Central Asian Regional Scientific Research Hydrometeorological Institute) obtained interesting results from study of scrption processes of pesticides, regarding the soil layer as a chromatographic column. The investigations were carried out on an apparatus developed at this institute.

Two sections operated at the conference: "Behavior and Migration of Pesticides in the Soil and Adjacent Media" and "Behavior and Migration of Technogenic Contaminants in the Soil and Adjacent Media."

A considerable part of the reports in the first section were devoted to the behavior of pesticides in the soil and their migration in plants.

A report by F. I. Vayntraub, et al. (All-Union Scientific Research Institute of Biological Methods for Protecting Crops, Kishinev) examined the lifetime of some organophosphorus pesticides in the soil and it was demonstrated that such organophosphorus substances as phosalone, metathione, phthalophos and siphos can persist in the soil for not more than one growing season.

V. V. Ivanchenko (Saratov Agricultural Institute), who studied the behavior of phosalone in the soil, demonstrated that among the many factors, such as type of soil, humus content, pH, temperature and others, soil moisture plays a special role in the retention and migration of pesticide.

A communication by T. M. Petrova and K. V. Novozhilov (All-Union Research Institute of Plant Protection) was devoted to an examination of the factors favoring the destruction of 12 insecticides in the soil and plants, their distribution in agricultural crops and the soil for different methods of use, and also movement of pesticides from the soil into plants.

The reports of F. I. Kopytova (All-Union Research Institute of Plant Protection) and A. N. Stroy (VNIIGINTOKS), Ye. S. Kovaleva and G. A. Talanov (VNIIVS) examined problems relating to the migration of organophosphorus

pesticides from the soil into plants and the duration of their retention in plants.

A number of interesting communications on the migration of toxic metals in soils and in plants were presented by specialists in the Department of Soil Science and Geography at Moscow State University in the second section.

By investigating the migration of Zn, Cd and Pb in the zone affected by a zinc smelting combine, R. A. Makarevich, A. I. Obukhov and N. G. Zyrin (Moscow State University) demonstrated that toxic metals, entering onto the soil surface with the effluent from the enterprises, are concentrated in the upper humus layer and little subject to migration and redistribution in the soil layer. The authors discovered a rather close dependence between the humus content in the upper soil layer and the concentration of heavy metals in it.

R. I. Pervunina (Institute of Experimental Meteorology), in collaboration with N. G. Zyrin (Moscow State University), made preliminary computations of the balance of cadmium distribution in the soil-plant system. These demonstrated that the loss of this element from the root-occupied layer, as a result of migration through the soil profile is 40-58%, whereas the loss with the crop yield is 0.03-0.24%.

At the conference much interest was shown in a report by N. P. Solntseva and Yu. I. Pikovskiy (Moscow State University). In the example of soddy-podzolic and soddy-gleyey soils in southern taiga landscapes he demonstrated the influence of petroleum contamination and contamination of mineralized waters on soil transformation. They detected a change in the reaction of the medium, an intensification of reduction processes, sodium chloride salinization and other disruptions of soil processes under the influence of these contaminants.

The results of an investigation of the influence of contaminating substances (fluorine, benzapyrene) on the microbiological indices of the soil were presented in communications by specialists of the Institute of Experimental Meteorology.

E. I. Gaponyuk, T. N. Morshina and N. P. Kremlenkova carried out an investigation of the influence of fluorine compounds on some physicochemical and biological properties of two types of soils -- soddy-podzolic and gray soils. They demonstrated that the nature of the effect of fluorine is different in gray soils and in soddy-woody soil and that there is a decrease in the activity of dehydrogenase, phosphatase and urease under the influence of fluorine when its content is 1000 mg/kg or above.

A similar study of the change in the activity of dehydrogenase, phosphatase and soil respiration under the influence of benzapyrene was carried out by Ye. M. Vishenkova, L. V. Vaneyeva, E. I. Gaponyuk, N. P. Kremlenkova and A. I. Shilina. The most sensitive microbiological indices of soil contamination by benzapyrene were found to be the actual dehydrogenase activity

and the soil respiration process. Actual dehydrogenase activity is suppressed under the influence of benzapyrene.

A report by A. S. Demchenko, L. G. Korotova, M. N. Tarasova and V. S. Zolotareva (Geochemical Institute, Novocherkassk) dealt with the problem of transport of hexachlorocyclohexane by surface runoff waters. The authors demonstrated that the transport of hexachlorocyclohexane from unirrigated basins is accomplished by surface runoff waters, primarily during the period of spring high water -- up to 80% of its surface runoff. In addition, the greatest transport is observed during the first days of the high water.

A communication by Ts. I. Bobovnikova (Institute of Experimental Meteorology) dealt with the role of atmospheric precipitation (snow and rain) and contamination of rivers by stable chlororganic pesticides. An example of this is the observations made by the author in the Moskva River basin. The quantity of DDT and γ-hexachlorocyclohexane during the period of the spring high water was almost equal to the quantity of these pesticides accumulating in the snow in the basin.

Such results were obtained by V. N. Bashkin and A. Yu. Kudeyarova (IAP [expansion unknown], Pushchino), who studied contamination of the Skniga River (a tributary of the Oka) by compounds of nitrogen and phosphorus. They demonstrated that the contamination of water by nitrogen compounds in a period of high water is completely attributable to its reserves in the snow cover in the area of the basin. However, the quantity of phosphorus transported by the river is more than three times greater than its reserves in the snow.

A resolution was passed calling for the next conference to be held in 1980.

NOTES FROM ABROAD

Moscow METEOROLOGIYA I GIDROLOGIYA in Russian No 9, Sep 79 p 128

[Article by B. I. Silkin]

[Text] As reported in SCIENCE NEWS, Vol 114, No 7, p 105, 1978, a scientific specialist at the Scripps Oceanographic Institute, J. Namias, at a symposium "Solar-Terrestrial Relationships and Their Influence on Weather and Climate" organized by Ohio State University at Columbus, presented a report devoted to the characteristic meteorological conditions accompanying a drought.

He made an analysis of the meteorological conditions accompanying such outstanding phenomena as the droughts which during 1976-1977 affected the Pacific Ocean Coast of the United States, in 1972 -- eastern Europe, including the territory of the USSR, in 1976 -- the British Isles, in 1952-1954 -- the southwestern United States and the intense drought of 1930, entering into the history of the United States West as the "year of dust storms."

The researcher established that all these catastrophes accompanied:
1) the appearance of descending air flows, sometimes attaining 700 m/day, which as a result of an increase in pressure increases temperature and decreases atmospheric humidity, prevents the rising of individual air masses and the condensation of moisture in them, capable of causing precipitation;
2) formation of cells with unusually high pressure directly over the region of the drought;
3) formation of unusually powerful "accompanying" high-pressure cells along both sides of the continental high pressure, usually existing only over the ocean. These "accompanying" cells maintain the continental pressure maximum proper.

In the researcher's opinion, the formation of "accompanying" cells and the appearance of repeating droughts can be favored by unusual air temperatures over the sea surface. The anomalous heating or cooling of water, occurring for different reasons, can cause an unusual increase in pressure over the ocean. Since the ocean retains thermal energy a longer time than the atmosphere, these high-pressure regions are capable of creating conditions in the atmosphere causing a drought even in the years which follow. The prolonging of droughts can also be favored by dust particles in the atmosphere preventing the formation of a cloud cover.

Without completely denying the probability of a solar influence on droughts, the speaker nevertheless emphasized that there must be a careful study of the global and local "terrestrial" factors also giving rise to catastrophic phenomena.

As reported in the NEW SCIENTIST, Vol 80, No 1130, p 605, 1978, the meteorologist R. Carrie (United States) has completed a detailed analysis of a long series of observations carried out at 100 meteorological stations in North America and their comparison with astrophysical data characterizing solar activity. He established a definite correlation between the air temperature registered at 55 of these stations and 11-year cyclicity of spot-forming activity on the sun. Such a correlation is particularly conspicuous in the meteorological data collected at stations which are situated in the northeastern part of the American continent where there are 51 of these meteorological stations.

According to the data from this analysis, the mean cyclicity in air temperature variations has a period of 10.7 years (±0.4 year) and the amplitude of its variations is 0.29°C (±0.15°C). In the data it is also possible to see evidence of the existence of still another, lesser cycle with an amplitude of 0.06°C and a period of 18.6 years, that is, equal to the lunar nodal period.

***

As reported in THE SCIENCES, Vol 18, No 9, p 4, 1978, auroras constitute a powerful electric discharge transpiring at altitudes of approximately 100 to 500 kilometers above the earth's surface in the atmosphere, most frequently over the Far North or Far South. The energy source for these auroras is the magnetosphere -- a natural "generator" which can produce approximately 100 billion watts, that is, two orders of magnitude greater than the quantity of electric power that is used annually in the United States.

This generator arises as a result of interaction between the earth's intrinsic magnetic field and the solar wind -- the flow of heated ionized hydrogen and helium flowing from the sun.

In many cases this phenomenon is accompanied by serious disruptions of radio communication and it leads to interruptions in the activity of radar systems and high-voltage transmission lines. For this reason a national economic need arises for the prediction of the appearance of auroras and their intensity. Up to the present time such attempts have been fruitless.

Recently a group of specialists headed by Syun-Ichi Akasofu (Geophysical Institute, University of Alaska, Fairbanks) completed the processing of data obtained as a result of the launching of an artificial satellite (International Satellite "Explorer"-"Sun-Earth"). The launching of this satellite, which took place in the summer of 1978, by NASA in the United States, is part of the program of international investigations of the magnetosphere.

An analysis of the information received from this satellite enabled Akasofu and his colleagues, taking into account the new data on velocity with which the solar wind is propagated, on the intensity and orientation of the magnetic field which it carries along, to formulate a forecast of an aurora. The appearance of this phenomenon and its future intensity can now be predicted for approximately two hours in advance.

[1-5303]

5303 -END-
CSO: 1864